

Posttranscriptional regulation of mitochondrial DNA expression
in mammalian mitochondria

I n a u g u r a l - D i s s e r t a t i o n

zur

Erlangung des Doktorgrades

der Mathematisch-Naturwissenschaftlichen Fakultät

der Universität zu Köln

vorgelegt von

JULIA HARMEL

aus Karlsruhe

Berichterstatter: Prof. Dr. Nils-Göran Larsson

Prof. Dr. Thomas Langer

Tag der mündlichen Prüfung: 21.01.2014

Table of Contents

Table of Contents	I
I. Table of abbreviations	VI
II. Zusammenfassung	XII
III. Abstract.....	XIV
1 Introduction	1
1.1 Structural organization and morphology of mammalian mitochondria	1
1.2 Mitochondria in aging and disease	4
1.3 Structural organization of mammalian mitochondrial DNA.....	5
1.4 Transcription of mammalian mitochondrial DNA.....	7
1.4.1 The core machinery of mammalian mitochondrial transcription	8
1.4.1.1 Mitochondrial RNA polymerase	8
1.4.1.2 Mitochondrial transcription factor A	9
1.4.1.3 Mitochondrial transcription factor B2.....	10
1.4.2 Initiation of mammalian mitochondrial DNA transcription.....	11
1.4.3 Transcription termination in mammalian mitochondrial DNA.....	11
1.4.3.1 Mitochondrial transcription termination factor 1.....	13
1.4.3.2 Mitochondrial transcription termination factor 2.....	14
1.4.3.3 Mitochondrial transcription termination factor 3.....	14
1.4.3.4 Mitochondrial transcription termination factor 4.....	15
1.4.4 Posttranscriptional modifications in mammalian mitochondria.....	15
1.4.4.1 Posttranscriptional tRNA modifications.....	15
1.4.4.2 Posttranscriptional rRNA modifications.....	16
1.4.4.3 Polyadenylation in mammalian mitochondria.....	17
1.4.5 The PPR protein family.....	19
1.4.5.1 The leucine-rich pentatricopeptide repeat motif - containing protein (LRPPRC)	20
1.5 Projects.....	21
2 Material and Methods	23
2.1 Material	23
2.1.1 Antibodies	23
2.1.1.1 Commercial antibodies.....	23
2.1.1.2 In-house generated antibodies	24

2.1.1.3	Secondary antibodies	24
2.1.2	Oligomers	24
2.1.3	Plasmids	25
2.1.4	Taqman probes	25
2.2	Transgenic mouse models	27
2.2.1	Generation of LRPPRC (wt) BAC TG 505 mice	27
2.2.1.1	Genotyping of LRPPRC (wt) BAC TG 505 mice.....	27
2.2.2	Generation of LRPPRC heterozygous knockout mice.....	27
2.2.2.1	Genotyping of LRPPRC heterozygous knockout mice.....	28
2.2.3	Generation of <i>Mterf1</i> knockout mice	28
2.2.3.1	Genotyping of <i>Mterf1</i> knockout mice	29
2.2.4	Generation of <i>Mterf2</i> knockout mice	30
2.2.4.1	Genotyping of <i>Mterf2</i> knockout mice	30
2.2.5	Generation of <i>Cry1</i> knockout mice	30
2.2.5.1	Genotyping of <i>Cry1</i> knockout mice.....	31
2.3	Bacterial cells	31
2.3.1	Transformation of chemically competent cells.....	31
2.3.2	Overnight culture of bacterial cells	32
2.4	Methods in molecular biology	33
2.4.1	Plasmid preparation	33
2.4.2	DNA isolation from mouse tissue.....	33
2.4.2.1	Phenol chloroform extraction	33
2.4.2.2	Short protocol for DNA isolation from mouse tails.....	33
2.4.2.3	DNA extraction with DNeasy® Blood and tissue Kit (Qiagen)	34
2.4.2.4	DNA extraction with Puregene® Core Kit A (Qiagen)	34
2.4.3	RNA isolation from mouse tissue.....	34
2.4.3.1	RNA isolation with ToTALLY RNA™ kit (Ambion)	34
2.4.3.2	RNA isolation with TRIzol® (Invitrogen)	34
2.4.4	Quantification methods of nucleic acids	35
2.4.4.1	DNA/RNA quantification with nanodrop	35
2.4.4.2	DNA quantification with Qubit® 1.0 fluorometer (Invitrogen)	35
2.4.5	DNA agarose gelelectrophoresis	35
2.4.6	Polymerase chain reaction.....	36
2.4.6.1	DNA amplification with GoTaq® DNA polymerase (Promega)	36
2.4.6.2	DNA amplification with Phusion® High Fidelity DNA polymerase	36
2.4.7	DNase treatment	37
2.4.8	Reverse transcription.....	37

2.4.9	Quantitative polymerase chain reaction.....	37
2.4.9.1	Quantitative PCR using Taqman® Universal PCR master mix.....	37
2.4.9.2	QPCR using a pipetting robot.....	38
2.5	Methods in protein biochemistry.....	39
2.5.1	Recombinant proteins.....	39
2.5.1.1	Expression of human recombinant TFAM, TFB2M and LRPPRC	39
2.5.1.2	Expression of human recombinant POLRMT and mouse LRPPRC.....	39
2.5.1.3	Purification of human recombinant POLRMT	39
2.5.1.4	Purification of human recombinant TFB2M.....	40
2.5.1.5	Purification of human recombinant TFAM	40
2.5.1.6	Purification of human recombinant LRPPRC.....	40
2.5.1.7	Purification of mouse recombinant POLRMT, TFB2M and TFAM	41
2.5.1.8	Purification of mouse recombinant LRPPRC.....	41
2.5.2	Protein quantification with Bradford.....	41
2.5.3	Isolation of mitochondria from mouse tissue.....	42
2.5.4	SDS-Polyacrylamide gelelectrophoresis	42
2.5.4.1	Selfmade gels	42
2.5.4.2	Purchased gels.....	43
2.5.5	Gel drying	43
2.5.5.1	Gel drying using Hoefer Slab Gel Dryer	43
2.5.5.2	Manual gel drying	44
2.5.6	Western Blot.....	44
2.5.7	Blue Native PAGE	45
2.5.8	Immunoprecipitation	45
2.5.9	Size exclusion chromatography	46
2.5.10	Absolute quantification of recombinant proteins	46
2.6	Methods handling radionucleotides.....	47
2.6.1	Radioactive probe labeling	47
2.6.1.1	Probe labelling with [α - ³² P] dCTP using Prime-It® II Random Primer Labeling Kit (Agilent).....	47
2.6.1.2	Oligonucleotide labelling with [γ - ³² P] ATP using T4-polynucleotide kinase	47
2.6.1.3	RNA labeling using Riboprobe System T7 Kit (Promega)	47
2.6.2	Measurement of radiation.....	48
2.6.3	Northern blot analysis	48
2.6.3.1	Membrane stripping	49
2.6.4	Southern blot analysis.....	49
2.6.5	<i>De novo</i> transcription assay.....	50
2.6.6	<i>In organello</i> translation	51

2.6.7	S1 protection assay	52
2.6.8	<i>In vitro</i> transcription	53
2.6.9	Electrophoresis mobility shift assay.....	54
2.6.10	ChIP-Sequencing.....	54
2.7	Mass spectrometry	56
2.7.1	Protein identification with LC-MS/MS after immunoprecipitation	56
2.7.2	Protein identification and quantification with LC-MS/MS.....	57
2.8	Cell culture	58
2.8.1	Maintenance of cultured HeLa cells	58
3	Results	59
3.1	Analysis of mitochondrial gene regulation at the transcriptional level in	
	<i>Mterf1</i> knockout mice	59
3.1.1	Generation of <i>Mterf1</i> knockout mice	59
3.1.2	<i>Mterf1</i> knockout mice are fertile and viable with normal respiratory chain activity.....	61
3.1.3	MTERF1 binds mtDNA but is not involved in maintenance and transcription initiation of mitochondrial DNA.....	62
3.1.4	MTERF1 prevents light strand transcription from interfering with the light strand promoter.....	65
3.1.5	A ketogenic diet does not impair the physiological conditions of <i>Mterf1</i> knockout mice.....	66
3.2	Analysis of mitochondrial gene regulation at the transcriptional level in	
	<i>Mterf2</i> knockout mice	69
3.2.1	Creation of <i>Mterf2</i> knockout mice	69
3.2.2	<i>Mterf2</i> knockout mice are fertile and viable under normal and stress conditions	70
3.2.3	MTERF2 is dispensable for maintenance and expression of mtDNA	73
3.2.4	Lack of MTERF2 is not compensated by other members of the MTERF-family	76
3.2.5	MTERF2 does not affect oxidative phosphorylation activity	77
3.2.6	<i>Cry1</i> expression levels are downregulated in <i>Mterf2</i> knockout mice	79
3.3	Analysis of mitochondrial gene regulation at the posttranscriptional level	
	in <i>Lrpprc</i>^{+/-} and <i>Lrpprc</i>^{+T} mice.....	81
3.3.1	<i>Lrpprc</i> heterozygous knockout mice and <i>Lrpprc</i> overexpressor mice are fertile and viable	81
3.3.2	LRPPRC does not regulate the amount of respiratory chain complexes	82

3.3.3 LRPPRC strongly influences levels of the ND5-Cytb precursor transcript ...	84
3.3.4 LRPPRC does not activate mitochondrial transcription	86
3.3.5 LRPPRC is abundant in mammalian mitochondria	90
4 Discussion	92
4.1 Future perspectives	102
References.....	106
Erklärung	118

I. Table of abbreviations

α	anti
γ ATP	gamma adenosintriphosphate
A	ampere
aa	aminoacids
ab	antibody
Amp	ampicillin
APS	ammonium peroxodisulfate
ATP	adenosintriphosphate
BAC	bacterial artificial chromosome
bp	basepairs
BSA	bovine serum albumin
BSF	bicoid stability factor
$^{\circ}$ C	degree Celsius
Ca^{2+}	calcium
CaCl_2	calcium chloride
cAMP	cyclic adenosine-3',5' - monophosphate
cDNA	complementary DNA
cGMP	cyclic guanosin-3',5' - monophosphate
ChIP	chromatin-immunoprecipitation
Cl^-	chloride
cm	centimetre
CMV-Promotor	<i>human cytomegalovirus minimal promoter</i>
COX	cytochrome c oxidase
Cry1	cryptochrome 1
CSB I-III	conserved sequence block I-III
C-terminus	carboxylterminus of a polypeptide
CTD	c- terminal domain
Cytb	cytochrome b
Da	Dalton
DEPC	diethylpyrocarbonate
dCTP	deoxy cytosine triphosphate
DMSO	dimethylsulfoxide
DNA	deoxyribonucleic acid

DNase	desoxyribonuclease
dNTP	desoxynucleosidtriphosphate
DTT	dithiothreitol
<i>E.coli</i>	<i>Escherichia coli</i>
EDTA	ethylenediaminetetraacetate
eGFP	<i>enhanced green fluorescent protein</i>
e.g.	for example (<i>exempli gratia</i>)
EGTA	ethyleneglycoldiamine tetraacetate
EMSA	electromobility shift assay
ES-cells	embryonic stemcells
<i>et al</i>	<i>et altera</i>
EtOH	ethanol
FAD	flavin adenine dinucleotide
Fig	figure
FRT	flp-recombinase target
g	gram
g	normal gravity acceleration (9,81 m x s ⁻¹)
gt	goat
GTP	guanosine-5'-triphosphate
GTT	glucose tolerance test
h	hour(s)
HA-Tag	hemagglutinin A-Tag
HeLa cells	immortal cervical cancer cell line from Henrietta Lacks
HCL	hydrochloric acid
HEPES	2-(4-(2-hydroxyethyl)-1-piperazinyl)-ethansulfonacid
HMG	high mobility group
HRP	horseradish peroxidase
HSP	heavy strand promoter
Ig	immunglobulin
IP	immunoprecipitation
J	Joule
K ⁺	potassium (Kalium)
KCl	potassium chloride (Kalium)
KO	knockout
KOH	potassium hydroxide
kb(p)	kilo base

kDa	kilodalton
l	liter
LB	<i>lysogeny broth</i>
LC- MS/MS	liquid chromatography mass spectrometry
LiCl	lithium chloride
loxP	<i>locus of crossover x in P1</i>
LRPPRC	leucine rich pentatricopeptide repeat-containing protein
LSP	light strand promoter
µg	microgram
µl	microliter
µm	micrometer
M	molar
MELAS	mitochondrial encephalomyopathy, lactic acidosis and stroke-like episodes
mg	milligram
Mg ²⁺	magnesium
MgCl ₂	magnesium chloride
Min	minute(s)
mRNA	<i>messenger RNA</i>
miRNA	<i>micro RNA</i>
ml	milliliter
MS	mass spectrometry
mtDNA	mitochondrial DNA
MTS	mitochondrial targeting sequence
MTERF1-4	mitochondrial transcription termination factor 1-4
mtPAP	mitochondrial polyA polymerase
mV	millivolt
n	number of experiments
Na ⁺	sodium (Natrium)
NaAc	sodium acetate
NaCl	sodium chloride
NAD	nicotinamide adenine dinucleotide
ND5	NADH dehydrogenase 5
ng	nanogram
nl	nanoliter
NLS	nuclear localization signal

nm	nanometer
NTD	N-terminal domain
N-terminus	amino terminus of a polypeptide chain
OD	optical density
o/n	overnight
p.A.	<i>pro analysi</i>
PA	paraformaldehyde
pAMI	vector containing the entire mouse mtDNA genome cloned in pACYC177 vector
PAGE	polyacrylamide gel electrophoresis
PBS	phosphate buffered saline
PCR	polymerase chain reaction
pH-value	hydrogen ion concentration
POLRMT	mitochondrial RNA polymerase
ppm	<i>parts per million</i>
PVDF	polyvinylidene fluoride
rb	rabbit
RNA	ribonucleic acid
RNase	ribonuclease
ROS	reactive oxygen species
RT	reverse transcription
RT-PCR	reverse transcriptase - polymerase chain reaction
s	second(s)
SD	standard deviation
SDS	sodium dodecylsulfate
SEM	standard error of the mean
SLIRP	SRA stem-loop interacting RNA-binding protein
SSC	saline sodium citrate
t	time
tRNA	transfer RNA
T	temperature
TAS	termination associated sequence
TAE	tris-acetate-EDTA-buffer
TBE	tris-borate-EDTA-buffer
TCA	trichloroacetic acid
TE	tris-EDTA
TEMED	N,N,N',N'-tetramethylethylenediamine

Table of abbreviations

TFAM	mitochondrial transcription factor A
TFB2M	mitochondrial transcription factor B2
Tris	2-amino-2-(hydroxymethyl)1,3-propanediol
U	unit
UTP	uridine triphosphate
UTR	untranslated region
V	voltage
W	Watt
wt	wild type

One-letter-code and three-letter-code of aminoacids:

A	Ala	Alanine
R	Arg	Arginine
N	Asn	Asparagine
D	Asp	Aspartic acid
C	Cys	Cysteine
E	Glu	Glutamic acid
Q	Gln	Glutamine
G	Gly	Glycine
H	His	Histidine
I	Ile	Isoleucine
L	Leu	Leucine
K	Lys	Lysine
M	Met	Methionine
F	Phe	Phenylalanine
P	Pro	Proline
S	Ser	Serine
T	Thr	Threonine
W	Trp	Tryptophan
Y	Tyr	Tyrosine
V	Val	Valine

II. Zusammenfassung

In nahezu allen eukaryotischen Zellen sind Mitochondrien die wichtigsten Zellorganellen für die Bereitstellung von Energie in Form von ATP. Neben der Energieproduktion spielen Mitochondrien auch eine wichtige Rolle in der Kalziumhomöostase, Apoptose oder der β -Oxidierung von Fettsäuren. Auf Grund ihrer Abstammung von Protobakterien besitzen diese Organellen ihre eigene DNA, die für einige mitochondriale OXPHOS Untereinheiten kodiert, aber auch die Information für tRNAs und rRNAs trägt, welche wichtige Komponenten der mitochondrialen Translationsmaschinerie darstellen. Die regulatorische Expression mitochondrialer DNA ist daher unverzichtbar für eine normal funktionierende Atmungskette. Mitochondriale Fehlfunktionen sind oftmals die Ursache für neurodegenerative Krankheiten, Krebs oder Diabetes und werden außerdem mit dem Alterungsprozess in Verbindung gebracht.

Erkenntnisse aus *in vitro* Studien führten über viele Jahrzehnte zu der Annahme, dass die Transkription der beiden ribosomalen RNAs auf dem schweren mitochondrialen DNA-Strang durch das Protein Mitochondrial transcription factor 1 (MTERF1) reguliert wird, indem es gleichzeitig mit der Promotorregion und seiner Bindestelle interagiert. Diese Studien wurden jedoch nie in einem Tiermodell bestätigt. In der vorliegenden Arbeit wird zum ersten Mal beschrieben, dass sich das Fehlen von MTERF1 in einem Mausmodell nicht auf ribosomale RNA-Level auswirkt. Stattdessen wurden erhöhte RNA-Level auf dem „antisense“ Strang der ribosomalen RNA, und gleichzeitig eine verminderte Promotoraktivität auf dem selben DNA-Strang beobachtet. Diese Daten lassen eine Rolle von MTERF1 in der Transkriptionstermination des leichten DNA-Strangs vermuten, um eine negative Beeinflussung der Transkriptionsmaschinerie auf den Promotor des leichten DNA – Strangs zu verhindern.

Studien in Mäusen defizient für MTERF2 ergeben gesunde und fruchtbare Tiere mit einer normalen Lebenserwartung. Die Behandlung dieser Mäuse mit einer ketogenen Diät führt allerdings zu einem muskelspezifischen Phänotyp, der mit einer verminderten Transkriptionsrate und defizienter oxidativer Phosphorylierung in den Mitochondrien einhergeht. Ein zweites in unserem Labor kreierte *Mterf2* knockout Mausmodell kann diese Beobachtungen jedoch nicht bestätigen. Sogenannte „viral traps“, wie sie auch bei der Produktion einer der *Mterf2* knockout Mausmodelle benutzt wurden, besitzen sehr starke Promotoren, die die Genexpression in unmittelbarer Umgebung des Zielgens beeinflussen können. Das Gen, das für das Protein chryptochrome 1 (CRY1) kodiert befindet sich nur 1,6 kb vom *Mterf2* Gen entfernt und seine Expression könnte von einem viral trap im *Mterf2* Gen negative beeinflusst werden. Dies könnte der Grund für die unterschiedlichen Phänotypen beider *Mterf2* knockout Mausmodelle sein. Zur Verifizierung dieser Hypothese wurden die

beiden *Mterf2* knockout Maus Modelle, *Cry1* knockout Mäuse und wildtyp Mäuse mittels molekularer Analysen direkt miteinander verglichen. Alle Mausmodelle weisen normale mitochondriale DNA Level, und unveränderte Transkriptionsraten und Proteinlevel von Untereinheiten des OXPHOS Systems auf, was eine Rolle von MTERF2 in mitochondrialer Transkription sehr unwahrscheinlich macht. Die eigentliche Funktion dieses Proteins *in vivo* ist jedoch immer noch unbekannt.

Ein wichtiger Faktor der posttranskriptionalen Regulation ist das leucine-rich pentatricopeptide repeat domain containing protein (LRPPRC). Trotz eindeutiger Erkenntnisse aus einem *Lrpprc* knockout Mausmodell, die eine Rolle von LRPPRC in der Stabilisierung mitochondrialer mRNAs, sowie der Koordination der Translation unterstützen, ist die *in vivo* Funktion dieses Proteins immer noch umstritten. So beschreibt eine kürzlich publizierte Studie LRPPRC als mitochondrialen Transkriptionsfaktor, der direkt mit dem Enzym POLRMT interagiert. Um die Funktion von LRPPRC unter physiologischen Bedingungen näher zu untersuchen stellten wir „bacterial artificial chromosome“ (BAC) transgene Mäuse her, die dieses Protein leicht überexprimieren und ebenso *Lrpprc* heterozygote Mäuse mit leicht reduzierten LRPPRC Proteinmengen. Moderat erhöhte oder verminderte LRPPRC protein Level wirkten sich nicht auf mitochondriale Transkriptlevel oder die absolute Transkriptionsaktivität in Mitochondrien aus, was eine Rolle von LRPPRC als mitochondrialen Transkriptionsfaktor sehr unwahrscheinlich macht. Desweiteren führte die Zugabe von rekombinantem LRPPRC zu einer *in vitro* Transkriptionsreaktion nicht zu einer Stimulation der Transkription, und Immunpräzipitationsexperimente sowie Gel permeations chromatographische Untersuchungen konnten keine Interaktion zwischen LRPPRC und POLRMT nachweisen.

III. Abstract

Mitochondria are the most important organelles for ATP supply in nearly all eukaryotic cells. Besides energy production, mitochondria also play important roles e.g. in calcium homeostasis, apoptosis or fatty acid β -oxidation. They originated from a proto-bacterium and therefore contain their own genome encoding for a subset of mitochondrial OXPHOS components as well as tRNAs and rRNAs necessary for the translation machinery. Regulation of mtDNA expression is indispensable for normal OXPHOS function and defective mitochondrial function can cause neurodegenerative diseases but is also linked to aging, cancer and diabetes.

Mitochondrial transcription factor 1 (MTERF1) has been reported to regulate H-strand transcription of the two ribosomal RNA genes through simultaneous binding of the heavy strand promoter and its termination site based on extensive *in vitro* studies during the last decades. However, evidence for its function *in vivo* is still missing. In this work, analysis of the first *Mterf1* knockout mouse model reveals that lack of MTERF1 has no effect on ribosomal RNA levels, but instead causes increased RNA levels on the antisense region of mitochondrial rRNAs. At the same time transcription initiation events are decreased at the light-strand promoter suggesting that MTERF1 has a role in transcription termination on the L-strand to prevent transcriptional interference at the light-strand promoter.

Studies in mice lacking the mitochondrial transcription termination factor 2 (MTERF2) show apparently healthy and fertile animals with normal lifespan. However, mice challenged with a ketogenic diet have been reported to develop a muscle-specific phenotype including decreased transcription and OXPHOS deficiency. A second *Mterf2* knockout mouse model, created in our lab, however, does not confirm the reported phenotype. The viral trap, a genetic tool used to interrupt *Mterf2* gene expression in one of the mouse models, could explain the observed differences since it contains a very strong promoter, which can influence the expression of other genes closely located to the target gene. A gene encoding cryptochrome 1 (CRY1) is situated 1,6 kb downstream of *Mterf2* and could be influenced by a viral trap targeting the *Mterf2* gene. In order to test this hypothesis, we simultaneously analyzed the two *Mterf2* knockout mouse models, a *Cry1* knockout mouse and controls and found that all mice were healthy and fertile with a normal lifespan. MtDNA levels, mitochondrial transcription as well as steady state levels of OXPHOS protein components are unaffected in mice lacking *Mterf2* or *Cry1*, contradicting a role of MTERF2 in mitochondrial transcription. However, *Cry1* expression is decreased in both *Mterf2* knockout mouse models, which suggests a putative influence of *Cry1* expression when the *Mterf2* gene is targeted.

The leucine-rich pentatricopeptide repeat domain containing protein (LRPPRC) is an important factor of posttranscriptional regulation of mtDNA expression. Although data from a

Lrpprc knockout mouse model and patient fibroblasts carrying decreased LRPPRC protein levels support a role of LRPPRC in mitochondrial mRNA transcript stability and coordination of translation, its *in vivo* function is still highly debated in the literature. A recent report demonstrated that LRPPRC is involved in mitochondrial transcription initiation through direct interaction with POLRMT. In order to study this protein in a physiological environment we created bacterial artificial chromosome transgenic mice slightly overexpressing LRPPRC and *Lrpprc* heterozygous knockout mice with moderately decreased LRPPRC levels. Slightly increased or decreased LRPPRC protein levels did not affect steady state transcript levels as well as *de novo* transcription suggesting that LRPPRC does not have a role in mitochondrial transcription. In addition, increasing amounts of LRPPRC did not stimulate transcription in a recombinant *in vitro* system and immunoprecipitation as well as size exclusion chromatography did not detect any interaction between LRPPRC and POLRMT.

1 Introduction

The first time mitochondria were mentioned in literature was in 1857 when Rudolph Albert von Kölliker described them as granular cytoplasmic compartments in the mammalian cells. It took another forty years until Carl Benda first used the name mitochondria in 1898, a name originated from the Greek words *mitos* (thread) and *chondrion* (grain) ((Liesa et al., 2009), (Benda et al. 1898). According to the endosymbiotic theory, mitochondria originated from α -proteobacteria around 1.5 billion years ago (Gray, 1999; Lang et al., 1997). During evolution, an alphaproteobacteria was introduced into an *archaeobacterial* cell, and the resulting endosymbiotic event lead to the contemporary eukaryotic cell. (Martin, W. & Mentel, M.et. al, 2010)(Gray et al., 2001)) The details about this process and the nature of the host and the physiological capabilities of the mitochondrial endosymbiont are still being debated (Gray et al., 2001). Mitochondria, often named as “powerhouses of the cell”, are the major source of cellular ATP production, but they also have other important biological functions such as Ca^{2+} homeostasis, fatty acid β oxidation, cell cycle control, and apoptosis (Antico Arciuch et al., 2012; Eaton et al., 1996; Liu et al., 1996; Vandecasteele et al., 2001). Furthermore, mitochondrial dysfunction is implicated in severe diseases including cancer, diabetes, neurodegenerative diseases, and aging and typically (but not exclusively) affects tissues and organs with a high energy demand such as heart, brain or muscle (Wallace; Wallace and Fan, 2010).

Genetic defects affecting mitochondrial function can appear at several regulatory levels, affecting mitochondrial DNA (mtDNA), as well as the nuclear genes encoding proteins involved in regulation of mitochondrial replication, transcription, translation and respiratory chain assembly, which all can generate serious mitochondrial dysfunction leading to a wide range of mitochondrial diseases.

1.1 Structural organization and morphology of mammalian mitochondria

The mammalian mitochondria consist of two membranes defining four distinct compartments within the organelle: the outer membrane, the intermembrane space, the inner membrane, and the matrix, each of them having its specific function. A remnant from their bacterial origin, mitochondria contain their own DNA, RNA and protein synthesis capabilities, making them semiautonomous organelles (Whelan and Zuckerbraun, 2013). During the course of evolution most of the mitochondrial encoded genes have been lost, transferred to the nucleus, or replaced by nuclear encoded proteins (Adams and Palmer, 2003). A typical animal

mitochondrial genome maintains a subset of genes encoding 13 proteins, 22 tRNAs and two rRNAs, all essential for the biogenesis of the oxidative phosphorylation system located in the mitochondrial matrix (Larsson and Clayton, 1995; Wallace, 1992). The question why these particular genes have not been shifted to the nucleus has not been definitely answered yet, but one of the possible explanations could be that the high degree of hydrophobicity of the mitochondrially encoded proteins makes their import in the mitochondria impossible (Heijne, 1986). Another explanation could be that distribution of mitochondrial genes encoding respiratory chain subunits in nucleus and mitochondria is optimal for metabolic regulations of the oxidative phosphorylation system (Allen, 2003).

The rest of the mitochondrial proteome, including mitochondrial replication, transcription and translation components, as well as the major part of the subunits of the oxidative phosphorylation system, is encoded in the nucleus, translated in the cytoplasm and imported into mitochondria (Larsson and Clayton, 1995).

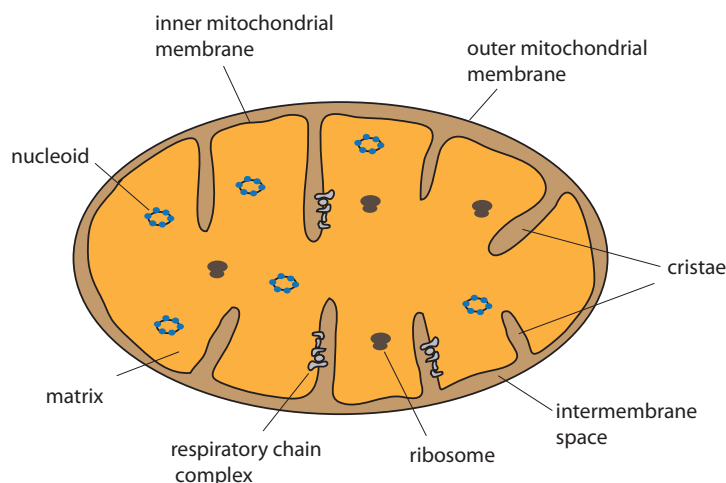


Figure 1.1: Schematic model of a mitochondrion.

The inner mitochondrial membrane is densely folded to form mitochondrial cristae structures, which provides a large surface to accommodate the oxidative phosphorylation system (Mannella et al., 1997; Perkins et al., 1997). There are five complexes (Complex I – Complex V) forming the oxidative phosphorylation system, whereas only three of them (Complex I, III and IV) transfer protons from the matrix into the intermembrane space in order to create a proton gradient between the intermembrane space and the matrix (Mitchell, 1961; Mourier and Larsson, 2011; Vafai and Mootha, 2012). Complex I and Complex II transfer electrons from NADH and FADH₂, respectively, to an electron carrier, coenzyme Q. Complex III receives electrons from reduced coenzyme Q and in turn forwards single electrons to cytochrome c. Complex IV, the last station for the electrons in the respiratory chain, accepts electrons from cytochrome c and uses them to reduce molecular oxygen to water. With the

exception of Complex II, the respiratory chain complexes couple electron transfer to the relocation of protons from the matrix to the intermembrane space, thus creating a proton gradient across the inner mitochondrial membrane (Mitchell, 1961). In the final step in oxidative phosphorylation, this membrane potential is to drive ATP synthesis by the F1FO-ATPase (Complex V) by allowing the protons to re-enter the mitochondrial matrix through this complex (Stock et al., 1999; Vafai and Mootha, 2012).

Importantly, shape and function of mammalian mitochondria cannot be subjected to a universal description as often seen in textbooks. Mitochondria form a dynamic network within the cell and also interact with other cellular organelles; they are migrating and constantly fusing and separating from each other in order to monitor, maintain and keep the system fully active by the exchange of organellar components (Nunnari et al., 1997) (Chen et al., 2007). In addition, the energy supply function of mitochondria can be highly tissue dependent. For example, while brain mitochondria preferentially oxidize ketones, mitochondria from skeletal muscle are specialized in fatty acid oxidation. Furthermore, cristae structure and mitochondrial content or size are tissue dependent and can be highly variable. Tissues with a higher energy demand, such as heart, tend to have mitochondria with a denser cristae structure (Vafai and Mootha, 2012).

Up to approximately 1500 mitochondrial proteins are known to be encoded by the nucleus and a subset of those interact with the 13 mitochondrial encoded proteins to form the oxidative phosphorylation system (Nunnari and Suomalainen, 2012; Pagliarini et al., 2008). The dependence of mitochondria on both nuclear and mitochondrial-encoded genes requires precise adjustment of regulatory mechanisms at many different levels, from replication and transcription to protein synthesis and assembly of respiratory chain complexes. Efficient communication between the nucleus and mitochondria is essential to maintain mitochondrial metabolism (Scarpulla, 2008).

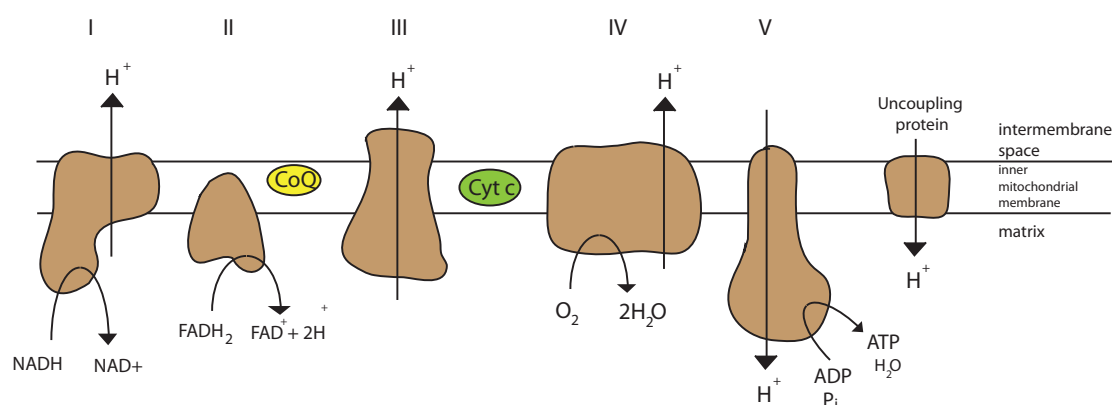


Figure 1.2: Schematic illustration of the five protein complexes constituting the mammalian oxidative phosphorylation system. Complex I-IV constitutes the respiratory chain. Modified from Mourier et al., PLoS Biol. 2011.

1.2 Mitochondria in aging and disease

Mitochondrial dysfunction can cause a broad range of multisystemic symptoms, such as diabetes, cardiomyopathy, deafness, retinal degeneration, dementia, ataxia, epilepsy, stroke and neuropathy, and is also implicated in the pathophysiology of several common diseases, e.g. Parkinson's disease (Larsson, 2010; Tuppen et al., 2010; Wallace). Mutations in mtDNA occur much more often than mutations in the nuclear DNA. Due to their involvement in a manifold range of metabolic signaling pathways, defective mitochondria (Nunnari and Suomalainen, 2012) can affect nearly every organ at any age (Nunnari and Suomalainen, 2012; Suomalainen, 2011). Mitochondrial malfunction can be caused by either point mutations or deletions of mitochondrial and/or nuclear DNA that affect the mitochondrial oxidative phosphorylation activity. MtDNA molecules carrying mutations or deletions can accumulate over time by the process of clonal expansion, due to the relaxed replication of mtDNA, which occurs independent from the cell cycle (Bogenhagen and Clayton, 1977). This leads to an apparently random distribution of mutated and non-mutated mtDNA molecules in different daughter cells, resulting in a mixture of normal and mutated mtDNA (heteroplasmy) with widely varying levels of mutated mtDNA in different cells of the same tissue. Cells from patients suffering from mitochondrial diseases are often heteroplasmic and the threshold at which mutated mtDNA induce respiratory chain deficiency differs depending on the type of mutation and can be ~90% for some tRNA mutations and ~60% for single large mtDNA deletions (Lagouge and Larsson, 2013). The proportion of wild type and mutated mtDNA molecules typically differs from cell to cell to result in a mosaic pattern of respiratory chain deficiency in the affected tissue (Stewart et al., 2008). The most common mitochondrial disorders are the Leigh syndrome, Kearns-Sayre syndrome (KSS) (Wallace, 1992), and Leber's Hereditary Optic Neuropathy (LHON) (Wallace et al., 1988), which all are neurodegenerative diseases.

Progressive accumulation of mtDNA mutations is not only causing a broad range of diseases, but is also occurring during the normal aging process. Many human diseases, e.g. cancer, type II diabetes, Alzheimer disease and Parkinson's disease are associated with aging and defective oxidative phosphorylation (Bender et al., 2006; Wallace, 2005). It is known that respiratory chain capacity as well as mtDNA copy number is decreasing with age in humans and mice. However, observed mitochondrial dysfunction in aged organisms does not automatically imply a causative role of mitochondria in the aging process, because this could also be a secondary effect of other degenerative processes.

Reactive oxygen species (ROS) have been considered to be the main culprit regarding the accumulation of mtDNA damage during aging (Fraga et al., 1990). Superoxide is primarily produced in complexes I and III of the respiratory chain, where it is considered as a

deleterious by-product formed during oxidative phosphorylation. Superoxide can be converted to hydrogen peroxide and a hydroxyl radical, which can cause oxidative damage to DNA, proteins and lipids. The so called “mitochondrial free radical theory of aging” claims that aging is the unavoidable outcome of a vicious cycle: mtDNA mutations cause respiratory chain deficiency leading to an increased ROS production, which in turn damages mtDNA as well as proteins and lipids (Miquel et al., 1980). The mtDNA mutator mouse was the first *in vivo* model, which provided evidence that accumulation of mtDNA mutations can lead to a premature aging phenotype, surprisingly without any major increase of ROS levels or oxidative damage (Trifunovic et al., 2004). In these mice the catalytic subunit of the mtDNA polymerase is defective in proofreading, which results in accumulation of mtDNA mutations and the production of an unusual linear, deleted mtDNA molecule. The mice display a range of phenotypes typically appearing during aging including greying of the hair, hearing loss, reduced fertility, weight loss and reduced life span (Kujoth et al., 2005; Trifunovic et al., 2004). In addition, mtDNA mutator mice suffer from severe oxidative phosphorylation deficiency, but interestingly no appreciable increase of ROS could be found in these mice (Trifunovic, 2005). In other studies, efforts to reduce ROS did not result in prolonged life span as expected according to the free radical theory of aging. ROS have also been proposed to function as signaling factors important for stress resistance and longevity, which suggests that increased ROS production initially has a protective role that induces cellular defenses (Hekimi et al., 2011; Lagouge and Larsson, 2013; Sena and Chandel, 2012). A role for mitochondrial dysfunction in aging is supported by many studies, but the idea that ROS is a driver of the ageing process is increasingly losing support (Hekimi et al., 2011; Viña et al., 2013). New methods capable of more accurate measurement of specific types of ROS levels as well as oxidative damage are needed to better understand the role of ROS in aging.

1.3 Structural organization of mammalian mitochondrial DNA

Mammalian mtDNA is a densely compacted molecule covered by many copies of the mitochondrial transcription factor A (TFAM) protein, which packages and bends mtDNA to mediate the formation of the nucleoid (Bogenhagen et al., 2008; Kukat et al., 2011). There are approximately 10^2 to 10^3 mtDNA molecules per mammalian cell, each being a circular, double stranded molecule of 16.6 kb in size. Due to a higher content of purines (guanosines and adenines) the heavy strand (H-strand), has a higher buoyant density in alkaline cesium chloride gradients than the light strand (L-strand), which is rich in pyrimidines (cytosines and thymidines) (Kasamatsu and Vinograd, 1974).

The H-strand encodes for most of the mitochondrial encoded mRNAs including cytochrome b (Cytb), NADH dehydrogenase 1 - 5 (ND1 - 5), cytochrome c oxidase I, II and III (COX I, II and III) and ATP synthase subunit 6 and 8 (ATP 6 and 8) (Larsson and Clayton, 1995). In addition, the H-strand encodes two ribosomal RNAs, 12S and 16S, and 14 tRNAs. According to the “tRNA punctuation model”, mRNAs are matured by processing the large polycistronic transcripts at the tRNAs and antisense tRNAs by specific enzymes (Ojala et al., 1981). However, this model cannot explain all processing of mRNAs as some of them do not contain flanking tRNAs at both ends, e.g. as seen in the junction of ATP6 and COXIII, as well as the junction between ND5 and the antisense ND6 sequence. There are two bicistronic mRNAs that are translated to generate two proteins (ATP8+ATP6 and ND4L+ND4) (Temperley et al., 2010). Both strands of mtDNA are transcribed as a single, almost genome-length transcript product and abundant precursor transcript products are found in mitochondria, including RNA19 (the 18S rRNA fused to the ND1 mRNA) and the Cytb-ND5 precursor (Rackham et al., 2011). It is unclear if these large RNA species are functional or if they represent RNA processing intermediates that will undergo processing. The remaining mitochondrial encoded RNAs, namely ND6 and 8 tRNAs, are encoded on the L-strand. ND6 is also unique as it encodes a large 3' UTR derived from the antisense ND5 sequence and as it lacks a polyA tail (Ruzzenente et al., 2012).

Mammalian mtDNA does not contain introns (Falkenberg et al., 2007; Taanman, 1998) and the only large non-coding region on the mammalian mtDNA molecule is the control region also called the displacement loop (D-loop) (Bogenhagen and Clayton, 1978). This region has obtained its name from an event occurring during initiation of replication of mtDNA, when a triple-stranded DNA structure containing a nascent H strand is formed. This region contains elements involved in regulation of mtDNA replication and transcription, such as the H- strand promoter (HSP), the L – strand promoter (LSP) and the origin for mtDNA replication of the H - strand (O_H). The origin of replication for the light strand (O_L) sits in a cluster of five tRNAs outside of the D-loop region (Falkenberg et al., 2007).

Additional functional sites present in the D-loop region are the conserved sequence blocks (CSB I - III) and the termination associated sequence (TAS), which are proposed to have roles in RNA primer formation and replication termination, respectively.

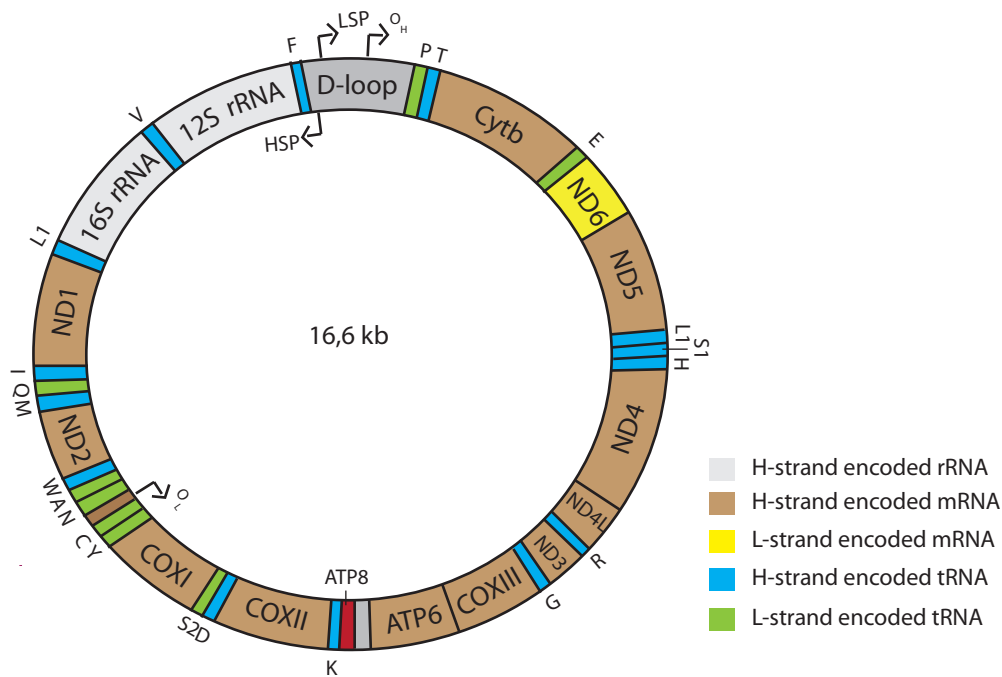


Figure 1.3: Schematic illustration of a mammalian mtDNA molecule. Mammalian mtDNA is a double-stranded circular molecule consisting of a heavy and a light strand. The molecule encodes 13 proteins, 2rRNAs and 22 tRNAs. Modified from Larsson, Annu. Rev. Biochem., 2010.

1.4 Transcription of mammalian mitochondrial DNA

MtDNA transcription plays a fundamental role in maintaining mitochondrial and cellular homeostasis, as all of the proteins encoded by mtDNA are essential components of the mitochondrial oxidative phosphorylation system. Some basic components of the mitochondrial transcription machinery were found in the mid-1980s, when experiments using purified mitochondrial extracts reconstituted mitochondrial transcription *in vitro* (Polosa et al., 2011). Mitochondrial transcription requires a core transcription machinery consisting of only three components RNA polymerase (POLRMT), mitochondrial transcription factor A (TFAM) and mitochondrial transcription factor B2 (TFB2M) (Falkenberg et al., 2002). The initiation of H-strand transcription is dependent on the HSP promoter and produces a large polycistronic precursor transcript encompassing nearly the entire mtDNA molecule. This precursor encodes 10 mRNAs, 2 rRNAs and 14 tRNAs which are subsequently processed into the single RNA species (Rossmannith and Karwan, 1998).

There are reports claiming the existence of a second HSP promoter (HSP2) that is located upstream of the tRNA^{Phe} gene. According to this model, HSP1 is responsible for the transcription of only the two ribosomal RNAs and their flanking tRNAs (tRNA^{Phe} and tRNA^{Val}), whereas HSP2 is producing a near genome length primary transcript. The existence

of the HSP1-dependent transcription unit was postulated to explain the 50- to 100-fold higher transcription rate of ribosomal RNAs compared to the genes transcribed from HSP2 (Gelfand and Attardi, 1981). In one study attempts to identify HSP2 activity in an *in vitro* system failed as POLRMT was not able to recognize HSP2 (Litonin et al., 2010), whereas two other studies report the reconstitution of transcription from HSP2 *in vitro* (Lodeiro et al., 2012; Zollo et al., 2012).

L- strand transcription initiated at the LSP promoter gives rise to a polycistronic transcript, which contains the gene for ND6 and eight tRNAs. In addition, a portion of LSP transcription is prematurely stopped and processed to obtain the 7S RNA primer necessary for replication.

1.4.1 The core machinery of mammalian mitochondrial transcription

1.4.1.1 Mitochondrial RNA polymerase

The enzyme catalyzing mammalian RNA transcription is the mitochondrial RNA polymerase (POLRMT). This protein is related to bacteriophage T7 single subunit RNA polymerases and consists of three different regions, the C-terminal domain (CTD), the N-terminal domain (NTD) and an N-terminal extension domain (NTE) (Arnold et al., 2012). The CTD of POLRMT shows the highest homology to its bacteriophage counterpart whereas the NTD exhibits only weak sequence similarity and NTE is even completely absent in the phage RNA polymerase. In contrast to its bacteriophage counterpart, POLRMT is not able to autonomously initiate transcription, but depends on the assistance of additional transcription factors (Arnold et al., 2012; Cermakian et al., 1997).

The CTD of POLRMT contains the catalytic domain of POLRMT responsible for nucleic acid template binding and catalyzing nucleotide incorporation (Arnold et al., 2012). X-ray crystal structure revealed a right hand shape of the CTD of human POLRMT containing “finger”, “palm “ and “thumb” subdomains (Ringel et al., 2011) involved in different functions such as nucleotide binding, substrate selection or interaction between enzyme and the DNA/RNA substrate (Ringel et al., 2011).

The finger subdomain of the CTD is defined by two characteristic structural elements, the O-helix, necessary for substrate selection, catalysis and translocation (Arnold et al., 2012) and the specificity loop, which is indispensable for promoter recognition in T7 RNA polymerases. Similarities of this region were also found in human POLRMT suggesting a homologous function of these structures.

The NTD of human POLRMT only shares weak sequence similarity with the phage RNA polymerase but has structural analogies such as β -hairpin and AT-rich recognition loop (Ringel et al., 2011), which are both partly interacting with the PPR domain of the NTE. In

T7 RNA polymerases, the AT-rich recognition loop mediates promoter recognition, whereas the β -hairpin helps to melt the promoter for initiation of transcription.

The N-terminal extension part is unique to mitochondrial RNA polymerases and has a huge diversity among animals, plants, fungi etc. The N-terminal domain contains a mitochondrial targeting sequence and two pentatricopeptide repeat (PPR) motifs, which are known to facilitate RNA-protein interactions (Lightowers and Chrzanowska-Lightowers, 2008; Small and Peeters, 2000). The motif contains nine α -helices of which four represent the PPR motifs. The function of the pentatricopeptide domain still remains to be elucidated.

After initiation of mitochondrial transcription, POLRMT catalyses nucleotide incorporation in the context of *de novo* RNA synthesis. This mechanism encompasses repeating cycles, consisting of four distinct steps including nucleotide binding, conformational change and translocation (Arnold et al., 2012). Due to its importance in mitochondrial transcription as well as mitochondrial replication mutations affecting POLRMT are expected to deep impact on the health of the organism.

1.4.1.2 Mitochondrial transcription factor A

TFAM is an essential multifunctional protein, which, besides its role in mitochondrial transcription initiation also has important roles in mtDNA packaging and maintenance. Due to its two high mobility group (HMG) box domains, TFAM belongs to the high mobility group (HMG) family, which is characterized by proteins being able to bind, unwind and package DNA (Parisi and Clayton, 1991). The HMG boxes enable TFAM to bind the minor DNA groove and bend mtDNA and a basic linker domain located between the two HMG boxes facilitates additional mtDNA contact sites (Gangelhoff et al., 2009; Ngo et al., 2011). The C-terminus of TFAM is reported to be essential for specific transcription initiation (Dairaghi et al., 1995).

It has been previously shown that TFAM covers mtDNA *in vivo* producing a discrete protein-mtDNA structure named the nucleoid (Kukat et al., 2011) and *in vitro* studies reported that TFAM alone is sufficient to package mtDNA, through DNA looping and supercoiling (Campbell et al., 2012).

Lack of TFAM in a knockout mouse model is embryonic lethal due to loss of mtDNA and abolished oxidative phosphorylation activity (Larsson et al., 1998). It was previously reported, that regulation of mtDNA copy number is directly connected to the TFAM protein levels. This was shown in a transgenic mouse model, where overexpression of human TFAM did not show altered mtDNA transcription activity or respiratory chain capacity, but increased

mtDNA copy number without affecting the endogenous TFAM expression in the mouse (Ekstrand et al., 2004).

Due to its HMG domains TFAM unspecifically binds DNA. During transcription initiation however, TFAM is known to preferentially interact with a region upstream of transcription initiation sites of HSP and LSP. The carboxy terminus of TFAM is essential for direct interactions with the other components of the transcription machinery, but not for its DNA binding properties in general (Dairaghi et al., 1995). At low concentrations, TFAM preferentially binds to the LSP, but as TFAM concentrations increase, transcription activity switches to HSP (HSP1) (Campbell et al., 2012). TFAM bound to the upstream promoter region of LSP has been reported to promote a U-turn like bending of mtDNA, facilitating a correct positioning of the TFAM carboxy-terminus for transcription initiation (Rubio-Cosials et al., 2011). X-ray diffraction studies revealed a bending angle about 180° when TFAM binds at the LSP (Campbell et al., 2012; Ngo et al., 2011), whereas non-specific DNA binding only reveals bend angles around 100° +/- 20°. The bending is thought to be important for mtDNA compaction (Kaufmann et al., 2007).

1.4.1.3 Mitochondrial transcription factor B2

The mitochondrial transcription factor B2 (TFB2M) as well as the paralogue mitochondrial transcription factor B1 (TFB1M) were thought to serve a similar function as the yeast transcription factor sc-mTFB. Although both proteins can activate transcription from a promoter containing DNA sequence in presence of TFAM and POLRMT *in vitro*, the efficiency of transcription activation of TFB1M is about 10 times lower compared to TFB2M (Falkenberg et al., 2002; McCulloch and Shadel, 2003). Besides their capability to bind DNA and to activate transcription, TFB1M and TFB2M also share sequence homology with the bacterial rRNA dimethyltransferases ((McCulloch and Shadel, 2003),(Falkenberg et al., 2002)). In fact, TFB1M is able to methylate two adenine residues in a conserved stem loop region of the 12S rRNA, which is an important post-transcriptional modification in the process of mitochondrial ribosomal biogenesis (Seidel-Rogol et al., 2003),(Metodieiev et al., 2009). It has been previously shown that missing dimethylation of 12S rRNA leads to abnormal assembly of ribosomal subunits in mitochondria. Therefore, TFB1M is thought to have its main function in ribosomal maturation rather than in transcriptional initiation (Metodieiev et al., 2009). This idea is consistent with the finding that overexpression of TFB1M does not promote mitochondrial transcription activation, whereas increased levels of TFB2M activates mitochondrial transcription and causes elevated steady-state levels of mitochondrial transcripts (Cotney et al., 2007) (Falkenberg et al., 2002)). Furthermore, TFB2M is reported to have a much higher transcriptional activity than TFB1M *in vitro*

(Falkenberg et al., 2002). In summary, TFB2M is indispensable for assisting in open complex formation during mitochondrial transcription initiation (Arnold et al., 2012; Sologub et al., 2009) and crosslink experiments revealed direct interaction of TFB2M with the promoter starting site, where it is involved in promoter melting to facilitate transcription initiation by POLRMT (Sologub et al., 2009).

1.4.2 Initiation of mammalian mitochondrial DNA transcription

The initial step for specific promoter recognition in mammalian mitochondria is mediated by TFAM binding at the specific start site upstream of the mitochondrial promoter region. With the help of its carboxy terminus domain TFAM covers an area between -14 and -35 upstream of the LSP (Litonin et al., 2010) and causes a U-turn like bend in the mtDNA conducted by partial unwinding of mtDNA to expose this area for recognition by the transcription machinery (Falkenberg et al., 2007; Gaspari et al., 2004). In order to initiate mitochondrial transcription, TFB2M forms a heterodimer with POLRMT being collectively recruited by TFAM to the transcription initiation site (Falkenberg et al., 2007). During this process TFB2M melts the promoter and stabilizes the open promoter complex by simultaneous binding of the RNA primer and mtDNA template (Sologub et al., 2009). Once recruited to the start site the specificity loop of POLRMT was found to interact with the promoter region in the major groove of mtDNA (Arnold et al., 2012). Then, TFAM and TFB2M dissociate from transcription initiation complex allow POLRMT to catalyze nucleotide incorporation in order to produce elongating RNA transcripts. Interestingly, it has been reported that POLRMT itself is not able to transcribe the entire mitochondrial genome (Smidansky et al., 2011) but rather depends on another mitochondrial protein TEFM (transcription elongation factor in mitochondria) (Minczuk et al., 2011). Knockdown of this protein leads to oxidative phosphorylation deficiency and decreased steady state transcript levels of promoter distal genes, supporting the idea, that POLRMT elongation capacity is limited and dependent on this additional protein (Minczuk et al., 2011).

Notably, transcription initiation in yeast doesn't require the yeast TFAM homologue Abf2. One can speculate that evolution of multicellular organisms required a more complex regulation of mtDNA transcription (Falkenberg et al., 2007).

1.4.3 Transcription termination in mammalian mitochondrial DNA

Mechanisms regarding mtDNA transcription termination in mammalian organisms are still poorly understood. Transcripts from HSP2 have been reported to encompass nearly the entire mitochondrial genome and to terminate in a region immediately upstream of the tRNA^{Phe}

gene, where a conserved A/T rich sequence motif has been detected (Camasamudram et al., 2003). Studies in a HeLa mtDNA transcription system revealed two uncharacterized proteins, which are supposed to bind in this area supporting transcriptional termination from HSP2 in a unidirectional manner (Camasamudram et al., 2003). However, further details about the termination mechanism and the nature of the two unknown proteins are needed for a complete understanding of this process.

The MTERF family in total comprises four proteins MTERF1 – MTERF4, which are all located in mitochondria and characterized through MTERF domains consisting of three α -helices, which are separated by loops (Roberti et al., 2009; Spähr et al., 2010). MTERF proteins have been identified in metazoans and plants, but not in fungi (Roberti et al., 2009). MTERF1 and MTERFF2-like protein are found in vertebrates, echinoderms and flies, whereas MTERF3 and MTERF4 are more broadly distributed in animals, and are thought to be the ancestral MTERF family members (Roberti et al., 2009). Despite being denoted as transcription termination factors, MTERF family members appear to hold a diversified functional spectrum influencing mtDNA expression at different levels.

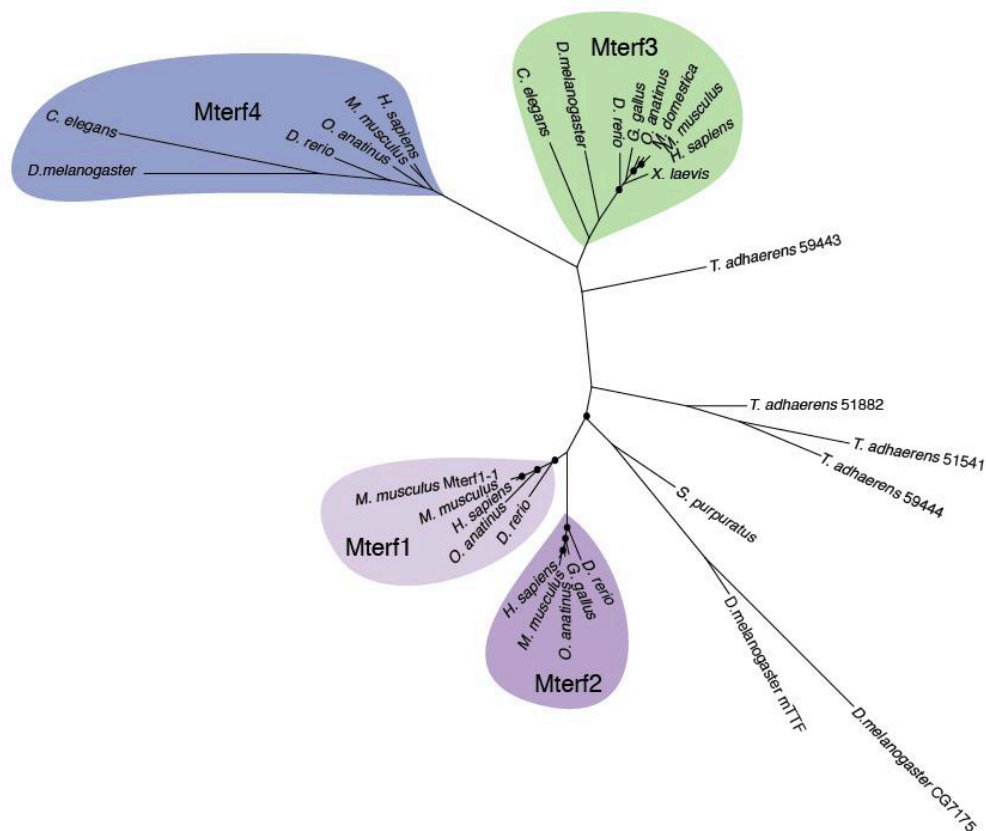


Figure 1.4: Phylogenetic tree of the MTERF family proteins. Illustrated by Bianca Habermann.

1.4.3.1 Mitochondrial transcription termination factor 1

Termination of transcripts initiated at the HSP1 promoter are proposed to be mediated by the DNA binding protein, mitochondrial transcription termination factor 1 (MTERF1) (Fernandez-Silva and Attardi, 1997). MTERF1 is the first identified member of the MTERF protein family and strongly binds within 28 bp in the tRNA^{Leu} region, where it is thought to block transcription of the ribosomal RNAs and their flanking tRNA^{Phe} and tRNA^{Val} (Roberti et al., 2006a). *In vitro* experiments have shown that MTERF1 promotes transcription termination in a bidirectional way, with an even higher termination efficiency of transcripts coming from the L-strand direction (Asin-Cayuela et al., 2005). Besides its function as transcriptional terminator, MTERF1 was also reported to be involved in HSP1 transcription activation by simultaneous binding at its termination site and a region in the HSP1. This binding is reported to result in a loop formation of the intermediate located rDNA (Martin et al., 2005) suggesting increased transcriptional efficiency through the direct delivery of POLRMT from the termination to the HSP1 transcription initiation site (Roberti et al., 2009). This hypothesis has been suggested to explain the finding that transcripts originating from the HSP1 are found to be more than 50-times more abundant compared to transcription from HSP2. Another study implicates MTERF1 in mitochondrial replication since a newly identified MTERF1-binding site in the non-coding region was associated with replication pausing and the strength of pausing was modulated by the expression level of MTERF1 (Hyvarinen et al., 2007). However, all of the data mentioned above arose from *in vitro* experiments and experiments regarding the function of MTERF1 *in vivo* is still lacking.

In patients carrying a A3243G mutation in the tRNA^{Leu(UUR)} region, which causes mitochondrial myopathy, encephalopathy, lactic acidosis and stroke-like episodes (MELAS) syndrome, MTERF1 is not able to interact with its binding site (Hess et al., 1991). Interestingly, molecular characterization of the patients does not support a role of MTERF1 in mitochondrial transcription termination in the disease pathology, but suggests the defect in translation being responsible for the clinical manifestations due to the abolished function of tRNA^{Leu(UUR)} (Chomyn et al., 1992).

Recently the atomic structure of MTERF1 bound to dsDNA has been solved with a clear definition of the binding mechanism to its specific binding sequence on mtDNA. MTERF1 holds a half-doughnut like shape and binds DNA as a monomer covering a 20 bp region (Yakubovskaya et al., 2010). The MTERF1 protein contains eight MTERF motifs, consisting of two α -helices separated by a hydrophobic core (Yakubovskaya et al., 2010). Due to a positively charged path it can wrap around the DNA and bind along the major groove, causing slight bending and a partial unwinding of the mtDNA. During this process the central

DNA part is affected by eversion of three nucleotides, promoting a firm sequence specific anchorage on mtDNA (Terzioglu et al., 2013; Yakubovskaya et al., 2010), supporting a function of MTERF1 as mitochondrial transcription termination factor. Moreover, a high resolution crystal structure proposes more interacting residues of *Mterf1* with the mitochondrial L-strand than the H-strand supporting a more effective termination activity on the L-strand (Yakubovskaya et al., 2010).

1.4.3.2 Mitochondrial transcription termination factor 2

MTERF2 has been demonstrated to be a component of the mitochondrial nucleoid with a relatively high abundance in the cell (Pellegrini et al., 2009). A recent *in vivo* study has reported MTERF2 being an important factor of mitochondrial transcription initiation (Wenz et al., 2009). Lack of *Mterf2* in a knockout mouse model did not cause any apparent phenotype. However, after feeding the mice with a ketogenic diet, decreased steady state levels of mitochondrial transcripts involving impaired oxidative phosphorylation activity have been observed specifically in muscle. A ketogenic diet is a high fat, low carbohydrate diet particularly challenging the mitochondrial metabolism by shifting it from glycolysis to oxidative phosphorylation (Kennedy et al., 2007). In addition, mRNA levels of MTERF1 and MTERF3 were reported to be upregulated in the absence of MTERF2. As a result, a model has been hypothesized in which MTERF2 binds to the HSP promoter region together with MTERF1 and MTERF3 and regulates mitochondrial transcription (Wenz et al., 2009). Notably, the knockout strategy chosen for the *Mterf2* knockout mouse model named “gene trap technology” is known to potentially affect genes, which are closely located to the target gene (Yamaguchi et al., 2012). Gene traps contain very strong promoters, which easily influence the activity of promoters in close proximity causing an additional unintended interruption or induction (Floss and Schnütgen, 2008; Springer, 2000). For this reason, the exact function of MTERF2 still remains unclear and further studies are needed to provide insights into its *in vivo* role.

1.4.3.3 Mitochondrial transcription termination factor 3

For a long time MTERF3 was considered as negative regulator of mitochondrial transcription termination. Due to embryonic lethality caused by the whole body knockout, conditional knockout mice specifically lacking MTERF3 in heart and skeletal muscle have been created and analysed (Park et al., 2007). Massively increased steady state transcript levels of most mitochondrial encoded genes and increased mitochondrial *de novo* transcription supported a role of MTERF3 as negative regulator of mitochondrial transcription (Park et al., 2007). However, a more detailed analysis regarding the *in vivo* function of MTERF3, supported by utilization of data from *Drosophila melanogaster Mterf3* knockout and knockdown flies,

revealed a novel unexpected function of this protein. Wredenberg et al could demonstrate, that MTERF3 binds 16S rRNA to promote the assembly of the large ribosomal subunit and at the same time assure proper translation. This function is conserved in the fly as well as in the mouse (Wredenberg et al., 2013).

1.4.3.4 Mitochondrial transcription termination factor 4

The last remaining member of the MTERF family is MTERF4. This protein has been recently reported to form a heterodimer with the 5-methylcytosine methyltransferase NSUN4 and recruits this enzyme to the large ribosomal subunit, where it is suggested to modify 16S rRNA to regulate mitochondrial ribosomal biogenesis and translation (Cámara et al., 2011). The MTERF4 is essential for embryonic development and therefore molecular analyses of conditional knockout mice with loss of this protein in heart and skeletal muscle revealed massive increase of mtDNA transcript levels, impaired translation and defective ribosomal assembly (Cámara et al., 2011). The atomic structure of MTERF4 is similar to the one of MTERF1 and MTERF3 already described above representing a half-doughnut shape, with a positively charged surface for nucleic acid interaction (Cámara et al., 2011).

1.4.4 Posttranscriptional modifications in mammalian mitochondria

1.4.4.1 Posttranscriptional tRNA modifications

Mammalian mitochondrial mRNAs are generated by processing and subsequent maturation of large polycistronic precursors synthesized by POLRMT. Despite their common derivation mitochondrial mRNAs, rRNAs and tRNAs can show distinct individual variations, illustrating the highly important function of post-transcriptional modifications (Mercer et al., 2011). An essential step after precursor transcription in mitochondria is the processing into individual RNA species. The “tRNA punctuation model”, which implies the co-transcriptional formation of cloverleaf structures of mitochondrial tRNA sequences, defines important tRNA processing sites on the mitochondrial precursor (Ojala et al., 1981). The main endonucleases involved in precursor maturation are RNase Z (ELAC2) and RNase P that are supposed to have recognition sites for the 3'-processing and the 5'-processing, respectively, and thus generate different processed RNA species in the mitochondria (Brzezniak et al., 2011; Holzmänn et al., 2008; Sanchez et al., 2011). RNase Z is encoded by the ELAC2 gene and exists in two isoforms including a version with the mitochondrial targeting sequence (MTS) located to mitochondria and a short version without MTS located in the nucleus (Brzezniak et al., 2011; Rossmannith, 2011). Mutations in the ELAC2 gene have been recently linked with hypertrophic cardiomyopathy, mitochondrial dysfunction (Haack et al., 2013) and prostate cancer (Tavtigian et al., 2001) and decreased levels of the mitochondrial RNase Z lead to defective 3' end processing of mitochondrial tRNAs as well as accumulation of mitochondrial

RNA precursor transcripts (Brzezniak et al., 2011). Furthermore, RNase Z is reported to interact with the pentatricopeptide repeat domain protein 1 (PTCD1), which is suggested to have a role in negative regulation of tRNA^{Leu (UUR)} and tRNA^{Leu (CUN)} 3' end maturation (Rackham et al., 2012).

The second enzyme known to be involved in tRNA maturation, RNase P, is responsible for tRNA 5' end processing. It is a multiple protein complex, consisting of mitochondrial RNase P protein 1 (MRPP1), MRPP2 and MRPP3 (Rossmannith, 2008). Whereas MRPP1 is believed to be involved in tRNA binding and methylation (Vilaro et al., 2012), MRPP2 seems to be required for RNase P activity and MRPP3 containing three PPR domains and a putative metallo-nuclease domain is required for mitochondrial tRNA binding and processing. Knockdown of RNase P subunits leads to increased mitochondrial precursor transcripts and consequently decreased levels of mature mRNAs and tRNAs (Holzmann and Rossmannith, 2009; Sanchez et al., 2011).

The subsequent step after cleavage of mitochondrial tRNAs is their maturation, which includes a multitude of tRNA modifications. Essential for tRNA maturation is the addition of a CCA triplet to their 3' end, which is required for amino acid coupling and binding of the aminoacyl-tRNA synthetase as well as the elongation factor Tu (Cusack, 1997; Levinger et al., 2004; Rackham et al., 2012). A second common modification is the pseudouridylation by the pseudouridylate synthase 1 (PUS1), whose absence was connected with mitochondrial myopathy and sideroblastic anemia (MLASA) if mutated (Bykhovskaya et al., 2004; Casas et al., 2004). Whereas the processes mentioned above are common for all mitochondrial tRNAs, there is also a broad spectrum of modifications specific for the function of individual tRNAs, as for example the 2-thiolation wobble modification mediated through the mitochondrial-specific 2-thiouridylase (MTU-1) in order to promote mitochondrial translation. The same function is held by mitochondrial translation optimization 1 homolog (MTO1) and mitochondrial GTP binding protein 3 (GTPBP3), which might be involved in 5-aurinomethyluridylation, another tRNA modification, found at the wobble position of tRNA^{Leu(UUR)} and tRNA^{Trp} (Li and Guan, 2002). Variations in the amount of tRNAs can have deep impact on the mitochondrial metabolism and further identification of tRNA modifying enzymes will broaden our understanding of regulation of mitochondrial gene expression.

1.4.4.2 Posttranscriptional rRNA modifications

Besides tRNAs, the mitochondrial ribosomal RNAs also undergo various modifications. However, very little is known so far about the enzymes involved in this process in mammalian mitochondria. Mitochondrial ribosomes consist of two subunits, the 28S small subunit and the 39S large subunit containing a 12S rRNA and a 16S rRNA, respectively (O'Brien, 1971). To date, studies of hamster cells have revealed that five nucleotides in the

rRNA of the small ribosomal subunit are modified (Dubin, 1974). All modifications are conserved in humans, but there are only two rRNA modifying enzymes yet identified in mammalian mitochondria being responsible for two of these five modifications. The N6-dimethylation of two highly conserved adenines m⁶₂A⁹³⁶ and m⁶₂A⁹³⁷ is mediated by TFB1M and dimethylation of these adenines is performed by an *S*-adenosylmethionine-dependent MTase domain (Falkenberg et al., 2002; McCulloch and Shadel, 2003). This process is shown to be required for full assembly of the 55S mitochondrial ribosome, as lack of TFB1M in a conditional knockout mouse model results in abolished formation of the small ribosomal subunit (Metodieiev et al., 2009). The enzymes responsible for the remaining modifications still await identification (Rorbach and Minczuk, 2012).

According to previous studies four modifications have been found in the 16S rRNA and to date just two methyltransferases are known to migrate with the large subunit: NSUN4/MTERF4 (Cámara et al., 2011) and RNMTL1 (Lee et al., 2013). While RNMTL1 was recently found to be responsible for the methylation at position Gm₁₃₇₀ the complex NSUN4/MTERF4 does not have a defined substrate yet since it belongs to the m5c methyltransferases and in 16S there are no known modifications of this kind. However, there is a putative m5c modification site in the 12S rRNA and it is speculated that NSUN4/MTERF4, while interacting with the large subunit, could methylate 12S rRNA in the small subunit mediating the contact between the two subunits. Nevertheless *in vivo* evidence for this model is still missing. Two putative methyltransferases of the 16S rRNA, MRM1 and MRM2, have been recently found to be possibly involved in methylation of uridyl 2'-O-ribose methylation at G₁₁₄₅ and U₁₃₆₉ respectively (Lee et al., 2013). However, *in vivo* evidence still remains to be presented.

1.4.4.3 Polyadenylation in mammalian mitochondria

The main maturation step for mitochondrial mRNAs after cleavage is 3'- polyadenylation mediated by the mitochondrial poly (A) polymerase (mtPAP) (Tomecki et al., 2004). Polyadenylation of mRNAs can have several functions, depending on the organism as well as the organelle. In bacteria and plants for example, polyadenylation of mitochondrial mRNAs mainly functions as degradation signal, since mature mRNAs are not polyadenylated at all (Chang and Tong, 2012). On the other hand, in trypanosomes polyadenylation in mitochondria occurs in connection with mRNA editing. Processed transcripts at all stages, from pre-edited and partially edited to fully edited, are stabilized through polyadenylation (Chang and Tong, 2012). In contrast, yeast mitochondrial mRNAs are not polyadenylated at all.

In the mammalian cytosol polyadenylation mainly ensures mRNA stability, export from the nucleus and initial support of transcription and translation, whereas in mammalian

mitochondria mRNA polyadenylation creates a functional stop codon for most of the mitochondrial mRNAs and likely also has other functions, which remain to be elucidated (Tomecki et al., 2004). The length of mammalian polyadenylated transcripts in mitochondria is markedly varying dependent on the cell type or the type of transcript. The ND6 transcript in mouse, for example, is not polyadenylated at all but encodes a large, non-coding 3' UTR.

The enzyme mediating polyadenylation in human mitochondria is the human mitochondrial poly A polymerase (human mt-PAP). Downregulation of mt-PAP causes substantially shortened poly(A) tails (Nagaike et al., 2005; Tomecki et al., 2004), confirming the idea that this enzyme is accountable for polyadenylation in human mitochondria. However, to date there is no consensus concerning the role of poly(A) extensions in the stability of mitochondrial mRNAs. Knockdown of human PAP revealed only partial degradation of some mitochondrial transcripts, whereas others were not affected. (Rorbach et al., 2011) Even though the role of mt-PAP is not well understood it has been shown that its function is essential for mitochondria since a mutation in the mt- PAP gene is associated to spastic ataxia (Crosby et al., 2010).

Notably, there is no mRNA detectable being completely free of adenine residues, when mt-PAP levels are reduced suggesting the existence of another, yet unidentified enzyme undertaking oligoadenylation (Crosby et al., 2010; Tomecki et al., 2004).

The polynucleotide phosphorylase (PNPase) is thought to be responsible for the degradation of mammalian mitochondrial mRNA transcripts, since the absence of this enzyme is reported to increase poly (A) tail length (Nagaike et al., 2005). However, its mitochondrial role is not solved completely, since this enzyme is supposed to be located in the inner mitochondrial membrane far away from mitochondrial mRNAs, which are located in the matrix.

In addition to PNPase another protein involved in the specific deadenylation of certain mitochondrial mRNAs was characterized. The enzyme PDE12 is believed to be responsible for deadenylation of only some specific mitochondrial RNAs. This enzyme is an exoribonuclease sharing sequence homologies with other RNA deadenylases (Rorbach et al., 2011). Its activity is suggested to affect only the stability of some mitochondrial transcripts, whereas steady state levels of other mRNAs remain normal, similar to the effect of PARN, described above. Notably, deadenylation of mitochondrial mRNAs was also shown to have negative affects on mitochondrial translation process (Rorbach et al., 2011) but its direct role in protein synthesis still remains to be elucidated.

1.4.5.1 The leucine-rich pentatricopeptide repeat motif - containing protein (LRPPRC)

LRPPRC is a 130 kDa, mitochondrial matrix protein featuring 22 PPR motifs. A recessive mutation creating an A354V amino acid substitution in the *Lrpprc* gene causes a neurodegenerative disease called Leigh syndrome French Canadian variant (LSFC) (Mootha et al., 2003). LSFC patients suffer from cytochrome c oxidase deficiency as well as reduced translational activity in mitochondria specifically in brain and liver (Merante et al., 1993; Xu et al., 2004). In addition, *in vitro* studies in cells from LSFC patients and cells where LRPPRC was knocked down revealed decreased mitochondrial mRNA levels suggesting a role in RNA stability (Sasarman et al., 2010).

These findings have been confirmed by studying mice with a conditional knockout of LRPPRC in heart and skeletal muscle, since homozygous knockout of LRPPRC in mice is embryonic lethal. The mice suffer from a strong decrease in cytochrome c oxidase activity, reduced mt-mRNA levels, polyadenylation and misregulated translation (Ruzzenente et al., 2012). It was also shown that LRPPRC plays an important role in stabilization of a non-translationally active mt-mRNA pool. Besides its suggested role in mRNA stabilization and polyadenylation, others have proposed that LRPPRC interact with POLRMT to activate mitochondrial transcription. Overexpression of LRPPRC in mouse liver has been reported to cause a compaction of cristae and stimulation of oxidative phosphorylation (Liu et al., 2011) and there are several publications within the last years describing a range of potential functions and interaction partners of LRPPRC (Ruzzenente et al., 2012; Sasarman et al., 2010). Cooper et al., for example, found LRPPRC in the nucleus, where it is supposed to bind PGC1-alpha and promote transcription of genes involved in gluconeogenesis (Cooper et al., 2006). Another report of this group describes a direct interaction of LRPPRC and POLRMT promoting mitochondrial transcription (Liu et al., 2011) or claiming an impact of varying LRPPRC levels on nuclear encoded mitochondrial proteins suggesting that varying mitochondrial RNA levels influence nuclear gene expression (Gohil et al., 2010), (Rackham and Filipovska, 2012). Furthermore there are data, suggesting that LRPPRC is a cytoplasmic translational activator that functions as a shuttling protein helping to export nuclear mRNAs to the cytosol (Topisirovic et al., 2009). However, the only commonly accepted binding partner of LRPPRC so far, is the SRA stem-loop interacting RNA binding protein (SLIRP). SLIRP is another mitochondrial RNA binding protein repressing transactivation of nuclear receptors, via SRA-binding (Hatchell et al., 2006). A recent mouse model lacking SLIRP reports this protein being important for spermatogenesis and sperm motility (Colley et al.,

2013). LRPPRC and SLIRP form a stable complex, which has been suggested to moderate mitochondrial RNA processing and stability (Sasarman et al., 2010)

Despite several reports about LRPPRC having a nuclear and cytoplasmic function, the main localization of this protein is in mitochondria (Sterky et al., 2010)

1.5 Projects

Regarding the regulatory processes coordinating mitochondrial and nuclear gene expression, potential regulatory events could take place at several levels, such as maintenance and replication of mtDNA (mtDNA), mtDNA transcription and mitochondrial translation as well as protein quality control. This work focuses on transcriptional regulation in mammalian mitochondria mediated by the MTERF family members MTERF1 and MTERF2 as well as on posttranscriptional regulation by LRPPRC.

Project I: To date MTERF1 has exclusively been studied *in vitro*, suggesting roles in H-strand transcription termination and mitochondrial replication, which all awaits confirmation in an *in vivo* model. In this work, the first *Mterf1* knockout mouse model is characterized, shedding the light on its role in a living organism.

Project II: A second member of the MTERF family, MTERF2, has recently been reported to have a role in transcription initiation. *Mterf2* knockout mice are claimed to develop decreased steady state transcript levels and impaired oxidative phosphorylation activity after treatment with a ketogenic diet for 6 months (Wenz et al., 2009). However, these results contradict existing data of our own *Mterf2* mouse model, which does not show any apparent phenotype even after exposing the mice to cold. A feasible explanation could be the different knockout strategies used to generate these animals. In contrast to homologous recombination, the gene trap technique often comprises strong viral promoters making it prone to disturb the expression of genes located close to the target gene. A gene encoding the mouse cryptochrome 1 (CRY1) is located in close proximity to the *Mterf2* gene and a gene trap in the latter position therefore increases the possibility of an unintended *Mterf2/Cry1* double knockout mouse model. In order to test this hypothesis and gain new insights in the *in vivo* function of MTERF2, we performed comparative molecular characterization of the two distinct generated *Mterf2* knockout mouse models and a mouse model lacking CRY1.

Project III: LRPPRC is an RNA-binding protein, which stabilizes mitochondrial mRNAs, promotes mitochondrial mRNA polyadenylation and coordinates mitochondrial translation as already discussed above. However, recent studies have suggested that LRPPRC may have additional roles in mitochondrial transcription by directly interacting with POLRMT to stimulate mitochondrial transcription (Liu et al., 2011). In this work we examined *Lrpprc* heterozygous knockout mice with moderately decreased LRPPRC expression as well as

Lrpprc overexpressor mice with moderately increased LRPPRC expression mediated by an artificial bacterial chromosome (BAC). The only slightly increased or decreased LRPPRC protein levels in both mouse models allowed us to study this protein under physiological conditions giving us the opportunity to gain novel insights in its *in vivo* function and to provide certainty concerning its role in mitochondrial RNA metabolism.

2 Material and Methods

2.1 Material

Used chemicals were ordered from Ambion, AppliChem, Fisher Scientific, Fluka, Merck KGaA, Roth, Sigma Aldrich and VWR. Enzymes and their according buffers were delivered from New England Biolabs. Transfer of nucleic acids was done on Amersham Hybond-N+ nylon (GE Healthcare) membranes from. Protein transfer was performed on Hybond- C extra (GE Healthcare) nitrocellulose membranes or Hybond-P PVDF (GE Healthcare) membranes. Radioactivity (^{32}P) to label nucleic acids was used from Perkin Elmer. Autoradiography was performed by using Amersham Hyperfilm MP (GE Healthcare) and ECL solutions were bought from Biorad. Protein samples for Western Blots were loaded on Invitrogen or Criterion gels from Biorad. For Blue Native PAGE experiments Invitrogen gels were used.

2.1.1 Antibodies

2.1.1.1 Commercial antibodies

The following primary antibodies were used:

Name	species	company
Complex I (NDUFA9 subunit)	mouse	Invitrogen
Complex II (SDHA subunit)	mouse	Invitrogen
Complex IV (COXI and COX3 subunits)	mouse	Invitrogen
Complex V (ATP5A1)	mouse	Invitrogen
MitoProfile total oxidative phosphorylation mixture	mouse	Mitosciences
Porin	mouse	Mitosciences
Anti FLAG	mouse	Sigma
POLRMT	rabbit	Abcam
SLIRP	rabbit	Abcam
Cryptochrome 1	mouse	Abcam

2.1.1.2 In-house generated antibodies

Name	Host
LRPPRC	rabbit
TFAM	rabbit
POLRMT	rabbit
TFB2M	rabbit
MTERF2	rabbit

2.1.1.3 Secondary antibodies

The following secondary antibodies were all purchased at GE Healthcare:

HRP-conjugated sheep anti mouse IgG

HRP-conjugated donkey anti rabbit IgG

HRP-conjugated goat anti rat IgG

2.1.2 Oligomers

All oligomers were customized and ordered at eurofins.

Primers used for genotyping:

LRP forward	5'- GGA GAA CAG GCC GCA TCA CAA- 3'
LRP reverse	5'- GTA ACC CCA CCC CCT TAT GT- 3'
LSFC forward	5'-AAA TTT GTT TCT CTT TGG ACT TAT TAG TTT-3'
LSFC reverse	5'- TTA TAA TAC TTA TGT GAA GAA CAC AGT GGA -3'
MTERF1 loxp forward	5'-GAT CTG TTA GCC TCA AGC TG-3'
MTERF1 loxP reverse	5'-ATG GGT ATT GCT TCA TTG TC-3'
MTERF1 KO forward	5'-GTT TAG TTT GCG AGA GGT TG-3'
MTERF1 KO reverse	5'-ATG GGT ATT GCT TCA TTG TC-3'
MTERF2 KO forward	5'- CCT TGC CAG CTT AAA TTG - 3'
MTERF2 KO reverse	5'- CTG CAG ATA ATC GCT TCC- 3'
DII mCry1	5'- TGA ATG AAC TGC AGG ACG AG -3'
ex5 V2 mCry1	5'- CAG GAG GAG AAA CTG ACG CAC T -3'
ex7 mCry1	5'- GTG TCT GGC TAA ATG GTG G - 3'

Primers used for amplification of mouse LRPPRC cDNA:

mLRP forward	5'- AAA CAT ATG CCA CCA TGG CCA TCG TTG CTG AG – 3'
mLRP reverse	5' - TTT GCG GCC GCT GAA GGG CTT TCC CT – 3'

2.1.3 Plasmids

The following constructs were used for generation of radiolabeled probes and were made without exception in the department of Prof. Nils Göran Larsson:

pCR2.1-*cox1*
 pCR2.1-*cytb*
 pCR2.1-12s
 pCR2.1-18s
 pCR2.1-*nd1*
 pCR–Blunt-II-*nd5*
 pCR–Blunt-II -*nd6*
 pCR–Blunt-II -16s

Plasmid used for expression of recombinant LRPPRC in E.coli:

pET-20(+)-*Lrpprc*

2.1.4 Taqman probes

The following probes were purchased at Life technologies

Species	Gene symbol	Gene Name	Reporter Dye
mouse	beta-actin	Actb	FAM
mouse	B2M	beta2-microglobulin	FAM
mouse	MMT-Cox1	mt cytochrome c oxidase	FAM
mouse	MMT-Cytb	mt cytochrome c	FAM
mouse	MMT-ND1	NADH dehydrogenase 1	FAM
mouse	MMT-ND5	mt NADH dehydrogenase 5	FAM
mouse	MMT-ND6	mt NADH dehydrogenase 6	FAM
mouse	MMT-12s	12s rRNA	FAM
mouse	MMT-7s	7s rRNA	FAM

mouse	Mterf4	MTERF4	FAM
mouse	Mterf3	MTERF3	FAM
mouse	Mterf2	MTERF2	FAM
mouse	Mterf1	MTERF1	FAM
mouse	LRP130	LRPPRC	FAM
mouse	16s	16s rRNA	FAM
mouse	SLIRP	SLIRP	FAM
mouse	Tfam	TFAM	FAM
mouse	Tfb2m	TFB2M	FAM
mouse	Tfb1m	TFB1M	FAM
mouse	PGC-1 alpha	PGC-1 alpha	FAM
mouse	Polrmt	POLRMT	FAM
mouse	POLG	POLG	FAM
mouse	Cry1	cryptochrome 1	FAM

2.2 Transgenic mouse models

2.2.1 Generation of LRPPRC (wt) BAC TG 505 mice

We got the whole mouse *Lrpprc* gene in a BAC clone of 241 kb (RP24-100M10), which was obtained from Children's Hospital Oakland-BAC-PAC Resources. To be able to distinguish between endogenous *Lrpprc* gene expression and the induced BAC clone, the BAC was modified by ET recombination. We introduced a silent mutation in exon 3, which eliminated a BglIII site, but did not alter the encoded amino acid. The modified BAC was purified by cesium chloride gradient centrifugation and injected into the pronuclei of fertilized oocytes. Founder mice holding the correct genotype (+/BAC-LRPPRC) were verified by PCR and restriction enzyme analysis of genomic DNA to proof loss of the BglIII site in the *Lrpprc* gene. Mice were maintained on an inbred C57BL6/N background.

2.2.1.1 Genotyping of LRPPRC (wt) BAC TG 505 mice

Tail DNA from offspring was genotyped for presence of the BAC transgene by analyzing 100 ng tail DNA with the GoTaq (Promega) PCR reaction kit according to the manufacturers instruction by adding forward primer (5'-AAA TTT GTT TCT CTT TGG ACT TAT TAG TTT-3') and reverse primer (5'- TTA TAA TAC TTA TGT GAA GAA CAC AGT GGA - 3'), 0.5 pmol each, for PCR with an initial denaturation for 3 min at 95°C, followed by 35 cycles with 30 sec at 95°C, 30 sec at 53°C and 45 sec at 73°C. The reaction was ended with extension for 5 min at 72°C. Afterwards samples were digested with Bgl II in NEB Buffer 3 (Biolabs) for 2 hrs at 37°C and then analyzed on a 1.8 % agarosegel at 135V for 45 min. Wildtype bands appear at 97 bp and 404 bp. Bands indicating the BAC transgene run at 500 bp.

2.2.2 Generation of LRPPRC heterozygous knockout mice

Isogenic 129R1 DNA was used for creation of a targeting vector for disruption of *Lrpprc* in embryonic stem cells (ESCs). A cDNA probe containing a partial region of the *Lrpprc* gene was used to identify a genomic clone containing the *Lrpprc* gene in a 129Sv RPCI-22M BAC library (Invitrogen). We cloned a 14-kb BAC fragment, containing exons 2–10 into a pBluescript II SK J vector (Stratagene) using ET recombination to generate pBS-LRPPRC. Next, we modified the pDELBOY-3X plasmid, containing a loxP sequence and an Frt-PGK-neomycin-Frt cassette, by introduction of MluI and BamHI sites in the XhoI site and an MluI site in the KpnI site. With these modifications we were able to remove the loxP sequence and

the Frt-PGK-neo-Frt cassette by performing MluI digestion, which was inserted into an MluI site of pBS-LRPPRC to create the plasmid pBS-LRPPRC-Neo. Subsequently, we removed a fragment comprising a loxP sequence and a KpnI restriction site from the pST7 plasmid and inserted it into the PacI site of the pBS-LRPPRC-Neo plasmid to create the targeting vector pBS-LRPPRC-TV. In summary, in this vector, a Frt-PGK-neomycin-Frt cassette and a loxP site were present between exons 2 and 3, whereas a second loxP site was present between exons 5 and 6. The targeting vector was linearized by NotI digestion, transformed into 129R1 cells and ESC clones were selected with gentamycin and analyzed by Southern blotting. In total, 196 ESC clones were analyzed by KpnI digestion and only two clones were identified where homologous recombination took place. Afterwards, chimeras were generated by blastocyst injection and we found germline transmission in both clones. Mating of *Lrpprc*^{+loxP-neo} mice with transgenic mice ubiquitously expressing Flp recombinase allowed us to remove the PGK- Neomycin cassette. The resulting *Lrpprc*^{+ /loxP} mice were mated with mice ubiquitously expressing cre recombinase to generate heterozygous knockout *Lrpprc*^{+/-} mice.

2.2.2.1 Genotyping of LRPPRC heterozygous knockout mice

100 ng tail DNA from offspring was used in a GoTaq (Promega) PCR reaction with the following primers: forward (5'- GGA GAA CAG GCC GCA TCA CAA- 3') reverse (5'- GTA ACC CCA CCC CCT TAT GT- 3') 0.5 pmol each. The PCR reaction was as described in the manufacturer's recommendation with an initial denaturation for 3 min at 95°C, followed by 35 cycles with 30 sec at 95°C, 30 sec at 60°C and 35 sec at 72°C. The reaction was ended with an extension for 5 min at 72°C. Samples were loaded on a 1.3% agarose gel and ran at 135V, 45min. A band at 280 bp indicated the knockout. No band was amplified in the wild type.

2.2.3 Generation of *Mterfl* knockout mice

CDNA probes containing the genes for *Mterfla* and *Mterflb* were used to identify a bacterial artificial clone (BAC) containing these genes in a 129Sv RPCI-22M BAC library (Invitrogen). We used a 12.4 kb EcoRI fragment containing all exons of *Mterfla* to clone it into pBluescript II SK+ (Stratagene) and generate pBS-T1a. Next, a loxP site in the intron following exon 2 was introduced in pBS-T1a using the PacI site for insertion of an oligonucleotide, thus creating the plasmid pBS-T1aLoxP. In the following, the Frt-PGK-neo-Frt-loxP cassette (Frt site-flanked neomycin resistance gene with an adjacent loxP site) was inserted into the KpnI site of pBS-T1aLoxP. To create the final *Mterfla* targeting vector (pBS-T1aKO), a KpnI fragment containing the Frt-PGK-neo-Frt-loxP cassette was cut from a

modified pDELBOY-3X plasmid containing a KpnI site introduced into the XhoI site. To create a double knockout of both actively transcribed *Mterfl* genes, a 13.6 kb KpnI fragment containing all exons of the *Mterflb* gene was cloned into pBluescript II SK+ (Stratagene) to generate pBS-T1b. Exon 2 of *Mterflb* was replaced by a hygromycin resistance cassette using a SfiI/SpeI site to create pBS-T1bKO.

Afterwards, embryonic stem cells were transfected with pBS-T1bKO and genomic DNA was isolated and digested with SacI. In total 145 clones were analyzed using Southern Blotting and one specifically targeted clone was found. Finally, pBS-T1aKO was used to transfect ESCs where *Mterflb* already had been targeted, and *Mterfla*-targeted ESC clones were identified by Southern blot analysis.

2.2.3.1 Genotyping of *Mterfl* knockout mice

Tail DNA from offsprings was extracted by following the DNA extraction protocol as described in section 2.4.2.1. Genotyping was done by using 100 ng DNA of tail DNA in a 20 μ l PCR reaction mix with GoTaq (Promega) PCR reaction kit according to the manufacturers instructions. The PCR reaction was performed with two sets of primers in order to distinguish floxed, wild type and knockout alleles. For floxed and wild type alleles the following primer sequences; lox^P forward (5'- GATCTGTTAGCCTCAAGCTG -3') and lox^P reverse (5'- ATGGGTATTGCTTCATTGTC -3'), with 0.5 pmol each were used in the PCR reaction with an initial denaturation for at 94°C for 5 min, followed by 30 cycles at 94°C with 30 sec, 60°C with 30 sec and 72°C for 30 sec. The reaction was ended with extension at 72°C for 5 min. The amplified bands were then analyzed on a 1.2 % agarose gel by distinguishing the wild type bands at 447 bp and floxed alleles at 547 bp. In order to define *Mterfla/Mterflb* double knockout, a second PCR for knockout allele was performed by using T1KO forward (5'- GTTTAGTTTGCGAGAGGTTG-3') and T1KO reverse (5'- ATGGGTATTGCTTCATTGTC-3') primer set with 0,5 pmol each in a 20 μ l PCR reaction mix followed by a PCR reaction with an initial denaturation at 94°C for 5 min, followed by 30 cycles at 94°C for 30 sec, 60°C for 30 sec, and 72°C for 45 sec with final extension at 72°C for 5 min. Amplified PCR products were then checked on a 1.2 % agarose gel to distinguish the wild type allele (no band amplification) from knockout allele, amplification at the size of 709bp.

2.2.4 Generation of *Mterf2* knockout mice

To generate the targeting vector, we identified a bacterial artificial chromosome (BAC) clone containing the *Mterf2* gene in a 129Sv RPCI-22M BAC library (Invitrogen) by using a cDNA probe. To construct the *Mterf2* targeting vector, a 12.5 kb NcoI fragment containing all exons of *Mterf2* was cloned into pBluescript II SK+ (Stratagene). The *Mterf2* gene sequence data was obtained from Celera in 2002. At that time, the targeting construct indicated an exon of mCG13745 on the antisense strand embedded in exon 3 of the *Mterf2* gene. Due to this coincidence, the targeting strategy of *Mterf2* gene has been changed. Instead of adding loxP sites to the active exon, site directed mutagenesis was performed to introduce mutations. The NsiI-BsrGI fragment was subcloned into pBS SKII+ and by site directed mutagenesis two mutations were introduced, one creating a premature STOP codon and the other a frameshift. The NsiI-BsrGI fragment containing the right mutations was cloned back into the right homology arm. On the 5 prime end of the targeting vector a 4.5 kb PacI-FseI homology arm was placed. The final targeting vector now contained a PacI-FseI homology arm-FRT-tkNEO-FRT-KpnI-NotI exon 3 with mutations.

The *Mterf2*-targeting vector was used to transfect ES cells and genomic DNA was isolated and digested with NheI. Digested DNA was transferred to nylon membranes by Southern blotting and probed with exon3 mCG13745 as a probe. Four specifically targeted clones were found among a total of 91 analyzed ES cell clones.

2.2.4.1 Genotyping of *Mterf2* knockout mice

100 ng tail DNA from offspring was used in a GoTaq (Promega) PCR reaction with the following primers: MTERF2 forward (5'- CCT TGC CAG CTT AAA TTG - 3') MTERF2 reverse (5'- CTG CAG ATA ATC GCT TCC- 3') 0,5 pmol each. The PCR reaction was as described in the manufacturers recommendation with an initial denaturation for 5 min at 94°C, followed by 35 cycles with 30 sec at 94°C, 45 sec at 55°C and 45 sec at 72°C. The reaction was ended with an extension for 5 min at 72°C. To distinguish wild type from knockout samples, PCR products were digested with HindIII in a total volume of 20µl for 2-3 hours at 37°C. Finally, samples were loaded on a 2% agarose gel and ran at 135V, 45min. A band at 500 bp indicated wild type, a band at 250 bp indicated *Mterf2* knockout.

2.2.5 Generation of *Cry1* knockout mice

Cry1 knockout mice were kindly provided from Dr E.H. Jacobs from the Erasmus University Medical Center, Department of Genetics in the workgroup Circadian Rhythms and Neuropsychiatric Disorders, Rotterdam

2.2.5.1 Genotyping of *CryI* knockout mice

Tail DNA from offsprings was extracted by following the DNA extraction protocol as described in section 2.4.2.1. Genotyping was done by using 100 ng DNA of tail DNA in a 20 μ l PCR reaction mix with GoTaq (Promega) PCR reaction kit according to the manufacturers instructions. The PCR reaction was performed with three different primers in order to distinguish wild type and knockout alleles. The following primer sequences were used: DII *Cry1* (5'- TGA ATG AAC TGC AGG ACG AG -3') ex5 V2 *Cry1* (5'- CAG GAG GAG AAA CTG ACG CAC T -3') and ex7 *Cry1* (5'- GTG TCT GGC TAA ATG GTG G - 3'), with 0.5 pmol each were used in the PCR reaction with an initial denaturation for at 94°C for 3 min, followed by 30 cycles at 94°C with 30 sec, 63°C with 60 sec and 72°C with 60 sec. The reaction was ended with extension at 72°C for 10 min. The amplified bands were then analyzed on a 0.8 – 1% % agarose gel by distinguishing the wild type bands at 1600 bp and knockout bands at 2200 bp.

2.3 Bacterial cells

2.3.1 Transformation of chemically competent cells

One shot® TOP 10 chemically competent bacteria (Invitrogen) were thawed on ice and supplied with 5ng plasmid DNA. The sample was mixed by flicking it several times followed by 30 min incubation on ice. A heat-shock at 42°C for 30 sec. and a 10 min incubation on ice allowed the DNA to enter the bacteria. Afterwards, 200 μ l S.O.C. media (Invitrogen) were added and bacteria were incubated at 37°C and 700 rpm for 30-60 min. Bacteria were plated on agar plates which contained 100 μ g/ml ampicillin to select for positively transformed clones. Agar plates were incubated o/n at 37°C.

LB (<i>lysogeny broth</i>)-media
10 g/l Tryptone
5 g/l yeast extract
10 g/l potassium chloride
15 g/l Agar-Agar

2.3.2 Overnight culture of bacterial cells

Bacterial colonies grown on an agar plate were picked with a sterile tip and transferred in 2-5ml LB-media containing an appropriate antibiotic. The culture was shaking overnight at 37°C. Next, bacteria were spinned down at 6.000x g, 5min, RT and kept at -20°C or used for DNA isolation.

2.4 Methods in molecular biology

2.4.1 Plasmid preparation

2ml (mini prep), 25ml (midi prep) or 100ml (maxi prep) of bacterial overnight culture supplied with an appropriate antibiotic were pelleted at 6.000 x g, 15 min at 4°C and DNA was isolated following the manufacturer's instruction for QIAGEN Plasmid Mini, Midi and Maxi Kits. In the final step DNA was dissolved in dH₂O and stored at -20°C.

2.4.2 DNA isolation from mouse tissue

2.4.2.1 Phenol chloroform extraction

A small piece of mouse tissue from heart, liver, brain, kidney, muscle or tail was incubated in 400 µl lysis solution supplied with 8µl proteinase K (10mg/ml) shaking at 55°C for 2-3 hrs, until the tissue was completely dissolved. Next, 75 µl of 8M potassium acetate and 0.5ml chloroform were added and the samples were vortexed for 10 sec. followed by incubation at -80 °C for at least 30min or o/n. Phase separation was achieved by centrifugation at maximum speed in a bench top centrifuge (Eppendorf). The upper (aqueous) phase was transferred to a new eppendorf tube and 1 ml 99% ethanol was added to each sample to precipitate the DNA. Tubes were inverted several times at room temperature and centrifuged at maximum speed in a benchtop centrifuge for 10min at RT. Pellets were rinsed with 0.5 ml 75% ethanol and spun for another 5 min at max speed. All residual ethanol was removed and the pellet was dissolved in an appropriate amount of dH₂O. For long term storage samples were stored at -20°C.

Lysis Buffer
0.5% sodium dodecyl sulfate
0.1 M NaCl
50mM Tris-HCl, pH8.0
2.4mM EDTA

2.4.2.2 Short protocol for DNA isolation from mouse tails

75µl of Buffer I were added to a mouse tail and incubated at 96°C, 1hr., shaking. Next, 75µl of Buffer II were added, samples were spinned down and stored at 4°C.

Buffer I (10X)	Buffer II (10X)
250mM NaOH	400mM Tris pH 7.5-8.0
2mM EDTA	

2.4.2.3 DNA extraction with DNeasy® Blood and tissue Kit (Qiagen)

For very pure DNA preparations a small piece of frozen tissue from mouse brain, heart, liver, kidney or muscle was cut into pieces and transferred into an eppendorf tube. Next, 180µl buffer ATL (Qiagen) and 20µl Proteinase K (Qiagen) were added and DNA was extracted following the manufacturer's instructions. DNA was kept at +4°C for short term and -20°C for long term storage.

2.4.2.4 DNA extraction with Puregene® Core Kit A (Qiagen)

A small piece of frozen tissue from mouse brain, heart, liver, kidney or muscle was grinded with mortar and pestle in liquid nitrogen. The frozen tissue powder was transferred into a new eppendorf tube and mixed with 300µl Cell lysis solution (Qiagen). DNA was extracted as recommended by the manufacturer and kept at +4°C for short term and -20°C for long term storage.

2.4.3 RNA isolation from mouse tissue

2.4.3.1 RNA isolation with ToTALLY RNA™ kit (Ambion)

A small piece of fresh or frozen tissue from mouse brain, heart, liver, kidney or muscle was extracted with Lysing Matrix D tubes from MP Bio and ToTALLY RNA™ kit from Ambion by following manufacturer's instructions. The final RNA pellet was dissolved in an appropriate amount of DEPC treated water at 50°C for 15 min. RNA was stored at -80°C.

2.4.3.2 RNA isolation with TRIzol® (Invitrogen)

A small piece of frozen tissue from mouse brain, heart, liver, kidney or muscle was grinded in liquid nitrogen using mortar and pestle. Next, 800µl TRIzol® were added to the still frozen sample and placed under the hood until it got liquid again. Samples were pipetted in a 2ml tube and homogenized by 20 strokes with a 23G syringe (BD Microlance). After incubation at RT for 5min, 200µl chloroform were added and mixed by vortexing, followed by another incubation at RT for 3 min. Phase separation was achieved by centrifugation of the samples at 15.000 x g at 4°C for 15 min. The upper aqueous phase was transferred into a new RNase-

free eppendorf tube and supplied with 500µl isopropanol. Next, samples were incubated at RT for 10 min, followed by a centrifugation at 15.000 x g at 4°C for 10 min. The pellet was washed with 1ml 70% ethanol at 15.000 x g at 4°C for 10 min and finally air-dried at 42°C in a heat block for 5-10 min. RNA pellet was dissolved in an appropriate volume of DEPC-treated water at 55°C for 15 min and stored at -80°C.

2.4.4 Quantification methods of nucleic acids

2.4.4.1 DNA/RNA quantification with nanodrop

DNA quantification was performed with NanoDrop 2000c (Thermo Scientific). 1µl of a DNA sample was placed on the pedestal and absorption was measured at 260nm. DH₂O was used as blank.

2.4.4.2 DNA quantification with Qubit® 1.0 fluorometer (Invitrogen)

DNA quantification with the Qubit® 1.0 fluorometer is based on intercalation of the reagent in double stranded DNA. For standard preparation 190µl working solution (Invitrogen) and 10µl Standard (Invitrogen) were vortexed and incubated at RT for 2 min. Sample preparation was performed by mixing 198µl working solution with 2µl DNA sample, vortexing and incubation at RT for 2 min. In the following, tubes were analysed in the Qubit® fluorometer (Invitrogen) according to the manufacturer's instructions.

2.4.5 DNA agarose gelelectrophoresis

For separation of DNA fragments, DNA samples were run on a 0.8%-1.8 % agarose gel, depending on size and number of the DNA fragments. 0.8-1.8 g agarose were mixed with 100ml 0.5 x TBE buffer and cooked in a microwave until the agarose got dissolved completely. Before the melted agarose was poured into a gel chamber, few microliter of ethidium bromide were added. After the gel was polymerized, DNA samples were loaded and run at 135 – 150 V. The gel was analysed in an UV imaging system (Syngene u:Genius).

1 x TBE
90mM Tris-Base
90mM H ₃ BO ₃
2.5 mM EDTA

2.4.6 Polymerase chain reaction

2.4.6.1 DNA amplification with GoTaq® DNA polymerase (Promega)

Amplification of DNA fragments was performed using PCR reactions. 50-200 ng DNA were used in a 20µl GoTaq® reaction (Promega) as recommended by the manufacturer using 0.2mM dNTPs and 0.5µl GoTag® polymerase in each reaction. If PCR product had to be digested 5x Green colorless GoTaq® Reaction Buffer instead of 5 x Green GoTaq® Reaction Buffer was used.

Standard thermal cycling conditions

Initial Denaturation:	95°C, 2 minutes
30 cycles	
Denaturation:	95°C, 30 sec
Annealing:	42–65°C (depending on the primer) 30 sec
Extension:	72°C, 2min
Final Extension:	72°C, 5 minutes
Soak:	4°C, forever

DNA products were analysed on 1.2% -1.8% agarose gels.

2.4.6.2 DNA amplification with Phusion® High Fidelity DNA polymerase

50-200ng DNA were applied in a 50µl Phusion® HF reaction (New England Biolabs) as recommended by the manufacturer's instructions using 1µl of each primer (final concentration 4µM).

Standard thermal cycling conditions

Initial Denaturation:	98°C, 30 seconds
30 cycles	
Denaturation:	98°C, 10 sec
Annealing:	45–72°C (depending on the primer) 30 sec
Extension:	72°C, 15-30 sec/kb
Final Extension:	72°C, 5 minutes
Soak:	4°C, forever

DNA products were analysed on 1.2% -1.8% agarose gels.

2.4.7 DNase treatment

To clear RNA samples from DNA, e.g. in correlation with reverse transcription, RNA samples (10µg/50µl) were mixed with 0.1 volumes of 10 x TURBO™ DNase buffer (Ambion) and 1µl TURBO™ DNase (Ambion) in a final volume of 50 µl and incubated at 37°C for 30 min. The reaction was inactivated by addition of 0.1 volumes DNase inactivation reagent (Ambion) and 5 min incubation at RT. Excess inactivation solution was pelleted at 10.000 x g for 1.5 min and the supernatant was transferred to a new RNase free eppendorf tube. If not used immediately for reverse transcription, RNA was stored at -80°C.

2.4.8 Reverse transcription

1-2µg of DNase treated RNA (see section 2.4.7) was dissolved in DEPC-water with a final volume of 10µl. Another 10µl of a reverse transcription mastermix containing 10 x RT buffer, 25 x dNTP mix, 10x random primers, reverse transcriptase, RNase inhibitor and nuclease-free H₂O as recommended in the manufacturer's instructions of the High capacity cDNA Reverse Transcription Kit (Applied Biosystems) RT reaction was performed in a thermocycler (Applied Biosystems) as recommended in the manufacturer's instructions. cDNA was stored at -20°C.

2.4.9 Quantitative polymerase chain reaction

2.4.9.1 Quantitative PCR using Taqman® Universal PCR master mix

Total RNA from mouse liver was extracted using the ToTALLY RNA™ kit (Ambion) (see section 2.4.3.1). Reverse transcription was performed using the High capacity cDNA Reverse Transcription Kit (Applied Biosystems) (see section 2.4.8). A small volume of each cDNA (5-10µl) was diluted 1:10 and 1µl of each cDNA, placed as triplicates, was pipetted in a 96- or 384- well plate. H₂O was used as control. In the following, a mastermix was prepared containing 12.5µl (4.8µl for 384-well plate) TaqMan® Universal PCR master mix (Invitrogen), 1.25µl (0.5µl for 384-well plate) probe and 10.25µl (3.7µl for 384-well plate) dH₂O per reaction. In case of 96- well plates 24 µl, in the case of 385-well plate 9µl mastermix were added to each cDNA. The plate was covered with a plastic film, shortly centrifuged and finally analyzed in a realtime PCR cycler (Applied Biosystems).

2.4.9.2 QPCR using a pipetting robot

To optimize pipetting accuracy especially for the performance of a 384-well plate qPCR, a pipetting robot (JANUS automated workstation, Perkin Elmer) was used. Mastermixes for each cDNA and probe were prepared in 1.5 ml eppendorf tubes as follows:

cDNA mastermix:

cDNA ($1\mu\text{l} \times 4$ (quadruplicates) \times number of primers $\times 1.3$ (pipetting error))

+

Taqman Mix ($5\mu\text{l} \times 4$ (quadruplicates) \times number of probes $\times 1.3$ (pipetting error))

Probe mastermix:

Taqman® probe ($0.5\mu\text{l} \times 4$ (quadruplicates) \times number of cDNAs $\times 1.3$ (pipetting error))

+

dH₂O ($3.5\mu\text{l} \times 4$ (quadruplicates) \times number of cDNAs $\times 1.3$ (pipetting error))

Tubes were placed in a JANUS automated workstation together with a 384-well plate and the robot was programmed to mix $6\mu\text{l}$ cDNA with $4\mu\text{l}$ probe mix by doing quadruplicates for every cDNA. Final analysis took place as described in section 2.4.8.

2.5 Methods in protein biochemistry

2.5.1 Recombinant proteins

2.5.1.1 Expression of human recombinant TFAM, TFB2M and LRPPRC

For mitochondrial *in vitro* transcription *Spodoptera frugiperda* (Sf9) cells were maintained and propagated in suspension in SFM 900 medium (Gibco-BRL) containing 5% fetal calf serum at 27 °C. Genes encoding human LRPPRC, TFB2M and TFAM (without leader peptide) were amplified from cDNAs by PCR, and cloned into the vector pBacPAK9 (Clontech). A 6×His tag had been introduced at the C terminus of all proteins. Autographa californica nuclear polyhedrosis viruses recombinant for the individual proteins were prepared as described in the BacPAK manual (Clontech). For protein expression, Sf9 cells were grown in suspension and collected 60–72 h after infection. Next, the infected cells were frozen in liquid nitrogen and thawed at 4 °C in lysis buffer containing 25 mM Tris-HCl (pH 8.0), 20 mM 2-mercaptoethanol, and 1× protease inhibitors (for all purifications the 100× stock of protease inhibitors contained 100 mM phenylmethylsulfonyl fluoride, 200 mM pepstatin A, 60 mM leupeptin and 200 mM benzamidine in 100% ethanol). After incubation on ice for 20 min, the cells were transferred to a Dounce homogenizer and lysed by 20 strokes of a tight-fitting pestle. After adding NaCl to a final concentration of 0.8 M, the homogenate was swirled gently for 40 min at 4 °C. The extract was cleared by centrifugation at 45,000 r.p.m. for 45 min at 4 °C using a Beckman TLA 100.3 rotor.

2.5.1.2 Expression of human recombinant POLRMT and mouse LRPPRC

Codon-optimized (DNA 2.0) DNAs encoding the mature form of mouse LRPPRC and human POLRMT fused to a 6xHis-tag at the N-terminus were cloned in the vector pJexpress 401 and heterologously expressed in Arctic express (DE3) cells (Stratagene) after induction with 0.2 mM isopropyl-1-thio-β-D-galactopyranoside at 16 °C for 20 hours.

2.5.1.3 Purification of human recombinant POLRMT

Extracts from cells were infected with 5 plaque-forming units (p.f.u.) of His-tagged POLRMT together with 5 p.f.u. of TFB2M. The extracts were supplemented with 10 mM imidazole and 2 ml of Ni²⁺-NTA matrix superflow (APBiotec) pre-equilibrated with buffer A were added. Next, we supplemented it with 10 mM imidazole and 0.3 M NaCl, and incubated it for 60 min at 4 °C with gentle rotation. His-POLRMT was further purified on a 1-ml HiTrap heparin

column (APBiotech) equilibrated in buffer B (0.1 M NaCl). After washing the column with three column volumes of buffer B (0.1 M NaCl), a linear gradient (10 ml) of buffer B (0.1–1 M) was used to elute the His-POLRMT protein at 0.8 M NaCl. The yield of His-POLRMT protein from 400 ml of culture was ~2 mg. The purity of the protein was estimated to be at least 95% by SDS–PAGE with Coomassie blue staining.

Buffer A
25 mM Tris-HCl (pH 8.0)
10% glycerol
20mM 2-mercaptoethanol
1M NaCl
Protease inhibitor

2.5.1.4 Purification of human recombinant TFB2M

His-TFB2M was purified by the method used for human recombinant His-POLRMT with the following modifications. Sf9 cells were infected with 10 p.f.u. of recombinant virus and TFB2M protein was eluted from the Hi-Trap Heparin column at 0.6 M NaCl.

2.5.1.5 Purification of human recombinant TFAM

TFAM was purified by the methods used for His-POLRMT with the following modifications. Sf9 cells were infected with 10 p.f.u. of recombinant virus. Dialyzed His-TFAM run from the Ni²⁺-NTA step through a Mono-Q column equilibrated with buffer B (0.1 M NaCl), and His-TFAM eluted in the flow through fractions. The yield of His-TFAM from 400 ml of culture was ~5 mg with a purity of at least 95%. All proteins were frozen in aliquots in liquid nitrogen and stored at –80 °C.

2.5.1.6 Purification of human recombinant LRPPRC

Human recombinant LRPPRC was purified over Ni²⁺-Agarose FF (Qiagen) as described before. LRPPRC was loaded on a 1 ml HiTrap Heparin column (Amersham Biosciences) equilibrated in buffer B containing 0.2 M NaCl. LRPPRC was eluted with a linear gradient (10 ml) of buffer B (0.2-1.2 M NaCl) and the peak fractions were diluted 3 times with buffer B (0 M NaCl), followed by further purification on a 1-ml Hi-Trap SP column (Amersham Biosciences) equilibrated in buffer B (0.2 M NaCl). After washing the column with three

column volumes of buffer B (0.2 M NaCl), LRPPRC was eluted with a linear gradient (10 ml) of buffer B (0.2-1.2 M NaCl) and the peak of protein eluted at 600 mM NaCl. The peak fractions were dialyzed against buffer B containing 0.2 M NaCl. The estimated purity of the purified LRPPRC was at least 95% as estimated from Coomassie blue stained SDS-PAGE gels.

Buffer B
20 mM Tris-HCl (pH 8.0)
0.5 mM EDTA (pH 8.0)
10% glycerol
1mM DTT

2.5.1.7 Purification of mouse recombinant POLRMT, TFB2M and TFAM

Recombinant proteins were purified to near homogeneity over Ni²⁺ - Agarose FF (Qiagen). The complexes were further purified on a 1 ml HiTrap Heparin column (Amersham Biosciences) equilibrated in buffer B (see section 2.5.1.6) (0.2 M NaCl) and a linear gradient (10 ml) of buffer B (0.2–1.2 M NaCl) was used as described above to elute the proteins.

2.5.1.8 Purification of mouse recombinant LRPPRC

LRPPRC was purified over a His-Select Ni₂⁺ (Sigma-Aldrich) resin and dialyzed against H-0.2 [25mM Tris-HCl (pH 7.8), 0.5mM EDTA, 10% (vol/vol) glycerol, 1 mM DTT, 200 mM NaCl] after the addition of tobaccoetch virus (TEV) protease at a 1:100 protease:protein ratio. Dialyzed LRPPRC was purified to homogeneity over a HiLoad 16/60 Superdex 200 pg gel-filtration column (GE Healthcare) in buffer H-0.2 lacking glycerol.

2.5.2 Protein quantification with Bradford

An undiluted or an 1:10 diluted protein solution as well as a BSA-standard curve (0.125, 0.25, 0.5, 1 and 2mg/ml BSA) were mixed with 1:50 with Bradford reagent (Sigma) and incubated at RT for 5-15 min. Samples were analysed in an Infinite® 200 PRO multimode reader (Tecan). Absorption was measured at 595nm.

2.5.3 Isolation of mitochondria from mouse tissue

Dissected heart, brain, muscle, liver or kidney from mouse was washed with mito isolation buffer, followed by homogenization on ice with a glass-teflon homogenizer (Sartorius, Potter S) in 10 ml (liver in 13 ml) mito isolation buffer 1X complete protease inhibitor cocktail (Roche) at 600rpm with 20 strokes. Next, the lysate was centrifuged for 10 min, at 1000xg, 4°C. The supernatant was transferred in a fresh, pre-cooled falcon tube and spinned for 10 min at 12.000 x g, 4°C. Mitochondria were washed with mito isolation buffer three times for 5 min at 12.000 x g, 4°C, before the pellet was resuspended in an appropriate volume of mito isolation buffer. For storage, mitochondria were frozen in liquid nitrogen and put into -80°C.

Mito isolation buffer
0.32M sucrose
1mM potassium EDTA
10mM Tris-HCl pH 7.4

2.5.4 SDS-Polyacrylamide gelelectrophoresis

2.5.4.1 Selfmade gels

For separation of proteins SDS-polyacrylamide gel electrophoresis was performed. For in organello translation experiments, protein samples were resuspended in 20µl 2 x gel loading dye (see 2.6.6) and pelleted at max. speed for 10 min. The gel was selfmade according to the following protocol:

17% Running gel	For 1 gel: 15ml
H ₂ O	5.325 ml
40 % Acrylamide/Bisacrylamide (29:1)	5.625 ml
1.5 M Tris/HCl, pH 8,8	3.75 ml
10 % SDS	150 µl
10 % APS (fresh made in H ₂ O)	150 µl
TEMED	6 µl

APS and TEMED were added immediately before pouring the gel to prevent precocious polymerization. A layer of 99% ethanol was pipetted on top of the running gel in order to have an even gel. After polymerization for 30min, a 5% stacking gel was added on top of the running gel, after removal of the ethanol:

5 % stacking gel	for 1 gel: 5 ml
H ₂ O	3.613 ml
40 % Acrylamide/Bisacrylamide (29:1)	0.637 ml
1,5 M Tris/HCl, pH 6.8	625 µl
10 % SDS	50 µl
10 % APS (fresh made in H ₂ O)	50 µl
TEMED	5 µl

APS and TEMED were added immediately before pouring the gel to prevent precocious polymerization. A 0.75 mm comb was placed in the stacking gel, which was removed after polymerization. Wells were washed with running buffer, before protein samples were loaded. Gel run at 100V, 10mA around 16 hrs.

2.5.4.2 Purchased gels

For western blotting and Blue native PAGE analysis the following customized gels were used:

Gel	Company
Criterion™ XT Bis-Tris Precast Gels 4-12%	Biorad
Criterion™ XT Bis-Tris Precast Gels 15%	Biorad
NuPAGE® Bis-Tris Precast Gels 4-12%	Invitrogen
NativePAGE™ Novex® 4-16% Bis-Tris Gels	Invitrogen

Gels run at 120V, 2 hrs (Biorad), 200V, 50 min (NuPAGE, Invitrogen) and 150V, 60min respectively. As a size marker prestained Spectra Multicolor Broad Range Protein Ladder (Generon) or Precision Plus Protein Dual Color Standards (Biorad) were used.

2.5.5 Gel drying

2.5.5.1 Gel drying using Hoefer Slab Gel Dryer

Polyacrylamide gels laying on filter paper were covered with clingfilm and placed in a Hoefer Slab Gel Dryer (Amersham Biosciences). A constantly active vacuum pump dehumidified the gel, whereas it was heated at 80°C for 1.5 hrs. Finally the clingfilm was removed from the gel and, if radioactive exposed to a phosphoimager screen.

2.5.5.2 Manual gel drying

Polyacrylamide gels were equilibrated in water for a minimum of 5 minutes to minimize gel cracking during drying. Next, the gel was placed between two sheets of cellophane that were pre-incubated in water using the GelAir Drying system from Biorad. All bubbles and wrinkles were removed and the gel was clamped between two frames and placed in one shelf of the GelAir dryer overnight to dry.

2.5.6 Western Blot

Isolated mitochondria, 20 µg, from heart, liver, kidney, brain and muscle were pelleted and resuspended in SDS Lämmli-Buffer. Samples were run on polyacrylamide gels (see section 5.5.4.2). and subsequently transferred to amersham nitrocellulose ECL membranes (GE Healthcare) using either the wet transfer system from Biorad or the semi-dry transfer system from Peqlab. For the wet transfer the criterion™ blotter system from Biorad was used. In a “sandwich-like” manner pre-wet sponges, four filter papers, the polyacrylamide gel and a nitrocellulose membrane were assembled in a gel holder cassette (Biorad) and blotted following the manufacturer's instructions at 80mA and 4°C, overnight. Using the semi-dry transfer, the same sandwich but without the sponges was made, everything pre-wet in transfer buffer and assembled in a peqlab semi dry blot following the manufacturer's recommendations. Next, the membrane was stained in Ponceau S, destained with TBS/T and blocked in 5% milk/TBS/T for 30 min at RT. Incubation with the primary antibody was performed either for two hours at RT or overnight at 4°C, depending on the quality of the antibody. Afterwards, the membrane was washed in TBS/T three times for 10 min and incubated with an appropriate secondary HRP-conjugated antibody for 1 hr at RT. After another washing series in TBS/T, three times for 10 min, the membrane was covered with a 1:1 ratio of the Immun-Star™ chemiluminescent substrate and enhancer (Biorad) for 2-3 min, followed by exposure to Amersham Hyperfilms (GE Healthcare).

SDS-Lämmli buffer (10 ml)		Ponceau S	Transfer buffer	10 x running buffer
0.5M Tris pH 6.8	1.6 ml	0.3 M acetic acid	Tris 12.1g	Tris base 30.3 g
10% SDS	4 ml	0.033 g Ponceau S	Glycine 72.3g	Glycine 144.1g
100% Glycerol	2 ml	40 ml dH ₂ O	fill up to 1L with dH ₂ O	SDS 10g
2-mercapto-ethanol	1 ml			fill up to 1L with dH ₂ O

bromphenol blue	2.5 mg			
H ₂ O	1.4 ml			

20x TBS

50mM Tris	121g
150mM NaCl	175g
dH ₂ O	up to 1L

2.5.7 Blue Native PAGE

To study the assembly of respiratory chain complexes Blue Native gel analyses was performed. Twenty µg of isolated mitochondria were pelleted and solubilized in cold 1 x NativePAGE Sample buffer (Invitrogen) containing 1% DDM. Proteins were incubated at 4°C for 15 min and pelleted at 20.000 x g for 30 min, 4°C. The supernatant was loaded on NativePAGE™ Novex® Bis-Tris gel and run at 150V for 60 min using NativePAGE™ Running buffer and NativePAGE™ Cathode buffer as described in the manufacturer's instructions. Later voltage was increased to 250 V for the remainder of the run. For blotting procedure see western blot section.

2.5.8 Immunoprecipitation

To analyze protein-protein interactions, 1mg human or mouse mitochondria with a concentration of 5µg/µl were incubated in lysis buffer B supplied with 1X complete protease inhibitor cocktail for 20 min on ice, followed by centrifugation at 13.000 x g for 45 min at 4°C. Next, the supernatant was incubated in 50µl ANTI-FLAG M2 affinity gel (Sigma) for 2hrs, at 4°C and protein partners were purified according to recommendations from the manufacturer (Sigma).

Lysis buffer B
50mM TrisHCl pH 7.4
1mM EDTA
150mM NaCl
5% glycerol
0,5 % TritonX

2.5.9 Size exclusion chromatography

Human mitochondria were isolated from HeLa cells by differential centrifugation in mito isolation buffer (see section 2.5.3) containing 1 x complete protease inhibitor cocktail (Roche). Mitochondria were lysed at a concentration of 5 mg/ml in lysis buffer B (see section 2.5.8) and 1X complete protease inhibitor cocktail for 20 min on ice followed by centrifugation at 13000xg for 45 min at 4°C. Next, 1 mg of the precleared lysate was subjected to size exclusion chromatography through Superose 6 column (GE Healthcare) in an ÄKTA chromatography system (GE Healthcare) which had been pre-equilibrated with lysis buffer B containing 0.05% TritonX. Fractions of 1 ml were collected, precipitated with TCA and analyzed by SDS-PAGE and immunoblotting.

2.5.10 Absolute quantification of recombinant proteins

Absolut quantification of mouse recombinant POLRMT, TFAM, TFB2M and LRPPRC without mitochondrial targeting sequence was performed by Xing Ping Li from the mass spectrometry facility of the Max Planck Institute for Biology of Ageing, Cologne. Standard curves with known protein concentrations were made for each of the recombinant proteins. Mitochondrial extracts from mouse liver were loaded each with one of the standards on a 4-15% Criterion™ precast gel (Biorad) and western Blots were performed as described before (see section 5.5.6) using antibodies against each recombinant protein. Molarity was calculated according to the molecular weight of the recombinant protein and its obtained concentration after comparison with the protein standard curve.

2.6 Methods handling radionucleotides

2.6.1 Radioactive probe labeling

2.6.1.1 Probe labelling with [α -³²P] dCTP using Prime-It® II Random Primer Labeling Kit (Agilent)

50 – 80 ng template DNA (1 μ l) were mixed with 10 μ l Random Primer Mix (Agilent) and 23 μ l dH₂O. reaction was heated for 5 min at 100°C, before addition of 10 μ l of 5 × dCTP primer buffer, 1 μ l Exo(-) Klenow enzyme (5 U/ μ l) and 5 μ l [α -³²P]dCTP at 3000 Ci/mmol (Perkin Elmer). Next, the reaction was incubated at 37°C for 30 min, to allow radioactive labelling of the oligonucleotides. Purification of the radiolabeled probe was performed in an illustra MicroSpin G-50 column (GE Healthcare) at 3000rpm for 2min. In the final step the radioactive oligonucleotides were cooked at 100°C for 5min, to melt the double strands. If not used immediately, probes were stored at -20°C.

2.6.1.2 Oligonucleotide labelling with [γ -³²P] ATP using T4-polynucleotide kinase

50 – 80 ng template DNA (1 μ l) were mixed with 12 μ l dH₂O, 2 μ l of 10 x polynucleotide kinase buffer (NEB), 1 μ l T4 polynucleotide kinase and 4 μ l [γ -³²P] ATP at 3000 Ci/mmol (Perkin Elmer). The reaction was heated at 37°C for 45 min, and subsequently purified in an illustra MicroSpin G-25 column (GE Healthcare) at 3000rpm for 2min. If not used immediately, probes were stored at -20°C.

2.6.1.3 RNA labeling using Riboprobe System T7 Kit (Promega)

20 μ g pCR-Blunt-II -*nd6* plasmid was digested with Spe I at 37°C, o/n. In the following, proteinase K treatment was performed in proteinase k buffer at 42°C for 1 hr. DNA was extracted by addition of 700 μ l phenol/chloroform and centrifuged at max. speed for 20 min. The upper, aqueous phase was transferred into a new eppendorf tube and mixed with an equal amount of chloroform. Phase separation was performed by centrifugation at max. speed for 15 min. Again the aqueous phase was taken and supplied with 40 μ l 3M NaAc pH5.2 and 1ml 99.5% EtOH. Sample was incubated at -80°C for 1-2 hrs. DNA was precipitated by centrifugation at max. speed for 20 min. Next. The pellet was washed with 70% EtOH for 10min, air-dried and resuspended in 40 μ l dH₂O. Subsequently, the DNA was used as template

for the Riboprobe in vitro transcription system (Promega). A transcription reaction containing of rNTPs, DTT, transcription buffer, RNasin ribonuclease inhibitor, linearized DNA template, [α -³²P] rCTP (50 μ Ci at 10 μ Ci/ μ l) and T7 polymerase was pipetted following the manufacturer's instructions and incubated at 37°C for 2hrs. After addition of DNase I and another incubation at 37°C for 15min, the probe was purified using a illustra MicroSpin G-50 column (GE Healthcare). If not used immediately, probes were stored at -20°C.

Proteinase k buffer
100 mM Tris
50mM EDTA
500mM NaCl
10% SDS
100 μ g/ml Proteinase K
490 μ l dH ₂ O

2.6.2 Measurement of radiation

For precise detection of ionizing radiation 1 μ l of the sample of interest was mixed with 10ml UltimaGold™ (Perkin Elmer) in small plastic containers and analysed in a Tri-Carb 2810 TR scintillation counter (Perkin Elmer) according to the manufacturer's instructions. For wipe test, the head of a cotton bud, that was wiped on 100cm² surface before was dropped into 10ml UltimaGold™ solution and handled as described above.

2.6.3 Northern blot analysis

2 μ g RNA from mouse brain, heart, liver, kidney or muscle were supplied with DEPC-water to a volume of 10 μ l. An equal volume of Glyoxal Sample Loading Dye (Ambion) was added and samples were heated at 55°C for 20 min. Next, RNA samples were loaded on an 1.4 % agarose gel containing formaldehyde and separated at 120V for appr. 2 hrs, until the blue front reached $\frac{3}{4}$ of the gel. Formaldehyde was removed from the gel by washing it in dH₂O three times for 15 min. Another 15 min incubation in 20 x SSC equilibrated the gel to the transfer buffer. Afterwards, RNA was transferred to a nylon membrane (Amersham Hybond™-N⁺) overnight, using 20 x SSC as transfer buffer. The membrane was activated in dH₂O for 15 min and equilibrated in 20 x SSC for 15 min before. Before hybridization with radiolabeled probes, the membrane was UV-crosslinked twice in an UVC 500 crosslinker, (Amersham Biosciences) at 200 mJ/cm². Pre-hybridization was performed by rotation of the

membrane in glass tubes in Amersham Rapid-Hyb Buffer (GE Healthcare) at 55 -65°C for 20 min. In the next step, a radiolabeled [α -³²P] dCTP probe was added to the hybridization buffer and incubated with the membrane for at least 2 hrs., rotating. To remove unbound radioactivity, the membrane was washed twice in 2 x SSC + 0.1% SDS, first at RT for 15 min, later at 55°C for 15 min. In the following, the membrane was welded and exposed to a phosphoimager screen for an appropriate time period depending on the radiation of the membrane. Finally the screen was analyzed and quantified in a phosphoimager (FujiFilm FLA-7000).

Agarose/Formaldehyde gel (100ml)		20 x SSC	
dH2O	72 ml	NaCl	175.3g
LE-Agarose (Ambion)	1,4 g	Sodium citrate	88.2 g
10 x NorthernMax MOPS (Ambion)	10 ml	dH2O	up to 1L
37% formaldehyde (Sigma)	18 ml		

2.6.3.1 Membrane stripping

To remove old radiolabeled oligonucleotides from the membrane, it was incubated for three times 15min, in boiling stripping solution. Afterwards the membrane was immediately used for another labelling or welded and stored at RT.

Stripping solution	400 ml
20 x SSC	1ml
0.5M EDTA	8ml
10% SDS	4ml
dH2O	387ml

2.6.4 Southern blot analysis

Genomic DNA from mouse heart, brain, liver, kidney and muscle was extracted and 10 μ g, DNA from mouse tissue were digested with SacI at 37°C overnight to linearize mtDNA. The next day an additional microliter SacI was added to the reaction and incubated 37°C for 2-3 hrs. DNA precipitation was performed by addition of 8 μ l 5M NaCl and 400 μ l 99.5% EtOH. Samples were mixed and incubated at -80°C for 2-3 hours, followed by a centrifugation for 30 min, RT at max. speed. The DNA pellet was washed with 70% EtOH for 20 min, RT, max. speed and afterwards air-dried. DNA was finally resuspended in 20 μ l TE-Buffer for 20 min at

65°C. Subsequently, 6 x Loading dye (Thermo Scientific) was added to the DNA samples which were finally loaded on a 0.6% agarose gel. Migration was performed o/n at 40V. The gel was shaking 5min in 250ml dH₂O plus 4ml HCl, followed by a series of washings in denaturation and neutralization buffer three times for 20 min each. Finally the gel was incubated in 20 x SSC for 20 min and blotted via wet transfer on a nylon membrane (Amersham HybondTM-N+) overnight using 20 x SSC as transfer buffer. In the following, the membrane was UV-crosslinked twice (UVC 500 crosslinker, Amersham Biosciences) at 200 mJ/cm² and pre-hybridized with 10ml Amersham Rapid-Hyb buffer (GE Healthcare) in rotation at 55°C. A radiolabeled plasmid (pAM1) containing cloned mouse mtDNA was used to detect mtDNA. A radiolabeled plasmid containing the nuclear encoded 18S rRNA gene was used to detect cytoplasmic 18S rRNA as a loading control. Probes were added to the hybridization buffer and incubated with the membrane for at least 2 hrs., rotating at 55°C. Membrane was stripped after each probe. In order to remove excess radioactivity, the membrane was washed twice in 2 x SSC + 0.1 % SDS after hybridization, first 15 min at RT, later 15 min at 55°C. To detect labeled mtDNA, the membrane was welded and exposed to a phosphoimager screen for an appropriate time period depending on the radiation of the membrane. Finally the screen was analyzed and quantified in a phosphoimager (FujiFilm FLA-7000).

TE Buffer	20 x SSC
10 mM Tris, pH 8.0	3M sodium chloride
1 mM EDTA	0.3M sodium citrate

2.6.5 *De novo* transcription assay

Freshly isolated mitochondria, 2mg, from heart, brain, liver, kidney and muscle tissue were pelleted and resuspended in 500µl transcription buffer. The mitochondrial suspension containing 50 µCi of [α -³²P] UTP (Amersham Biosciences) was incubated by rotating the mixture for 1 hour at 37°C. After the incubation, the mitochondria were pelleted and washed twice with resuspension buffer. Mitochondrial RNA was isolated from the final pellet by using the ToTALLY RNA Kit (Ambion) and resuspended in 30-50 µl glyoxal loading buffer with dye (Ambion). Samples were separated in a 1,2% agarose gel containing formaldehyde at 120V for 2hrs. Further procedures were as described in the northern blot section above.

Transcription buffer	Resuspension buffer
25mM sucrose	10% glycerol
75 mM sorbitol	10mM Tris-HCl pH 6.8
100mM KCl	0.15mM MgCl ₂
10mM K ₂ HPO ₄	
50mM EDTA	
5mM MgCl ₂	
1mM ADP	
10mM glutamate	
2.5mM malate	
10mM Tris-HCl, pH 7.4	
1mg/ml BSA	

2.6.6 *In organello* translation

To analyse *de novo* synthesis of mitochondrial encoded proteins we performed *in organello* translation assays. They were performed with 1mg mitochondria isolated by differential centrifugation in isolation buffer A and washed twice with translation buffer. In the following, mitochondria were pelleted and incubated in 2ml translation buffer at 37°C with gentle rotation for 5 min. Mitochondria were washed one more time in translation buffer before 30µCi Easy Tag Express³⁵S Protein labeling mix [³⁵S]-methionine (> 1000Ci/mmol) (Perkin Elmer) were added, followed by incubation in rotation at 37°C for 1 hr. Next, proteins were washed with isolation buffer A and resuspended in a conventional SDS-PAGE loading buffer. 10µl of each sample were loaded on a 17% acrylamide gel and separated at 100V, 10mA for 16 hrs, 4°C. The gel was incubated in fixing solution, stained in coomassie blue, destained with destainer and finally incubated in Amersham Amplify Fluorographic Solution (GE Healthcare) for 30 min at RT. Subsequently, the gel was dried using Hoefer Slab Gel Dryer (Amersham Biosciences) (see section 2.5.5.1) at 80°C for 1.5 hrs. and finally exposed to a phosphoimager screen 1-3 days.

Translation buffer		Translation Mix 2x		2x gel loading buffer	
2 x translation mix	5 ml	200 mM mannitol		100 mM Tris-HCl, pH 6.8	
Amino acids (6 mg/ml each)	100 µl	20 mM sodium succinate		20% glycerol	
200 mM ATP	250 µl	160 mM KCl		4% SDS	
50 mM GTP	40 µl	10 mM MgCl ₂		0.5 mg/ml bromphenol blue	
1 M creatine phosphate	60 µl	2 mM KPi pH 7,4		100mM DTT (fresh!!)	
10 mg/ml creatine kinase	60 µl	50 mM HEPES pH 7,4			
Cysteine (6 mg/ml)	100µl	adjusted to pH7			
Tyrosine (3 mg/ml)	200 µl				
dd H ₂ O	4,595ml				

10ml

Fixing solution	Coomassie Blue	Destainer
50% methanol	0.1% Coomassie Brilliant Blue R-250	40% methanol
10% glacial acid	50% methanol	10% glacial acetic acid
	10% glacial acid	

Amino acids (100x stock with 6 mg/ml each):

Ala, Arg, Asp, Asn, Glu, Gln, Gly, His, Ile, Leu, Lys, Phe, Pro, Ser, Thr, Trp, Val

2.6.7 S1 protection assay

To quantify the amount of transcripts upstream of the MTERF1 binding site, S1 protection assay was performed with 20µg mitochondrial RNA from mouse liver. Two samples of an oligonucleotide covering the MTERF1 binding site and a short region upstream as well as two control samples (oligonucleotides from another region) and a RNA ladder were labelled with [γ -³²P] ATP. Samples were combined and distributed among all RNA samples plus an additional control tube. After addition of 1/10 volume 5M NH₄OAc and 2.5 volumes ethanol, RNA was precipitated at -20°C for at least 15min or overnight. Next, RNA was pelleted at max. speed, 15 min, 4°C, washed with 70% RNase-free EtOH and resuspended in 10µl Hybridization Buffer III (Life technologies). In the following, RNA was heated at 90-95°C for 3-4 min for RNA denaturation and subsequently incubated at 42°C o/n. In each sample a

reaction containing 133.5 μ l dH₂O, 15 μ l 10 x S1 buffer and 1.5 μ l S1 enzyme was added, for the control sample, the S1 enzyme was missing. Samples were incubated at 37°C for 30 min, until the reaction was stopped by addition of RNase Inactivation solution III (RPA III kit, life technologies) and incubation at -20°C for 15 min. or overnight. RNA was pelleted at max. speed for 15 min at 4°C, washed with 70% RNase-free EtOH, resuspended in 30 μ l Loading buffer II (Ambion) and finally boiled at 90-95°C for 3 min. Samples were loaded on a 6% polyacrylamide 7M Urea gel. The gel was pre-runned in 1x TBE at 10mA for 30 min. After samples were loaded, gel was running at 10mA for 2-3 hrs. Finally, the gel was dried in a Hoefer Slab Gel Dryer (Amersham Biosciences) (see section 2.5.5.1) and exposed to a phosphoimager screen for 2 days.

6% polyacrylamide 7M Urea gel	
Urea	105.1 g
19:1 40% acrylamide	37.5ml
10x TBE	25ml
dH ₂ O	82.4ml

For 50ml gel 200 μ l 25% APS and 60 μ l TEMED were used.

2.6.8 *In vitro* transcription

DNA fragments corresponding to bp 1–741 (LSP and HSP), 1–477 (LSP) or 499–741 (HSP) of human mtDNA14 were cloned into pUC18. After linearization, the plasmid constructs were used to measure promoter-specific transcription in a run-off assay. *In vitro* transcription reactions contained 100 fmol of indicated template, 20 mM Tris-HCl (pH 8.0), 10 mM MgCl₂, 1 mM DTT, 100 μ g/ml bovine serum albumin, 400 μ M ATP, 150 μ M CTP and GTP, 10 μ M UTP, 0.2 μ M α -³²P UTP (3,000 Ci/mmol), 4 U of RNasin (APBiotech), 400 fmol POLRMT, 400 fmol TFB2M, and 5 pmol TFAM (15 pmol TFAM was added when the LSP/HSP template was used). The reaction volume was 25 μ l and the final concentration of NaCl was adjusted to exactly 80 mM NaCl in all reactions. The concentrations of LRPPRC were the following: 0, 0.4, 0.8, 1.6 and 3.2 pmol. Reactions were stopped after 30 min at 32 °C by adding 200 μ l of stop buffer (10 mM Tris-HCl [pH 8.0], 0.2 M NaCl, 1 mM EDTA and 0.1 mg/ml glycogen). The samples were treated with 0.5% SDS and 100 μ g/ml proteinase K for 45 min at 42 °C, and precipitated by adding 0.6 ml of ice-cold ethanol. The pellets were dissolved in 10 μ l of gel loading buffer (98% formamide, 10 mM EDTA [pH 8.0], 0.025%

xylene cyanol FF, 0.025% bromophenol blue) and heated at 95 °C for 5 min. Transcription reaction products were analyzed in a 6% denaturing polyacrylamide gel in 1 × TBE buffer.

2.6.9 Electrophoresis mobility shift assay

The RNA binding activity of LRPPRC was assayed by EMSA using the HSP (499–741) run-off transcript as a template. A ten times *in vitro* transcription reaction (250 µl) was performed as described in the *in vitro* transcription section. After 30 minutes, 2 µl of DNase I (1U/µl) was added to the reaction and placed on the benchtop at room temperature for 10 minutes before the radioactive labeled RNA was purified using RNeasy Mini kit (Qiagen). The RNA was eluted in 50 µl RNase-free water. The RNA binding reactions were performed in a volume of 20 µl containing 5 µl of the purified RNA, 25 mM Tris-HCl [pH 7.8], 1 mM DTT, 10 mM MgCl₂, 0.1 mg/ml BSA, 10% glycerol, and different concentrations of LRPPRC (0, 0.4, 0.8, 1.6, 3.2 pmol). The reactions were incubated for 20 min on ice before separation on a 4% polyacrylamide gel in 0.5 × TBE buffer, 2 hrs at 100 V.

2.6.10 ChIP-Sequencing

HeLa-S3 cells were cultured in DMEM (Invitrogen) with 10% fetal bovine serum in a perfusion culture using a three liter Biobundle bioreactor (Applikon) equipped with a 10mm spin filter and a bubble-free aeration system. The temperature was set to 37°C, the pH was 7.2 adjusted with CO₂ and 0.3M NaOH, the stirring rate was 200 rpm and dO₂ was 40% of air saturation. Mitochondria were purified and cross-linked in 1% formaldehyde in PBS for 10 min at room temperature. 125 mM glycine was added to the reaction, which was incubated for another 5 min. After two washes in cold PBS the mitochondrial pellet was frozen in liquid nitrogen. The mitochondria were lysed in lysis buffer (25 mM HEPES-KOH (pH 7.6), 10% glycerol, 5 mM MgCl₂, 0.5 mM EDTA, 0.5% Tween-20, 150 mM KCl, 1 mM phenylmethylsulfonyl fluoride, 2 mM pepstatin A, 0.6 mM leupeptin and 2 mM benzamidine), homogenized with a Dounce homogenizer, sonicated in a Bioruptor UCD-200 (Diagenode) to an mtDNA size of ~250 bp and centrifuged at 14.000 x g for 5 min. The extract was pooled and divided into aliquots of 400 µl (~5.8 · 10⁸ cells). For immunoprecipitation of MTERF1, 24 µl of a rabbit polyclonal antibody was added to one aliquot and incubated over night at 4 °C in a rotary shaker. As a control, a rabbit antiserum was added to another aliquot and incubated in the same way. Next, 50 µl of 50% (v/v) suspension of Protein A beads (GE Healthcare) in lysis buffer was added to the samples and incubated for 1 hr at 4 °C. The samples were then transferred to 0.45 mm Ultrafree-MC filter units

(Millipore) and the beads were washed once in wash buffer (0.1% SDS, 50 mM HEPES-KOH (pH 7.5), 1% Triton-X, 0.1% sodium deoxycholate, 1 mM EDTA, 150 mM NaCl) at 4 °C, twice at room temperature followed by two washes with deoxycholate buffer (10 mM Tris-HCl (pH 8), 1 mM EDTA, 0.5% sodium deoxycholate, 0.5% NP-40, 0.25 M LiCl). The beads were then rinsed with 10 mM Tris and 1 mM EDTA (pH 8) and incubated with 0.2 µg of RNase A for 30 min at 37 °C. Next, the DNA/protein was eluted by incubating the beads in 50 mM Tris, 10 mM EDTA and 1.5% SDS at 65 °C for 2 hr. To reverse the cross-linking, the samples were incubated over night at 65 °C and proteins were removed by treating the samples with 20 µg of proteinase K at 56 °C for 2 hr. The DNA was extracted using phenol-chloroform followed by ethanol precipitation. The DNA was further prepared using standard protocols provided by Illumina and deep-sequenced by using Illumina's Solexa sequencer [Beijing Genomics Institute]. Quality control statistics were generated with FastQC (<http://www.bioinformatics.bbsrc.ac.uk/projects/fastqc>). An alternate mitochondrial genome was generated for alignment of our sequencing data since the mtDNA of the HeLa cells was found to have some SNPs and Indels. Read alignments to the alternate mitochondrial genome were performed using BWA (0.5.9 - r16) with default parameters.

2.7 Mass spectrometry

2.7.1 Protein identification with LC-MS/MS after immunoprecipitation

50ul of 25mM ammonium bicarbonate was added to each pellet and vortexed to dissolve the protein pellet completely. 3ul of 1% RapiGest (Waters Corporation, Milford, USA) was added for denaturing the proteins. The protein solution was incubated at 80°C for 10 min on a Thermomixer. After addition of 2.5µl aliquot of 50mM DTT (Sigma–Aldrich) the solution was heated at 60°C for 15 min. The protein solution was then cooled down to room temperature and centrifuged. After the addition of 2.5µl aliquot of 150mM iodoacetamide (Sigma–Aldrich), the solution was stored in the dark at room temperature for 30 min. The tryptic digestion was performed by adding Trypsin Gold mass spectrometry grade (Promega, Madison, MI, USA) at a 1:50 (w/w) ratio and incubated at 37°C overnight. 1µl of 37% HCL was added to adjust the pH below 2. After being vortexed and centrifuged at 13000xg for 30 min, the supernatant was collected and transferred to a clean microcentrifuge tube. The protein digest was dried in Speed-Vac and resuspended with 10ul of 0.1% of formic acid. Samples were analyzed by LC-ESI-MS/MS with an Amazon ion trap ETD (Bruker, Bremen, Germany) coupled to an Aquity nanoUPLC with sample manager (Waters, Manchester, UK) using a 40 min gradient (3% to 55% ACN) at 300 nL/min flow, 15 min washing step (95% ACN) followed by re-equilibration for 20 min (3% ACN). The ion trap was operated in positive MS mode at enhanced resolution speed of 8100 m/z/s. ICC target was set to 400000 and the maximum accumulation time to 50 ms.

Scan range was m/z 300-1300. The source capillary was operated at -4500 V and the end plate offset was -500 V. The nebulizer pressure was 15 PSI, dry gas flow 4.0 L/min and the dry gas temperature 200°C. MS/MS parameters: number of precursors were 10, threshold absolute 25000, MS/MS fragmentation amplitude was 0.8 V, isolation width 2.5 m/z, scan speed 32500 m/z/s, scan range m/z 100-2400, ICC target 100000, maximum accumulation time 100 ms, precursor was excluded after one spectra and released after 0.17 min. The raw data were processed with DataAnalysis (Version 4.0 SP 2, Bruker, Bremen Germany). The processed data were imported into ProteinScape 2.1.0577 (Bruker, Bremen, Germany) and the extracted MS/MS data were submitted to an in-house MASCOT server (version 2.3, Matrix Science, London, UK). Proteins were identified by searching in the peptide lists for Knowledgebase 2012_11 (538585 sequences and 191240774 residues). The following

parameters were used: taxonomy *Mus musculus* (16580 sequences); Enzyme: trypsin; Max Missed Cleavages: 1; Fixed modifications: carbamidomethyl (C); Variable modifications : oxidation (M); Peptide Mass Tolerance : ± 0.8 Da; Fragment Mass Tolerance: ± 0.8 Da. ((1))

2.7.2 Protein identification and quantification with LC-MS/MS

Samples were diluted with 100mM ammonium bicarbonate to gain a concentration of about 200ng/ μ l according to Bradford method. Tryptic digestion was performed by adding Trypsin Gold mass spectrometry grade (Promega, Madison, MI, USA) at a 1:50 (w/w) ratio and incubation at 37°C overnight. Protein identification and quantification were performed with a Xevo Q-ToF (Waters Corporation, Milford, USA) coupled with a nanoACQUITY UPLC™ (Waters Corporation, Milford USA). The digest was 10 fold diluted with 0.1% of formic acid. 1 μ l of standard Alcohol dehydrogenase 1 (ADH) tryptic digest (50fmol/ μ l) (Waters Corporation, Milford, USA) was added to 0.5 μ l of the sample digest. 1.5 μ l of the digest mixer was loaded into a C18 trap column of 180 μ m X 20 mm with 10 μ l/min of 3% of solvent A (0.1% Formic Acid) for 2 min. The digest was then separated and eluted with an analytical column of 75 μ m x 150mm C18 BEH 1.7 μ m (Waters Corporation, Milford USA). The gradient was 3% to 35% of acetonitrile in 0.1% formic acid over 10min at a flow rate of 400nl/min. The Xevo Q-ToF was operated in LC/MS^E mode over the m/z range of 50-1800 in nano electrospray mode. The capillary, sample cone, extraction cone and collision energy were 3.3kV, 25.0V, 2.0V, and 6.0V respectively. During elevated energy scan, the collision energy was ramped from 15V to 35V. Glufibrinopeptide B of m/z 785.84 was used as Lock Mass for mass correction. At least 3 replicates of one sample were analyzed. Data was collected using MassLynx™ 4.1 and processed and searched using ProteinLynx™ Global Server 2.5.2. (Waters Corporation, Milford USA). Following parameters were used for database search: enzyme “trypsin”, minimal fragments ion per peptide matched “2”, minimal fragments ion per protein matched “7”, missed cleavages “1”, variable modification “oxidation Methionine”, peptide tolerance “automatic”, fragment tolerance “automatic”, false positive rate “4%”. Calibration protein P00330 (ADH1_YEAST), calibration protein concentration 50fmol. The mouse database was from Uniprot release knowledgebase_2012_11.

2.8 Cell culture

2.8.1 Maintenance of cultured HeLa cells

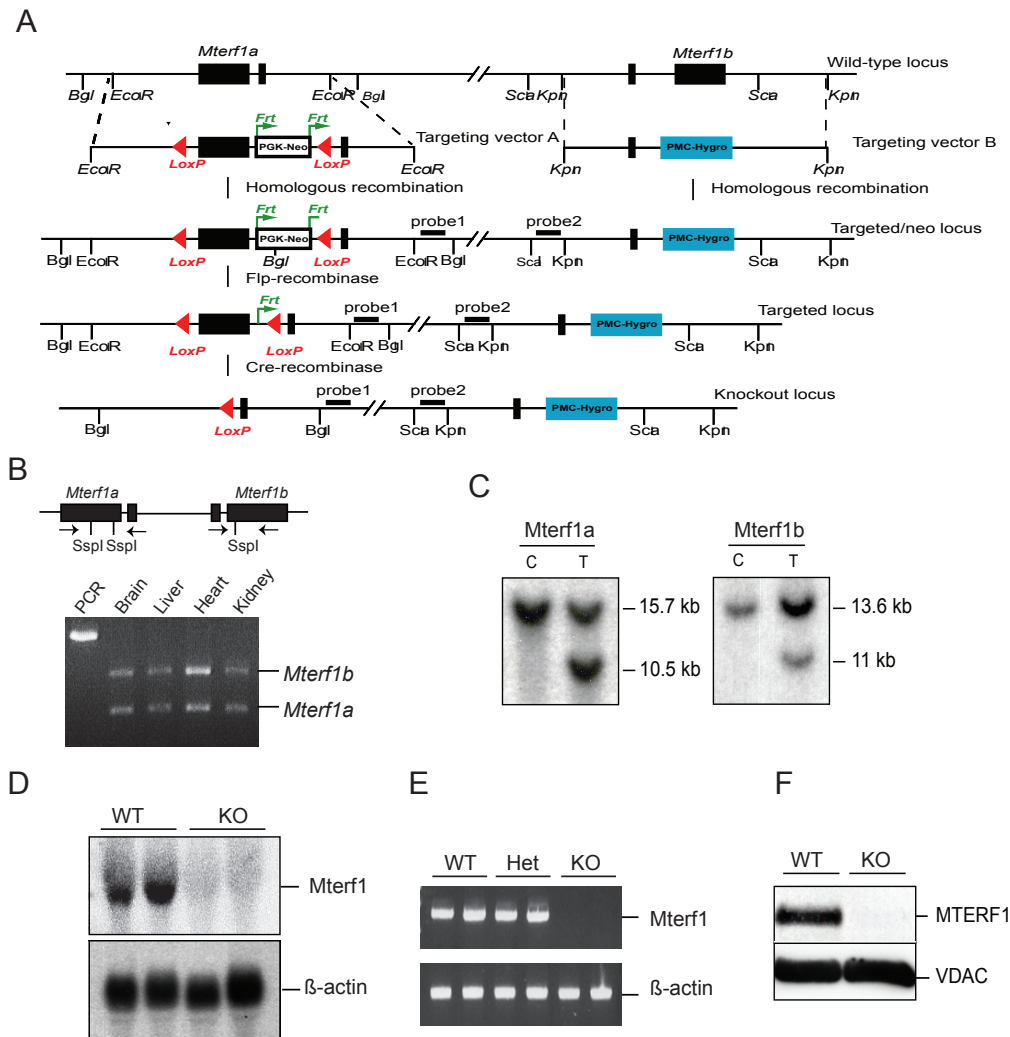
HeLa cells were grown at 37°C, 5% CO₂ and 95% humidity in 10cm dishes supplied with 10ml Dulbecco's Modified Eagle Medium (DMEM; Gibco) containing 10% Fetal Bovine Serum and penicilline (100µg/ml /streptomycine (100µg/ml). If cells were 100% confluent, media was removed and cells were washed with Phosphate Buffered Saline (Gibco) and subsequently incubated with 0.5% Trypsin/EDTA (Gibco) at 37°C for 2-3min. The cells disattached from the dish could be collected in 10ml DMEM media with 10% FBS and 100µg/ml penicillin / streptomycine. If not distributed to other dishes, cells were pelleted at 800 rpm, 5min, washed with PBS and used for experimental analysis.

3 Results

3.1 Analysis of mitochondrial gene regulation at the transcriptional level in *Mterf1* knockout mice

3.1.1 Generation of *Mterf1* knockout mice

Extensive studies have been done regarding the role of MTERF1, however all available data in the literature regarding this protein are based exclusively on in vitro studies. In order to obtain new insights about the in vivo function of MTERF1, a whole body knockout mouse model was created. MTERF1 is encoded by two homologous genes (*Mterf1a* and *Mterf1b*), which are both actively transcribed from mouse chromosome 5. Since the expression rate of both genes is similar in various tissues, *Mterf1a* and *Mterf1b* had to be disrupted in order to create a *Mterf1* knockout (*Mterf1*^{-/-}) mouse (**Figure 3.1 B**). Due to the immediate proximity of *Mterf1a* and *Mterf1b* it was not possible to disrupt both genes with two independent homologous recombination events at the same time. Therefore, *Mterf1a* and *Mterf1b* had to be disrupted individually by two separate targeting vectors in the same mouse embryonic stem cell clone to obtain a double knockout of both *Mterf1* genes, named *Mterf1* knockout mouse. First, a targeting vector A with loxP sites flanking exon1 of *Mterf1a* was electroporated into embryonic stem cells. In the next step exon 2 of the *Mterf1b* gene was replaced by a hygromycin cassette (targeting vector B) in stem cell clones already positive for targeting vector A (**Figure 3.1 A**). Clones electroporated with both targeting vectors were screened by using Southern Blot analysis with specific probes for the *Mterf1a* or *Mterf1b* gene regions (**Figure 3.1 C**). The clones carrying both targeting vectors were expanded and used for blastocyst injection as further step in the creation of mice heterozygous for both copies of the *Mterf1* gene. Obtained *Mterf1*^{+/^{loxP} mice were finally mated with mice expressing Fip and cre recombinases, respectively to remove the PGK-neo cassette and disrupt exon2 of the *Mterf1a* gene (**Figure 3.1 A**). In order to minimize genetic background effects heterozygous *Mterf1* knockout mice were backcrossed to wild type C57Bl6/N mice for six generations and intercrossed to produce homozygous knockout animals. Northern blot experiments with RNA from heart tissue demonstrated the absence of the *Mterf1* gene in *Mterf1* knockout mice (**Figure 3.1 D**). The lack of *Mterf1* gene copies were confirmed by qPCR and western blot analyses, where both could not reveal a signal of *Mterf1* gene and protein product in the knockout mice, respectively (**Figure 3.1 E and F**).}

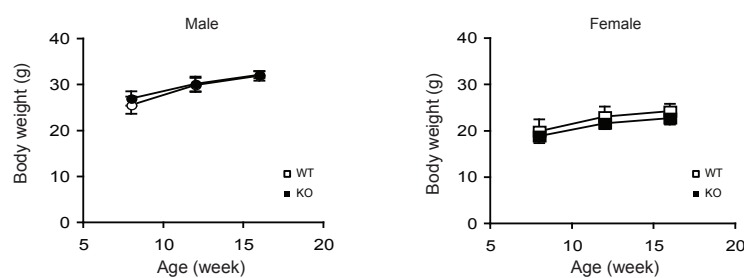


Terzioglu et al., Cell metabolism, 2013

Figure 3.1: Disruption of *Mterf1a* and *Mterf1b* in the germline. A. Targeting strategy for disruption of the *Mterf1* gene. Probes and restriction sites used for the ES cell screening are indicated. B. Map of *Mterf1a* and *Mterf1b* with indication of restriction sites for *SspI*. Arrows indicate primers used for RT-PCR (upper panel). Relative expression of *Mterf1a* and *Mterf1b* mRNAs determined by restriction enzyme digestion of cDNA from different tissues (lower panel). C. Southern blot analysis in embryonic stem cell to screen for homologous recombination events. D. Northern Blot analysis of *Mterf1* knockout and control mice to analyze *Mterf1* mRNA expression RNA isolated from heart tissue. β -actin was used as loading control. E. Quantitative PCR analysis of *Mterf1* mRNA expression in wild type and *Mterf1* knockout mice. β -actin was used as loading control. F. Western Blot analysis to detect MTERF1 protein steady state levels in liver protein extract from *Mterf1* wild type and control animals. VDAC was used as loading control.

3.1.2 *Mterfl* knockout mice are fertile and viable with normal respiratory chain activity

Mice lacking the *Mterfl* gene were apparently healthy with no obvious phenotype. The animals were fertile with a normal lifespan and weight gain like their wild type littermates (**Figure 3.2**). Regarding the extensive *in vitro* data of previous MTERF1 knockdown studies, the normal appearance of *Mterfl* knockout mice was quite surprising. For that reason we continued studying this model very carefully to not overlook minor molecular differences in *Mterfl* knockout mice compared to the wild type. We measured respiratory chain enzyme activity as well as mitochondrial ATP production on isolated mitochondria from heart of *Mterfl* knockout and wild type mice. There was no difference detected in the activities of NADH-coenzyme Q reductase (complex I), NADH-cytochrome c reductase (complex I and III), succinate dehydrogenase (complex II), succinate-cytochrome c reductase (Complex II and III) and



Terzioglu et al., Cell metabolism, 2013

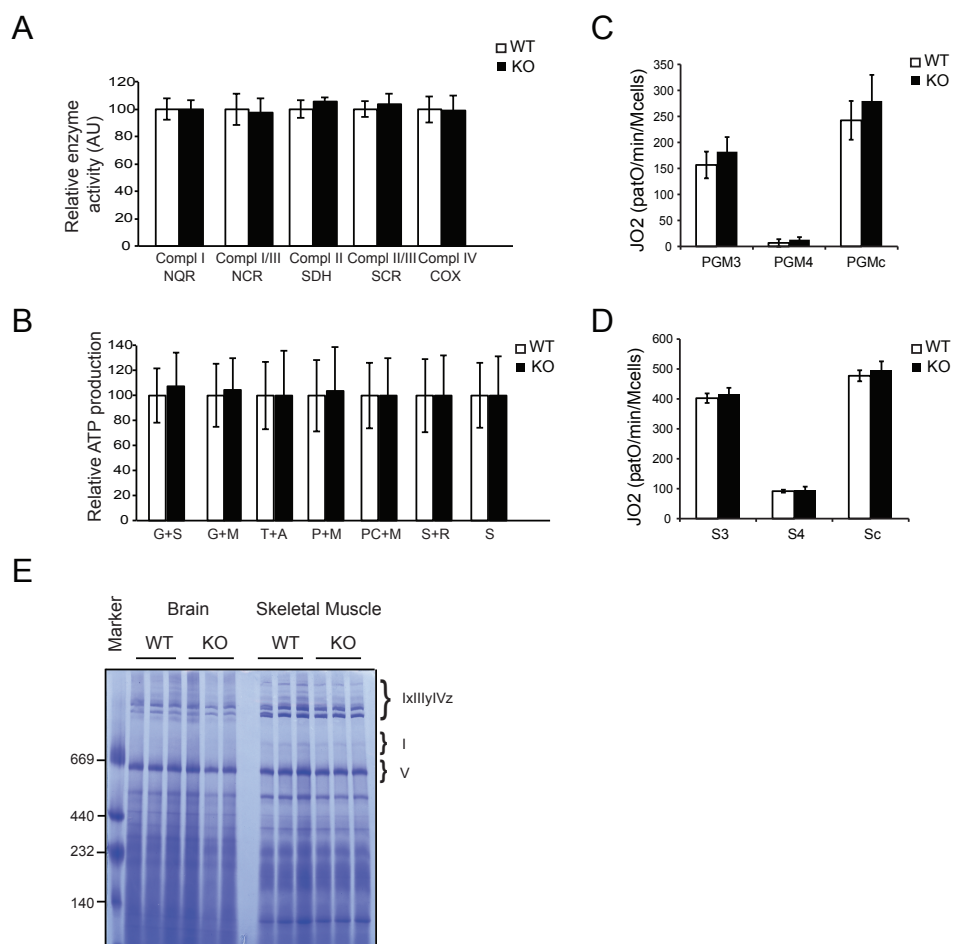
Figure 3.2: Body weight curves. Determination of body weight in wild type and *Mterfl* knockout mice. N=5 (males) and n= 5 (females). Error bars indicate s.e.m..

cytochrome c oxidase (complex IV) between wild type and *Mterfl* knockout animals and also measurements of the ATP production rate applying different substrates was unaffected in the knockout mice (**Figure 3.3 A,B**). Furthermore, total oxygen consumption in isolated splenocytes, a highly proliferative cell type, was investigated by studying respiration activity of different complexes dependent on the substrate (**Figure 3.3 C,D**) but again, *Mterfl* knockout mice were not affected.

Aside from the bioenergetic approach we also assessed the assembly and functionality of respiratory chain complexes in *Mterfl* wild type and knockout mice by performing Blue Native PAGE experiments in isolated mitochondria from brain and skeletal muscle. Coomassie staining of the Blue Native gels revealed normal steady state and assembly levels of all respiratory chain complexes (**Figure 3.3 E**). These data strongly support, that loss of MTERF1 does not influence oxidative phosphorylation capacity.

3.1.3 MTERF1 binds mtDNA but is not involved in maintenance and transcription initiation of mitochondrial DNA

MTERF1 is known to strongly bind DNA (Yakubovskaya et al., 2010), we therefore continued the characterization by evaluating its role in mtDNA maintenance. DNA from heart was used for Southern blot experiments but no difference between *Mterf1* knockout mice and their wild type controls was found (Figure 3.4 A,B). Numerous *in vitro* studies concerning the function of MTERF1 suggest a role in mtDNA transcription regulation, in particular HSP1 transcription of the ribosomal RNAs by enabling loop formation (Martin et al., 2005). However, steady state transcript levels of all mitochondrial encoded mRNAs and rRNAs in heart mitochondria appeared to be unchanged in *Mterf1* knockout mice compared to wild type controls. (Figure 3.4 C,D).



Terzioglu et al., Cell metabolism, 2013

Figure 3.3: Bioenergetic measurements and Blue Native PAGE analysis in *Mterf1* knockout mice. A. Measurement of respiratory chain enzyme activities in wild type (n=5) and *Mterf1* knockout (n=5) mice. The relative enzyme activities for NADH-coenzyme Q reductase (complex I), NADH-cytochrome c reductase (complexes I and III), succinate dehydrogenase (complex II), succinate-cytochrome c reductase (complexes II and III) and cytochrome c oxidase (complex IV) are shown. Error bars indicate s.e.m. B. Measurement of mitochondrial ATP production rate in wild type (n=5) and *Mterf1* knockout (n=5) mice with glutamate and succinate (G+S), glutamate and malate (G+M), tetramethyl-p-phenylenediamine (TMPD) and ascorbate (T+A), pyruvate and malate (P+M), palmitoyl-L-carnitine and malate (PC+M), succinate and rotenone (S+R) and succinate (S). Error bars indicate s.e.m. C. Oxygen consumption in whole splenocytes isolated from wild type and *Mterf1* knockout

mice. Cells were incubated in pyruvate, glutamate and malate (PGM) to deliver electrons to complex I. Permeabilized cell respiration was analysed in the phosphorylating (state 3; PGM3), non-phosphorylating (state 4; PGM4) and uncoupled (PGMc) states. Error bars indicate s.e.m. D. Oxygen consumption in whole splenocytes isolated from wild type and *Mterf1* knockout mice. Cells were incubated in succinate and rotenone to deliver electrons to complex II. Permeabilized cell respiration was analysed in the phosphorylating (state3; S3) non-phosphorylating (state 4; S4) and uncoupled (Sc) states. Error bars indicate s.e.m. E. BN-PAGE analysis of levels of assembled respiratory chain complexes from wild type (n=3) and *Mterf1* knockout (n=3) mice.

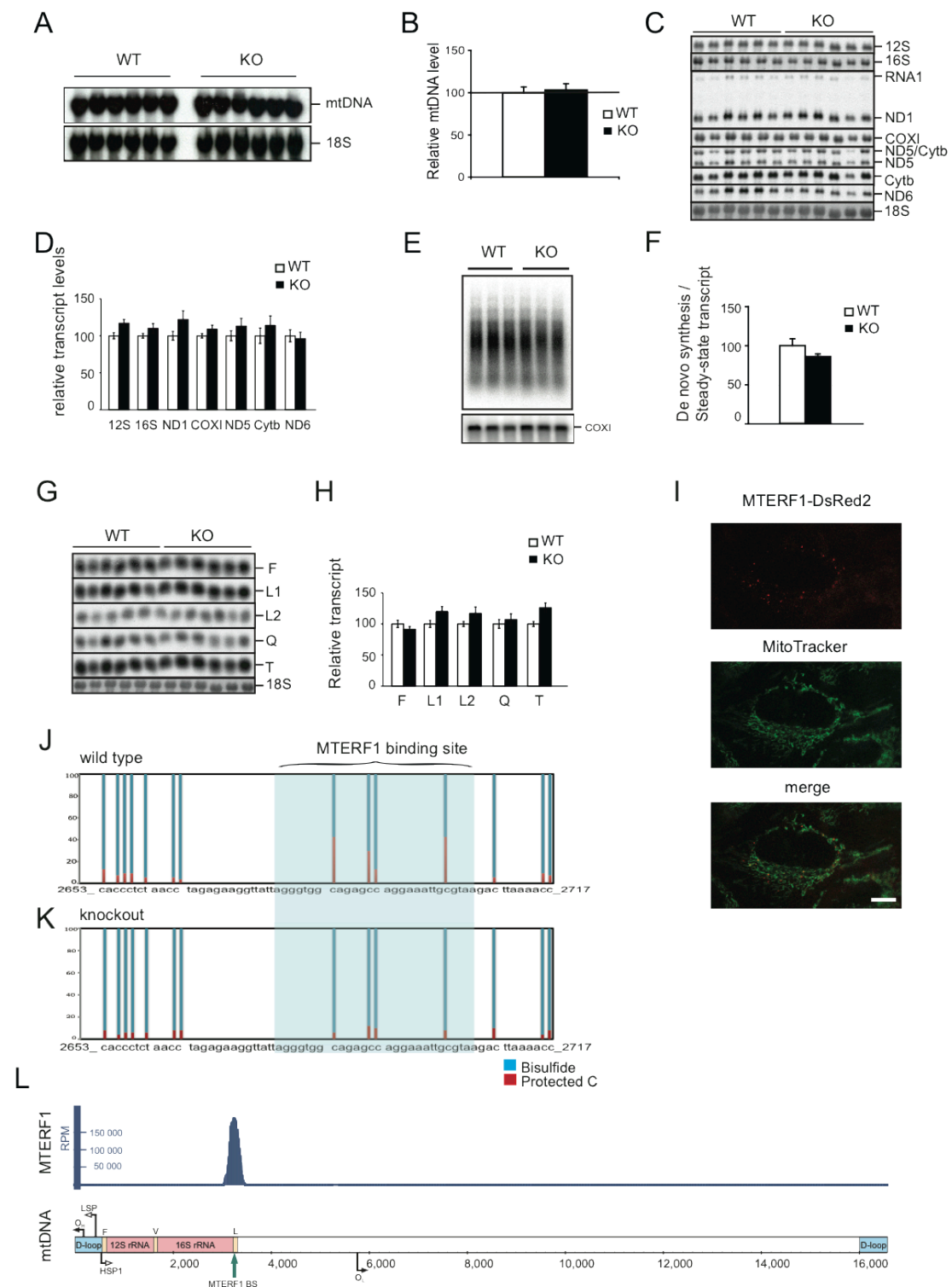
Furthermore tRNA steady state levels, which are good indicators for *de novo* transcription activity, were normal in mice lacking MTERF1, as shown in a northern blot with isolated RNA from heart tissue of control and *Mterf1* knockout mice (**Figure 3.4 G,H**). Consequentially, *in organello* transcription assays in isolated heart mitochondria from wild type and knockout animals did also not reveal any difference (**Figure 3.4 E,F**). These findings were rather unexpected and questioned the tenability of a loop formation.

The absence of any molecular effect in the *Mterf1* knockout mouse disposed us to re-examine the intracellular localization of MTERF1 and its mtDNA binding site.

Immunofluorescence microscopy studies found MTERF1 situated in mitochondria, co-localizing with mitochondrial nucleoids (**Figure 3.4 I**) consistent with previous studies claiming MTERF1 being a DNA-binding protein (Jiménez-Menéndez et al., 2010; Yakubovskaya et al., 2010). To define the exact mtDNA-binding site, chromatin immunoprecipitation, followed by next-generation sequencing (ChIP-seq) was performed. We found a strong interaction within the tRNA^{Leu} gene, confirming previous studies about the MTERF1 binding site (Asin-Cayuela et al., 2005; Fernandez-Silva et al., 2007) (**Figure 3.4 L**). However, besides the previous mentioned interaction no binding site in the HSP promoter region could be found. This is in contrast to a previous report, claiming that MTERF1 simultaneously interacts with the HSP1 promoter region and the tRNA^{Leu(UUR)} gene region to promote mtDNA loop formation, as already mentioned before (Martin et al., 2005).

In the following, we were engaged with the question if there is another protein able to occupy the MTERF1 binding site and competing against the protein. To address this issue we performed footprinting analysis in *Mterf1* knockout cells by using mouse embryonic fibroblasts from *Mterf1* knockout and control mice. The cells were transfected with a mitochondrially targeted cytosine DNA methyltransferase, which methylates unprotected cytosines at the mtDNA. Next, isolated mtDNA was treated with bisulfite to convert non-methylated cytosines into uracil. After PCR amplification and sequencing of the DNA samples we found the MTERF1 binding site unprotected in *Mterf1* knockout MEFs meaning that no other protein is occupying this area in the absence of MTERF1 (**Figure 3.4 J,K**).

Taken together, these data do not support the idea of MTERF1 being involved into the regulation of ribosomal biogenesis *in vivo*.



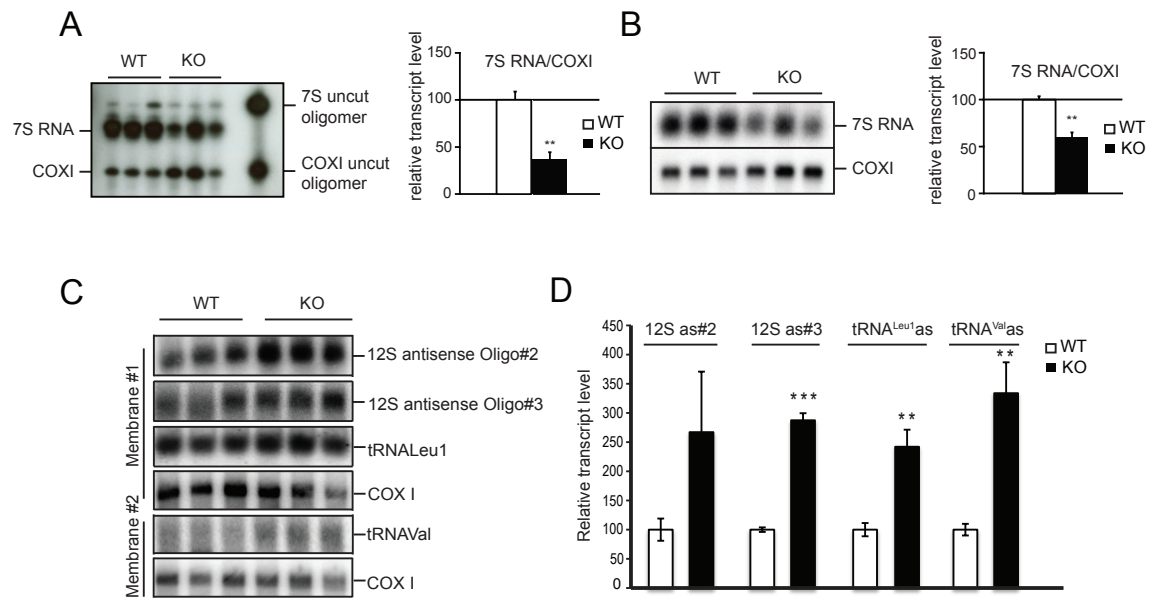
Terzioglu et al., Cell metabolism, 2013

Figure 3.4 :Analysis of MTERF1 DNA-binding sites and mtDNA expression. A Southern Blot analysis in heart tissue of wild type (n=5) and *Mterf1* knockout (n=5) mice. Nuclear encoded 18S was used as loading control. B Quantification of A. Error bars indicate s.e.m. C. Northern Blot analysis of mitochondrial mRNAs and rRNAs with RNA isolated from heart tissue of control (n=5) and *Mterf1* knockout (n=6) mice. D. Quantification of C. Error bars indicate s.e.m. E. *In organello* transcription assay in heart tissue of wild type (n=3) and *Mterf1* knockout (n=3) mice. COXI was used as loading control. F. Quantification of E. Error bars indicate s.e.m. G. Northern Blot analysis of mitochondrial

tRNAs in RNA isolated from heart tissue of control (n=6) and *Mterf1* knockout (n=6) mice. H. Quantification of G. Error bars indicate s.e.m. I. Subcellular localization of DsRed2-tagged MTERF1 fusion protein in HeLa cells. Mitochondria are stained with MitoTracker Green FM. The scale bar corresponds to 10 μ m. J. Methylation assay to assess cytosine methylation protection at the binding site for MTERF1 in cell lines from wild type mice. K. Methylation assay to assess cytosine methylation protection at the binding site for MTERF1 in cell lines from *Mterf1* knockout mice. L. Chip-Seq profile of MTERF1 binding to mDNA. MTERF1 reads were normalized against no-antibody control. Peak detection was performed using CisGenome (reads per million [RPM]).

3.1.4 MTERF1 prevents light strand transcription from interfering with the light strand promoter

Due to a missing effect in heavy strand transcription in *Mterf1* knockout mice, we continued our experiments by focusing on the light strand. S1 protection experiments using heart mitochondrial RNA isolated from *Mterf1* wild type and knockout animals were performed with probes covering a region immediately downstream of the LSP. Surprisingly, we found a serious decrease of transcripts in this area in *Mterf1* knockout mice compared to controls (**Figure 3.5 A**). We confirmed these findings with northern blots, which revealed decreased 7S RNA levels in the absence of MTERF1 but not in the controls (**Figure 3.5 B**). These findings indicated reduced transcription initiation events at LSP, since varying 7S RNA levels were reported to be good indicators for *de novo* transcription activity (Cámara et al., 2011; Park et al., 2007; Ruzzenente et al., 2012; Wredenberg et al., 2013). In order to get more profound information concerning the regulation of LSP transcription, we carried out northern blot analysis with probes binding different rRNA antisense transcripts, downstream and in close proximity to the MTERF1 binding site. Antisense transcription was clearly increased in animals lacking MTERF1, suggesting that MTERF1 prevents the RNA polymerase from continuing transcription on the light strand in order to avoid promoter interference at the LSP (**Figure 3.5 C,D**).



Terzioglu et al., Cell metabolism, 2013

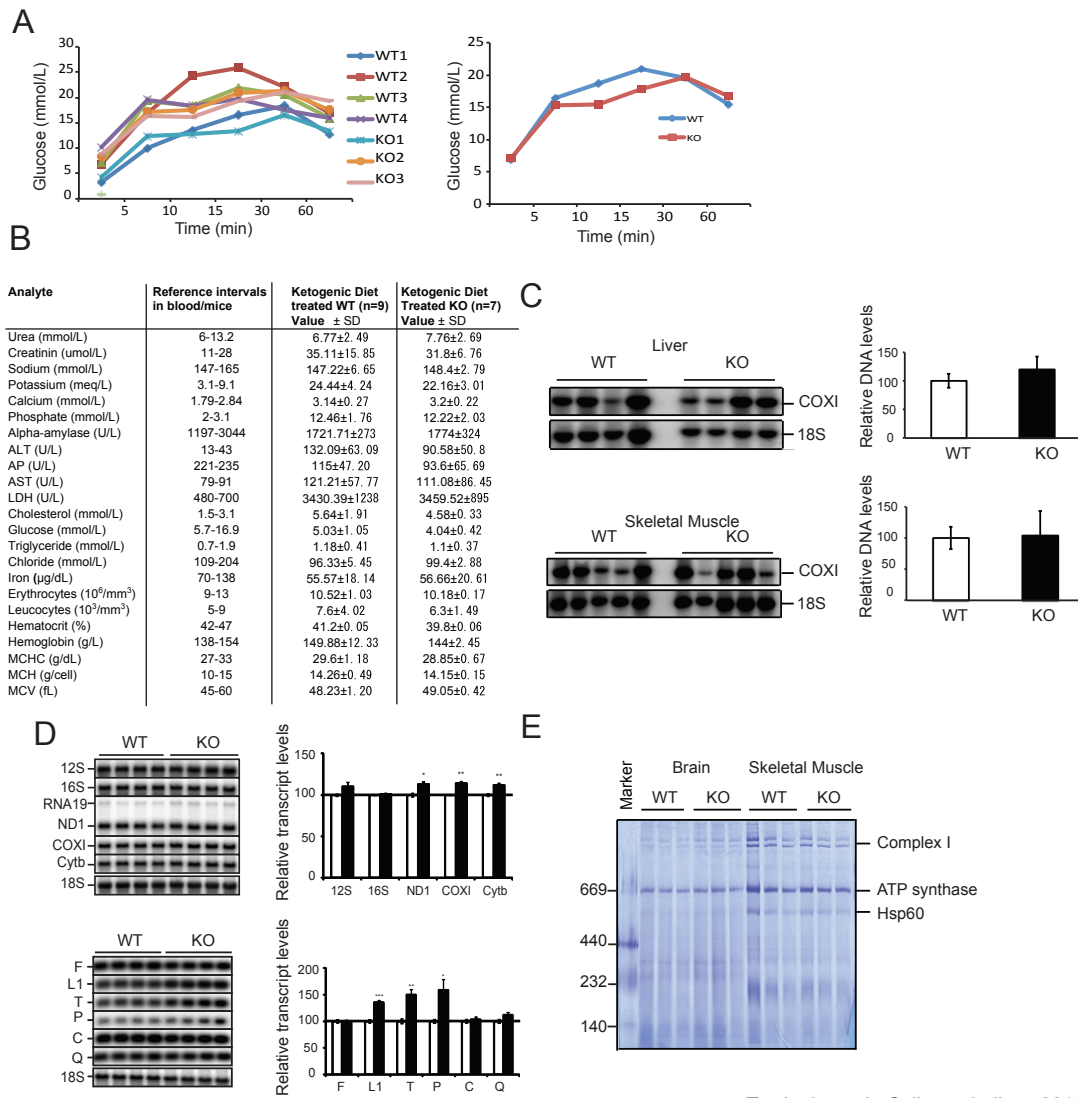
Figure 3.5: Analysis of transcription initiation at the LSP. A. S1 protection assay (left panel) and quantification of this analysis (right panel) in heart of control (n=3) and *Mterf1* knockout (n=3) animals to determine relative levels of the LSP-proximal 7S RNA transcript. Error bars indicate s.e.m., **P < 0.01 student's t-test. B. Northern Blot analysis (left panel) and quantification of this analysis (right panel) to determine relative levels of the LSP-proximal 7S RNA transcript of control (n=3) and *Mterf1* knockout (n=3) animals. Error bars indicate s.e.m. **P < 0.01 student's t-test. C. Northern Blot analysis in kidney tissue of wild type (n=3) and *Mterf1* knockout (n=3) animals to assess levels of L-strand transcripts downstream of the MTERF1 binding site. COXI was used as loading control. D. Quantification of C. Error bars indicate s.e.m. ***P < 0.001, **P < 0.01 student's t-test.

3.1.5 A ketogenic diet does not impair the physiological conditions of *Mterf1* knockout mice.

We wanted to investigate if the physiological importance of MTERF1 is more critical when the need for oxidative phosphorylation is high. For that reason *Mterf1* knockout mice were fed with a ketogenic diet for 9 months. This diet consists of high fat and low carbohydrate portions and shifts metabolism from glycolysis to oxidative phosphorylation (Kennedy et al., 2007). A previous study has shown the effectiveness of such a diet to provoke phenotypes in apparently healthy animals lacking MTERF2 expression (Wenz et al., 2009).

We performed basic molecular characterization on *Mterf1* knockout and control mice, which were treated with ketogenic diet and found normal mtDNA level by doing southern blot analysis with isolated DNA from liver and skeletal muscle in both mouse models (Figure 3.6 C). Steady state levels of mitochondrial transcripts were checked with northern blot experiments of RNA isolated from heart of *Mterf1* knockout and control animals. No difference was found in mice lacking MTERF1 compared to wild type controls and also the assembly of respiratory chain complexes was unaffected as demonstrated in Blue native

PAGE analysis of mitochondrial protein extracts from brain and skeletal muscle (**Figure 3.6 D,E**) In addition, glucose tolerance tests and check-up of standard clinical chemistry blood parameters could not trace any phenotype in *Mterfl* knockout mice (**Figure 3.6 A,B**). Even though we were unable to find any difference in *Mterfl* knockout mice treated with ketogenic diet compared to controls, one cannot exclude the possibility, that there are slight shifts regarding the oxidative phosphorylation capacity, which are not detectable with the available methods.



Terzioglu et al., Cell metabolism, 2013

Figure 3.6: Phenotyping of *Mterfl* knockout mice after treatment with ketogenic diet. A Glucose tolerance test of *Mterfl* knockout (n=3) and wild-type (n=4) mice after treatment with ketogenic diet. The left panel shows the data for each animal. The right panel shows the mean values in *Mterfl* knockout and wild-type mice. B. Analysis of standard clinical chemistry blood parameters in *Mterfl* knockout (n=12) and wild-type (n=10) mice after treatment with ketogenic diet. C. Southern blot analysis in Liver and Skeletal muscle from control (n=4 for Liver, n=5 for Skeletal Muscle) and *Mterfl* knockout (n=4 for Liver, n=5 for Skeletal Muscle) mice (left panel) and quantification (right panel) of steady-state levels of mtDNA in heart from *Mterfl* knockout (n=4) and wild-type (n=4) mice after treatment with ketogenic diet. D. Northern blot analysis (left panel) and quantification (right panel) of steady-state levels of mtDNA-encoded transcripts in heart from *Mterfl* knockout (n=4) and wild-type

(n=4) mice after treatment with ketogenic diet. Error bars indicate SEM; Student's t test was used to assess statistical significance: * = p<0.05, ** = p<0.01, *** = p<0.001 E. BN-PAGE analysis of steady-state levels of respiratory chain complexes in Brain and Skeletal Muscle of *Mterf1* knockout (n=3) and wild-type (n=3) mice after treatment with ketogenic diet.

The text of section 3.1 was modified according to Terzioglu et al., *MTERF1 binds mtDNA to prevent transcriptional interference at the light-strand promoter but is dispensable for rRNA gene transcription regulation*, Cell metabolism 17, 618-626.

3.2 Analysis of mitochondrial gene regulation at the transcriptional level in *Mterf2* knockout mice

3.2.1 Creation of *Mterf2* knockout mice

Mterf2 is located on mouse chromosome 10 and spans a region about 8.5 kilobases. The gene contains three exons from which only exon 3 is coding and produces a 1565 bp long immature transcript. This transcript then gives rise to a 385 amino acid residue mature protein with a predicted size of 39 kDa. Edman degradation revealed a 35 residue long targeting peptide (amino acids 1-35) present in the precursor protein and absent in the mature MTERF2 (Pellegrini et al., 2009). At the time, while designing a targeting strategy for the *Mterf2* gene publicly available sequencing data proposed another possible coding region on the antisense strand. In fact, exon 4 of the proposed mCG13745 gene was found to be embedded in the exon 3 of *Mterf2* (Figure 3.7 A). In this particular case, floxing and deletion of *Mterf2*-exon 3 would also cause the deletion of mCG13745-exon 4 and the resulting phenotype would not represent exclusively *Mterf2*. Therefore, deletion of only the target gene had to take place without disrupting the antisense region. As an alternative way to inactivate the *Mterf2*-exon 3 through homologous recombination, site directed mutagenesis at two different positions was introduced; one causing an artificial STOP codon and the other a frame shift in the *Mterf2*-exon 3 coding sequence (Figure 3.7 A). In addition, a neomycin cassette flanked by two *frt* (flippase recognition target) sites was introduced upstream of exon 3 in order to have a screening marker for the targeted ES cell clones carrying the targeting vector. Electroporated ES cells were screened for the targeting vector by DNA isolation from each clone and digestion with *NheI* before used for southern blot analysis. Detection of the targeted allele with southern blot was confirmed by using a probe covering the exon 4 of mCG13745 region (Figure 3.7 B). After confirmation of positively tested ES cell clones via southern blot (Figure 3.7 C), they were expanded and used for blastocyst injection to produce *Mterf2* knockout mice. Contribution of the targeted ESC clones was monitored with the produced chimeras and further matings of these provided germ line transmission of the targeted allele at heterozygote state. The removal of the neomycin cassette in these mice was ensured by crossing them with mice expressing the *Flp* recombinase. As a result of the heterozygote matings *Mterf2* knockout mice were finally achieved by a STOP codon and frameshift mutations created in exon 3 of the *Mterf2* gene without interfering with the expression of the mCG13745 gene. The absence of MTERF2 protein in *Mterf2* knockout mice was proven by western Blot analysis using an antibody against MTERF2 (Figure 3.7 D).

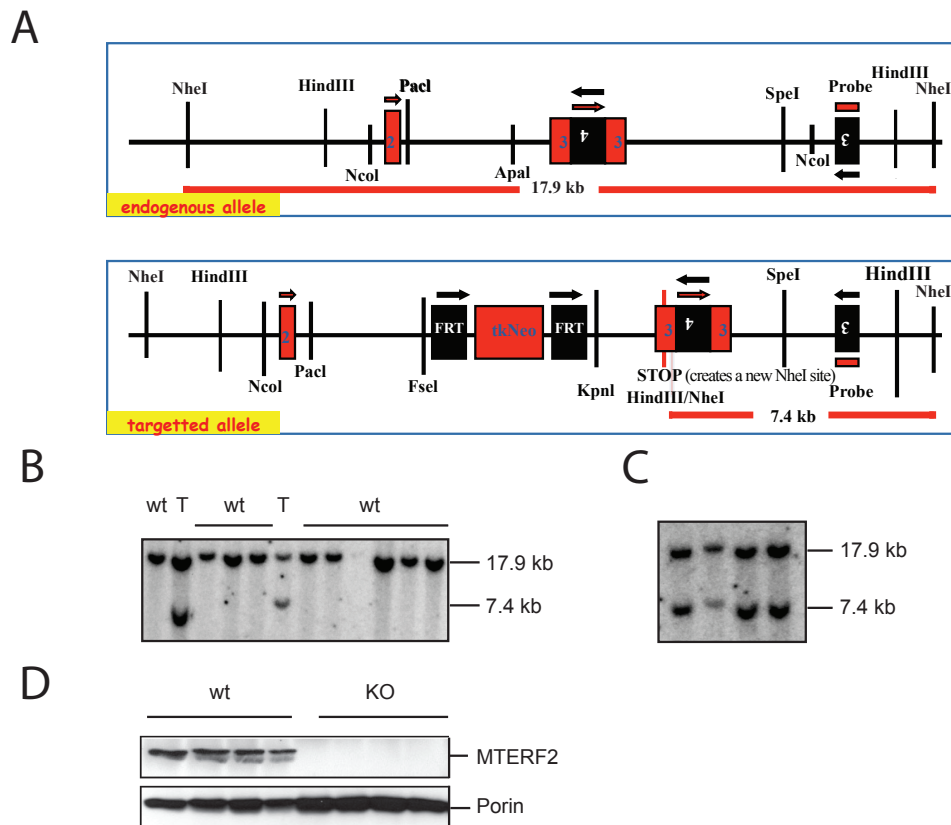


Figure 3.7: Targeting and screening of the *Mterf2* knockout mouse. A. Targeting strategy for disruption of the *Mterf2* gene (red boxes). Another overlapping gene candidate (mCG13745) on the antisense region is shown in black boxes. Probes and restriction enzyme sites used for the ES cell screening are indicated B. Southern Blot analysis to screen for targeted ES cells. Wild type band migrates at 17.9 kb, knockout band migrates at 7.4 kb. C. Southern Blot analysis to confirm targeted ES cell clones. D. Western Blot in heart tissue of wild type (n=4) and *Mterf2* knockout (n=4) animals to check MTERF2 protein levels. Porin was used as loading control.

3.2.2 *Mterf2* knockout mice are fertile and viable under normal and stress conditions

Mice lacking MTERF2 are apparently healthy, fertile and have a normal life span. Previous studies analyzing the absence of MTERF2 in knockout mice created by a gene trap strategy did not report any obvious difference in lifespan and general body conditions as well (Wenz et al., 2009). We followed up the body weight gain in a group of animals containing male and female wild type and *Mterf2* knockout mice backcrossed in the sixth generation between four weeks and 13 weeks of age (**Figure 3.8 A**). There was no statistically significant difference in weight between wild-type and MTERF2 knockout mice, although we observed a tendency to weight reduction when both sexes of the different genotypes were grouped together (**Figure 3.8 A**). In order to check physiological differences in control and *Mterf2* knockout mice, glucose tolerance tests (GTT) were performed. Defective glucose clearance from the blood after glucose injection can be an indicator for mitochondrial malfunction, since reduced levels of mtDNA have been shown to affect the expression of nuclear-encoded glucose transporter

(Rolo and Palmeira, 2006) and mitochondrial dysfunction has been reported in prediabetic patients (Lee et al., 1998; Rolo and Palmeira, 2006). For this reason, we injected 2g/kg glucose in 25 weeks old male and female animals and found a normal recovery of glucose levels in mice lacking MTERF2 compared to wild type supporting the idea of a normal mitochondrial biogenesis (Figure 3.8 B).

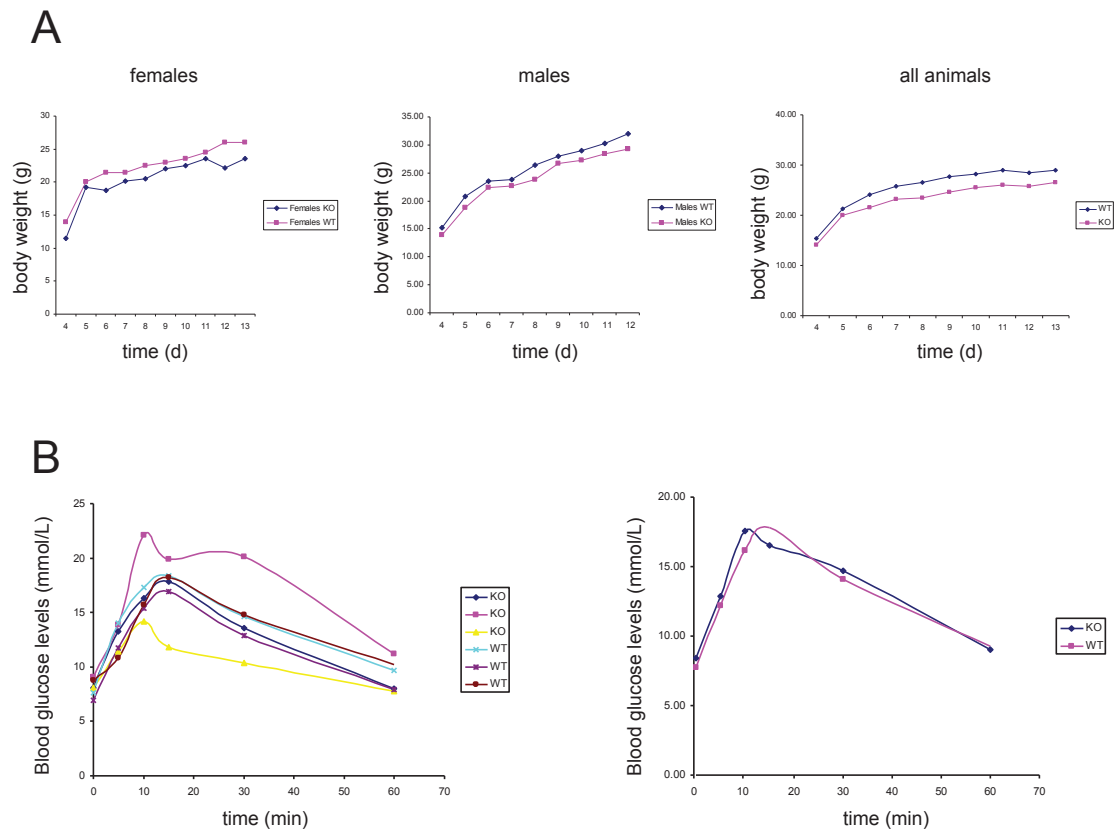


Figure 3.8: Body weight curves and glucose tolerance tests in *Mterf2* knockout and control mice.
 A. Body weight curves of female (left panel), male (middle panel) and all animals (right panel) of wild type (n=10) and *Mterf2* knockout (n=10) from 4 to 13 weeks of age. B. Glucose tolerance test in wild type (n=3) and *Mterf2* knockout (n=3) mice. 2g/kg glucose was injected per animal. The left panel shows individual data of all tested animals, the right panel indicates average values for wild type and *Mterf2* knockout animals, respectively.

Concerning their *Mterf2* knockout mouse model Wenz and co-workers found a muscle specific phenotype when animals were subjected to a ketogenic diet (Wenz et al., 2009). This high-fat, low-carbohydrate diet forces a metabolic shift from glycolysis towards oxidative phosphorylation in the cell. The metabolic shift provides a sensitive environment to uncover slight deficiencies in mitochondria, which are easily compensated under normal conditions. *Mterf2* knockout animals fed with this diet for about 6 months were shown to develop muscle weakness and orientation problems (Wenz et al., 2009), but also defects in oxidative

phosphorylation activity, since these mice had decreased expression levels of mitochondrial encoded genes (Wenz et al., 2009).

Another way of stressing mice to reveal slight phenotypic differences in mitochondrial physiology is to expose them at low temperatures. Under cage conditions with standard diet and temperature our *Mterf2* knockout mice did not show any apparent phenotype. We therefore decided to expose these animals to metabolic stress by keeping them at 4°C for six months. Cold temperatures lead to physiological changes including increased oxidative phosphorylation activity with increased oxygen consumption (Mollica et al., 2005). *Mterf2* knockout and control mice were individually placed in metabolic cages and subjected to normal (30°C) and cold (4°C) temperatures. Oxygen consumption was measured over three hours but there was no difference between control and *Mterf2* knockout animals for both temperatures (Figure 3.9 A,B). Another approach to study was the treatment with norepinephrine (NE), a hormone related to adrenaline causing shock-like symptoms when given in a certain amount, but again there was no change in oxygen consumption in wild type and *Mterf2* knockout mice at 30°C and 4°C (Figure 3.9 C,D). Furthermore, muscle weight as well as absolute fat content in cold exposed animals at 15 weeks age was not changed in comparison with controls under stress conditions (Figure 3.9 E,F). In summary, lack of MTERF2 does not impair metabolic standard values under normal and stress conditions.

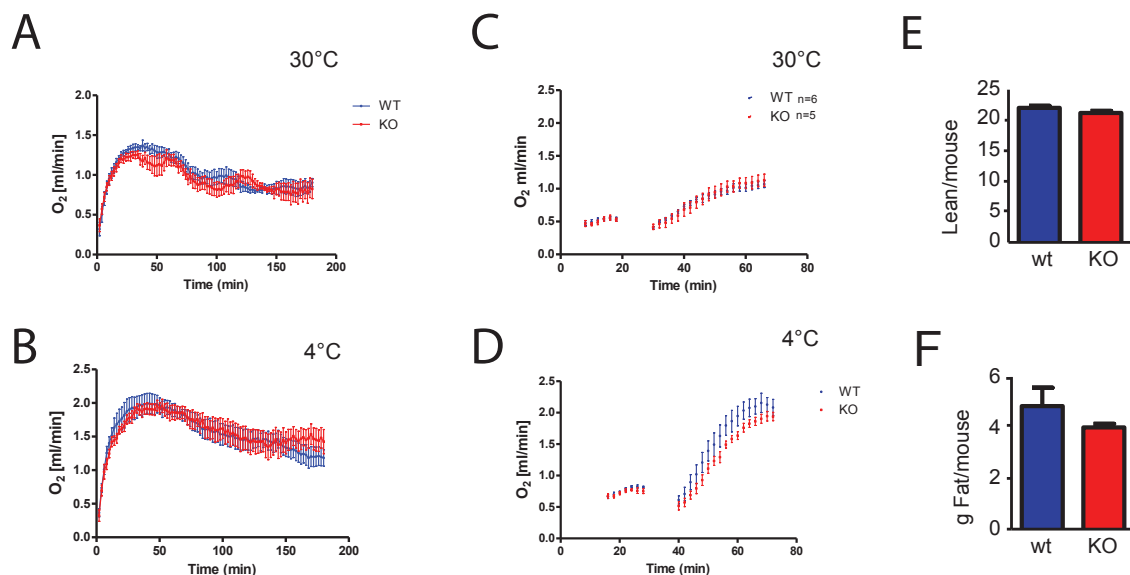


Figure 3.9: Metabolic phenotyping of control and *Mterf2* knockout mice. A. Oxygen consumption of wild type (n=6) and *Mterf2* knockout (n=6) mice at physiological temperature (30°C). Mice were measured individually about three hours. B. Oxygen consumption of wild type (n=6) and *Mterf2* knockout (n=6) mice at 4°C. Mice were measured individually about three hours. C. Oxygen consumption of wild type (n=6) and *Mterf2* knockout (n=5) mice treated with norepinephrine at 30°C. D. Oxygen consumption of wild type (n=6) and *Mterf2* knockout (n=5) mice treated with norepinephrine at 4°C. E. Muscle weight (lean) of wild type (n=6) and *Mterf2* knockout (n=6) mice. Error bars indicated s.e.m. F. Measurement of fat content at 4°C in 10 weeks old wild type (n=6) and *Mterf2* knockout (n=6) mice. Error bars indicate s.e.m..

3.2.3 MTERF2 is dispensable for maintenance and expression of mtDNA

The existence of two different *Mterf2* knockout mouse models showing different phenotypes was a surprising fact, which tempted us to figure out the reason for this discrepancy. One obvious distinction between the two knockout mouse models is the gene trap strategy used for disruption of the *Mterf2* gene in one of the mouse models. A gene coding for cryptochrome 1 (CRY1), functioning in regulation of circadian rhythms, is situated in close proximity to *Mterf2*. In order to study a potential impact of the gene trap on the CRY1 promoter we decided to directly compare control animals with both *Mterf2* knockout mice models (named T2N (created by homologous recombination) and T2M (created by gene trap)) and mice lacking CRY1. At the same time, the *in vivo* function of MTERF2 was still in the main focus of our studies.

We performed Southern Blot analyses with DNA isolated from heart tissue to assess mtDNA levels in wild type and all three knockout mouse models by using a COXI probe to detect mtDNA and 18S as nuclear encoded loading control. MtDNA levels were not affected by lack of MTERF2 in both *Mterf2* knockout mouse models, but seem to increase in *Cry1* knockout mice (**Figure 3.10**).

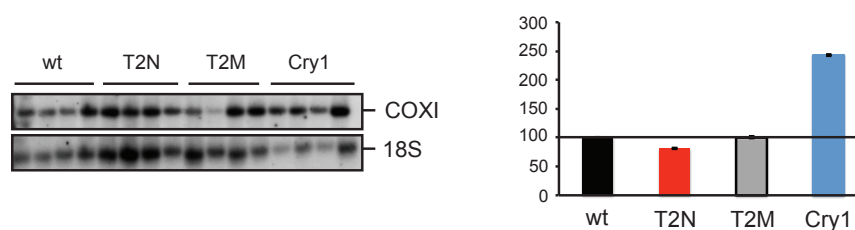


Figure 3.10: MtDNA levels in controls, *Mterf2* knockout mice (T2N and T2M) and *Cry1* knockout mice. A. Southern Blot analysis in heart tissue of wild type (n=4), *Mterf2* N (n=4), *Mterf2* M (n=4) and *mCry1* knockout (n=4) mice. 18S was used as nuclear encoded loading control. B. Quantification of A. Error bars indicate s.e.m.

A previous report claims MTERF2 has a role in mitochondrial transcription causing decreased steady state transcript levels and therefore defects in oxidative phosphorylation activity in the absence of this protein (Wenz et al., 2009). However, we could not confirm these data in our mouse models, since northern blot analysis with RNA isolated from heart, kidney, liver, skeletal muscle and brain revealed normal transcript levels of mitochondrial encoded genes in all tissues tested from *Mterf2* N knockout, *Mterf2* M knockout and *Cry1* knockout mice (**Figure 3.11**).

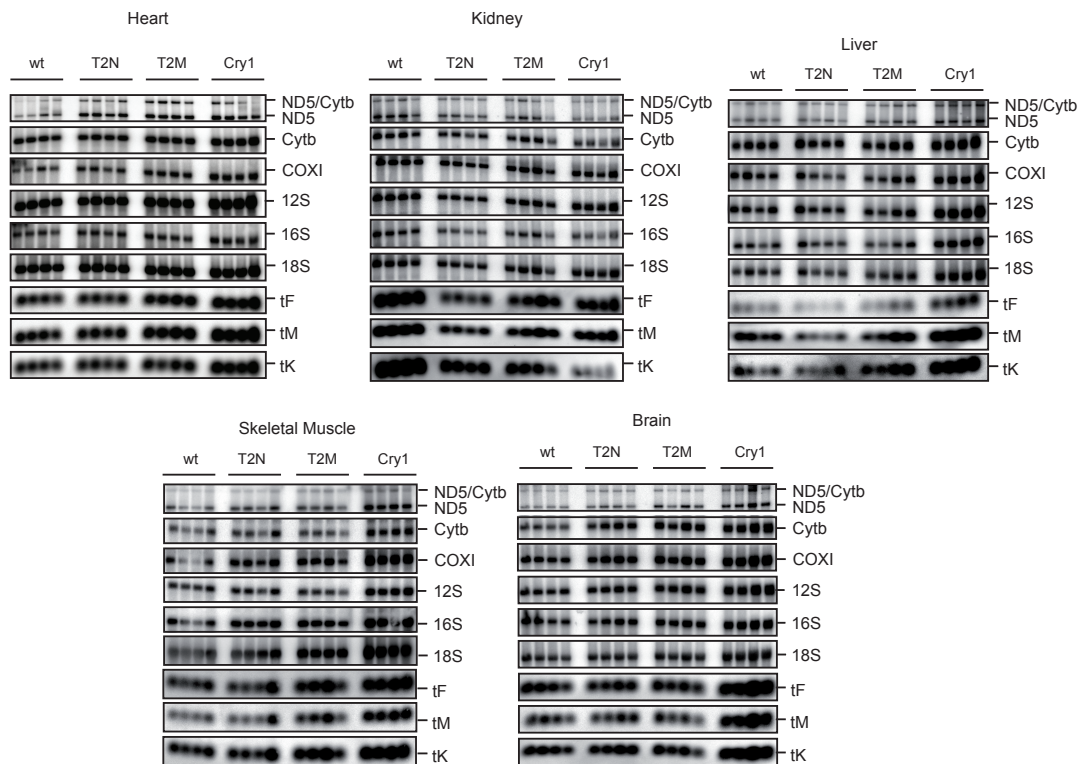


Figure 3.11: Steady state mitochondrial transcript levels in heart, kidney, liver, skeletal muscle and brain are unchanged in wild type, *Mterf2* N knockout, *Mterf2* M knockout and *Cry1* knockout mice. Northern Blot analysis with RNA from heart, kidney, liver, skeletal muscle and brain in control (n=4), *Mterf2* N (n=4), *Mterf2* M (n=4) and *Cry1* (n=4) knockout mice. 18S was used as loading control. Membranes were stripped after each probe.

We also checked rRNA as well as tRNA levels in mutant animals and controls, revealing unaffected steady state levels in heart, kidney, liver, skeletal muscle and brain in all knockout mouse models (**Figure 3.11**). These data suggest normal ribosomal biogenesis as well as unchanged *de novo* synthesis of mitochondrial transcripts in *Mterf2* N, *Mterf2* M and *Cry1* knockout mouse models as already discussed above in section 3.1.3. In order to confirm these data, we performed additional qPCR experiments in cDNAs of brain, liver and skeletal muscle from control, *Mterf2* N, *Mterf2* M and *Cry1* knockout mice. Probes detecting Cytb, COXI, COXII, ND6, 12S and 16S were used, but no difference in the transcript levels between knockout mice and controls were found confirming the data from northern blot analyses (**Figure 3.12 A**). We also assessed expression levels of nuclear encoded mitochondrial transcription factors, with cDNAs from liver and skeletal muscle of *Mterf2* N, *Mterf2* M and *Cry1* knockout mice (**Figure 3.12 B**). Probes for studying steady state mRNA levels of the core transcription machinery were used, but we found no differences in expression of POLRMT, TFB2M and TFAM (**Figure 3.12 B**). This contradicts previous reports showing a compensational, muscle-specific increase in expression of mitochondrial

transcription factors during the absence of MTERF2 (Wenz et al., 2009). Regarding mitochondrial biogenesis, the nuclear transcriptional co-activator PGC 1-alpha and also TFAM, an important factor for mtDNA packing and maintenance, was found normally expressed in mice lacking MTERF2 or CRY1, respectively (**Figure 3.12 B**). Finally, a probe detecting pol gamma mRNA revealed unchanged expression levels in control, *Mterf2* N, *Mterf2* M and *Cry1* knockout mouse models, making it unlikely that MTERF2 has a role in mitochondrial replication (**Figure 3.12 B**). It was surprising to notice, that even the *Mterf2* knockout mice created by gene trap were not affected in the mitochondrial transcription levels as shown before. In addition, lack of CRY1 does not affect these steady state transcript levels defeating our idea the reported defects in *Mterf2* knockout mice could be caused by the influence of the gene trap promoter on the *Cry1* gene.

Taken together, these data suggest that MTERF2 is dispensable for expression and maintenance of mtDNA.

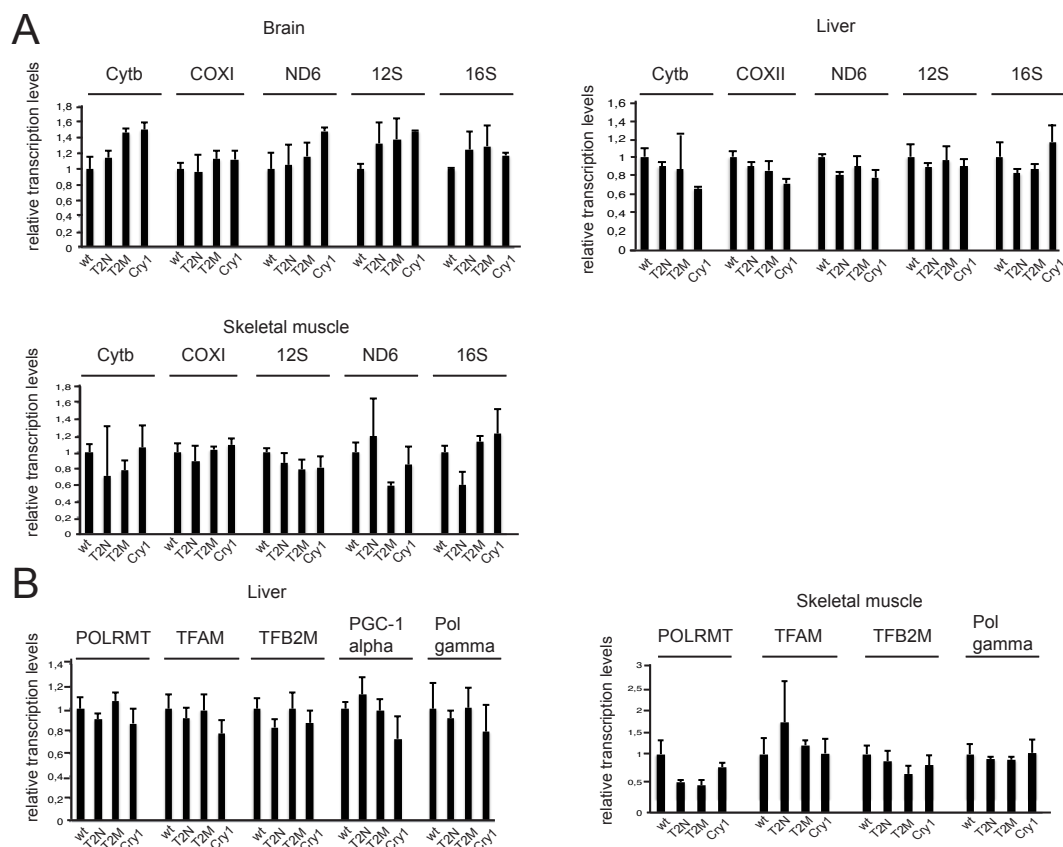


Figure 3.12: Steady state mRNA levels of mitochondrial encoded genes and mitochondrial transcription factors. A. QPCR analysis to study expression levels of mitochondrial encoded genes with cDNA isolated from brain, liver and skeletal muscle of control, *Mterf2* N, *Mterf2* M and *Cry1* knockout mice. Error bars indicate s.e.m. B. QPCR analysis to study expression levels of mitochondrial transcription factors with cDNA isolated from liver and skeletal muscle of control, *Mterf2* N, *Mterf2* M and *Cry1* knockout mice. Error bars indicate s.e.m..

3.2.4 Lack of MTERF2 is not compensated by other members of the MTERF-family

The healthy appearance of *Mterf2* knockout mice could be the result of functional compensation by another protein. Previous reports revealed upregulated levels of MTERF3 in *Mterf2* knockout mice (Wenz et al., 2009) suggesting a compensational transcription activation. We therefore decided to study steady state mRNA levels of all four MTERF family members to determine whether loss of MTERF2 in our mouse models reveals similar results. QPCR experiments were performed using cDNA from liver and skeletal muscle of control, *Mterf2* N, *Mterf2* M and *Cry1* knockout mice. We used probes detecting *Mterf1*, *Mterf2*, *Mterf3* and *Mterf4* and found normal expression of these genes in all knockout mouse models compared to wild type controls (**Figure 3.13**). MTERF2 expression levels were normal as expected in *Cry1* knockout mice, whereas no expression could be detected in *Mterf2* M knockout mice due to disruption of the *Mterf2* gene by the use of a gene trap. *Mterf2* N knockout mice however, carry a STOP codon in the coding sequence allowing normal transcription of MTERF2. However, the MTERF2 transcript cannot be translated to MTERF2 protein. In summary, lack of MTERF2 does not cause any compensational response regarding other MTERF family proteins (**Figure 3.13**).

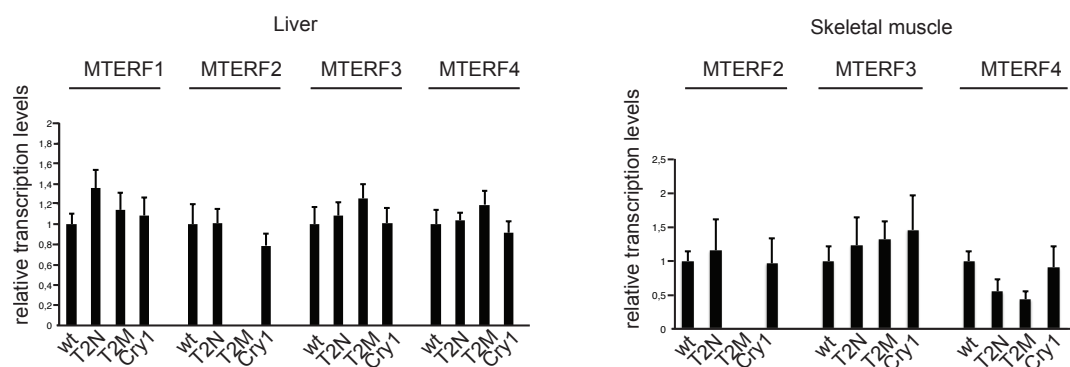


Figure 3.13: Expression levels of MTERF family proteins. QPCR analysis to study expression levels of MTERF family proteins with cDNA isolated from liver and skeletal muscle of control, *Mterf2* N, *Mterf2* M and *Cry1* knockout mice. Error bars indicate s.e.m..

In order to gain further ideas at which level MTERF2 has a role in mitochondrial metabolism, Western Blot analysis was performed in order to check MTERF2 protein levels in different knockout mouse models. Total mitochondrial extract from heart mitochondria of *Lrpprc* knockout mice, *Mterf3* knockout mice, *Mterf4* knockout mice and *Tfam* knockout mice revealed normal MTERF2 steady state protein levels, suggesting that MTERF2 is not directly

interacting with the mitochondrial ribosome, since mice lacking MTERF3 or MTERF4 suffer from deficient mitochondrial ribosomal assembly and decreased translational activity (**Figure 3.14**). Furthermore, LRPPRC is a good indicator for mitochondrial RNA levels since its protein levels always follow the RNA amount in mammalian mitochondria. Unaffected MTERF2 protein levels in this mouse indicate, that this protein rather does not directly interact with mitochondrial RNAs. *Tfam* knockout mice lack mtDNA and as a consequence mitochondrial transcription. Normal MTERF2 protein levels in these mice confirm our data shown above indicating that MTERF2 does not have a role in mtDNA expression. Further analysis concerning RNA binding capabilities or *de novo* translation analyses are necessary to define a function of MTERF2 in mitochondrial RNA metabolism.

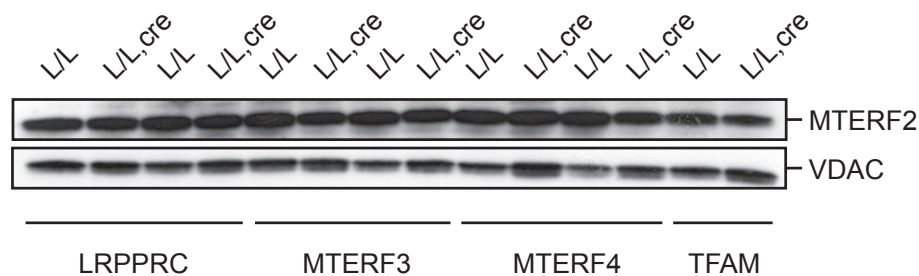


Figure 3.14: MTERF2 protein levels in different knockout mouse models. Western Blot analysis in mitochondrial extracts from heart of *Lrpprc*, *Mterf3*, *Mterf4* and *Tfam* knockout mice (L/L,cre) and controls (L/L) in order to check MTERF2 protein levels. VDAC was used as loading control.

3.2.5 MTERF2 does not affect oxidative phosphorylation activity

Loss of MTERF2 is shown to cause decreased steady state levels of subunits of the respiratory chain complexes (Wenz et al., 2009), a consequence of the reduced expression levels of mitochondrial encoded genes. In order to examine whether we can reproduce these data at least in *Mterf2* M and/or the *Cry1* knockout mouse model, we performed western blot experiments in mitochondrial extracts from brain, heart, kidney, liver and skeletal muscle. An antibody cocktail was used, containing antibodies against respiratory chain subunits of all complexes. We found normal levels of NDUFB8 (complex I), SDHA (complex II), UQCRC2 (complex III), COX1 (complex IV) and ATP5A1 (complex V) in all tissues of *Mterf2* N, *Mterf2* M and *Cry1* knockout mice (**Figure 3.15**).

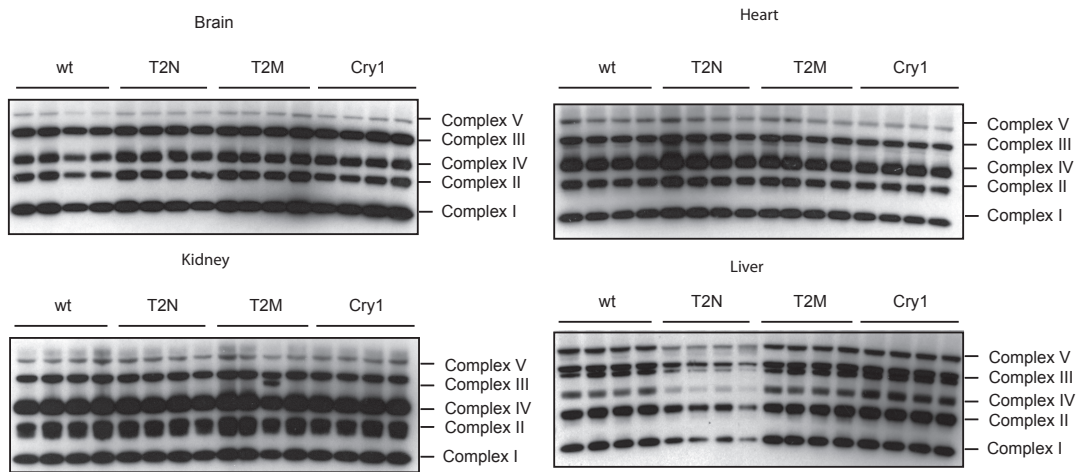


Figure 3.15: Steady state protein levels of respiratory chain subunits in wild type *Mterf2* N, *Mterf2* M and *Cry1* knockout mice. Western Blot experiments in total mitochondrial extracts of brain, heart, kidney and liver of Control (n=4), *Mterf2* N (n=4), *Mterf2* M (n=4) and *Cry1* (n=4) knockout mice. Antibody cocktail detecting NDUFB8 (complex I), SDHA (complex II), UQCRC2 (complex III), COX1 (complex IV) and ATP5A1 (complex V) was used. Nuclear encoded complex II was used as loading control.

In addition, Blue native PAGE analysis was performed in mitochondrial extracts from brain, heart, kidney and skeletal muscle to study the assembly of supercomplexes, but again we found unaffected patterns of assembled respiratory chain complexes and supercomplexes in *Mterf2* N, *Mterf2* M and *Cry1* knockout mice (**Figure 3.16**). In summary, these data together with the other results shown above do not support previous reports claiming that MTERF2 is a mitochondrial transcription factor. Our data suggest that MTERF2 is not involved in mitochondrial transcription or mtDNA maintenance, because mtDNA expression levels as well as steady state protein levels of the mitochondrial transcription machinery, and mitochondrial encoded genes appeared unaffected. Further experiments focusing on *in vivo* translation, RNA binding and binding partner experiments are planned to reveal the *in vivo* function of MTERF2.

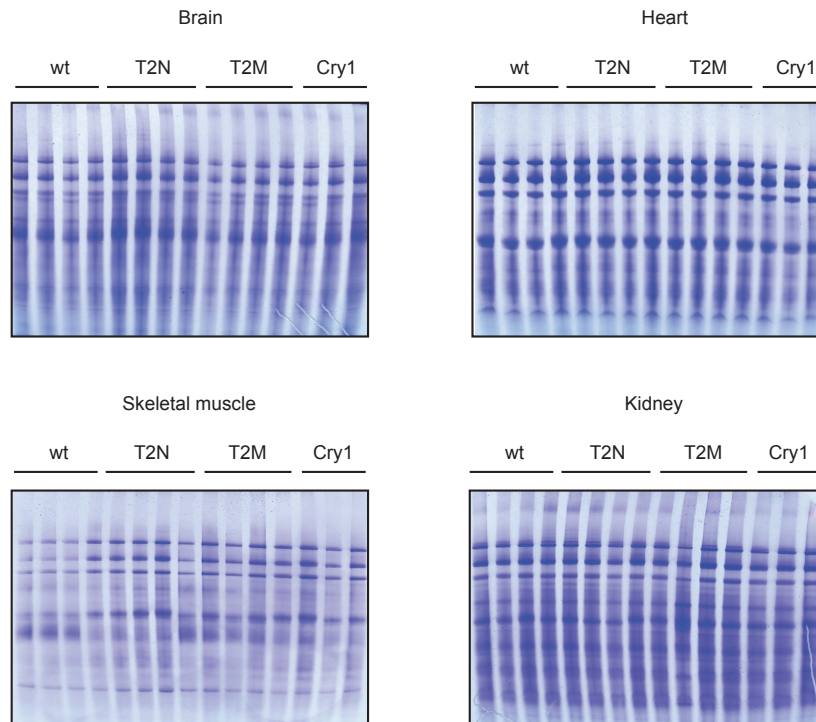


Figure 3.16: Super complex assembly is not affected by loss of MTERF2 and CRY1. Blue Native PAGE analysis with total mitochondrial extracts from brain, heart, skeletal muscle and kidney of wild type (n=4), *Mterf2* N (n=4), *Mterf2* M (n=4) and *Cry1* (n=4) knockout mice.

3.2.6 *Cry1* expression levels are downregulated in *Mterf2* knockout mice

Contrary to our expectations we noticed that *Cry1* knockout mice do not show any apparent phenotype resembling the results reported for *Mterf2* M knockout mice. Due to the close proximity of *Cry1* to the *Mterf2* gene, it was prone to be influenced by strong neighbouring promoters as for example a gene trap. In order to study *Cry1* levels in *Mterf2* N and *Mterf2* M knockout mouse models qPCR experiments were performed, using a probe detecting mRNAs of the gene of interest. Surprisingly, we found a forty to sixty percent decrease of *Cry1* expression levels in liver, heart, brain and skeletal muscle in both *Mterf2* N and *Mterf2* M knockout models meaning that reduced steady state mRNA levels in these animals are independent from the knockout strategy (**Figure 3.17**). It is rather likely, that loss of MTERF2 protein is responsible for the reduced CRY1 levels. Further studies have to be done uncovering the role of MTERF2 on *Cry1* expression.

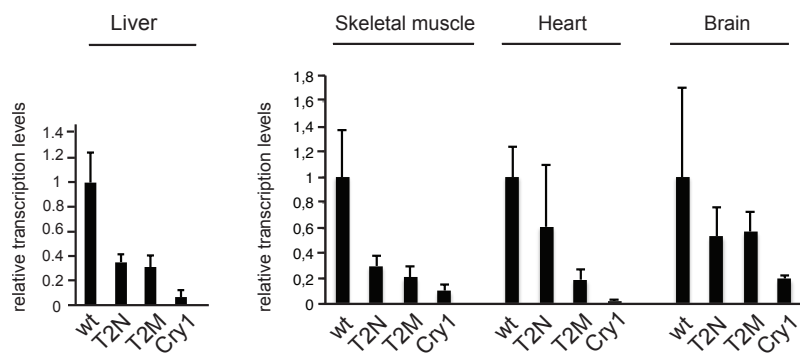


Figure 3.17: Steady state expression levels of *Cry1* in different tissues. QPCR analysis to study *Cry1* levels in cDNA of liver, skeletal muscle, heart and brain from control (n=4), *Mterf2* N (n=4), *Mterf2* M (n=4) and *Cry1* (n=4) knockout mice. Error bars indicate s.e.m..

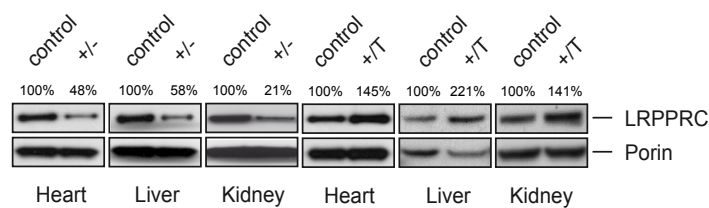
3.3 Analysis of mitochondrial gene regulation at the posttranscriptional level in *Lrpprc*^{+/-} and *Lrpprc*^{+/T} mice

3.3.1 *Lrpprc* heterozygous knockout mice and *Lrpprc* overexpressor mice are fertile and viable

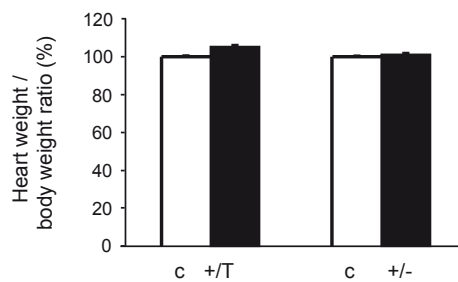
In order to gain more profound insights into the process of posttranscriptional regulation we decided to analyze mice with moderately decreased or increased LRPPRC expression.

Therefore, *Lrpprc*^{+loxP} mice were mated to mice expressing cre recombinase under the control of the β -actin promoter to generate heterozygous *Lrpprc* knockout (*Lrpprc*^{+/-}) mice (Ruzzenente et al., 2012).

A



B



Harmel et al., JBC, 2013

Figure 3.18: Heart to body weight ratio is not affected by moderately altered levels of LRPPRC.

A. Western blot analysis of LRPPRC levels in mitochondrial extracts of heart, liver and kidney from control, heterozygous *Lrpprc* knockout (+/-) and *Lrpprc* overexpressing (+/T) mice at age 10 weeks. Porin was used as loading control. The relative levels of LRPPRC are indicated above the lanes. B. Heart weight to body weight ratios in control, heterozygous *Lrpprc* knockout (+/-) and *Lrpprc* overexpressing (+/T) mice at age 10 weeks. Number of studied animals: n= 6 (control), n= 6 (+/-), n=6 (+/T). Error bars indicate SD.

In these mice LRPPRC protein levels in heart, liver and kidney were decreased about 50%, as expected (Figure 3.18 A). Increased heart to body weight ratio often gives evidence for a

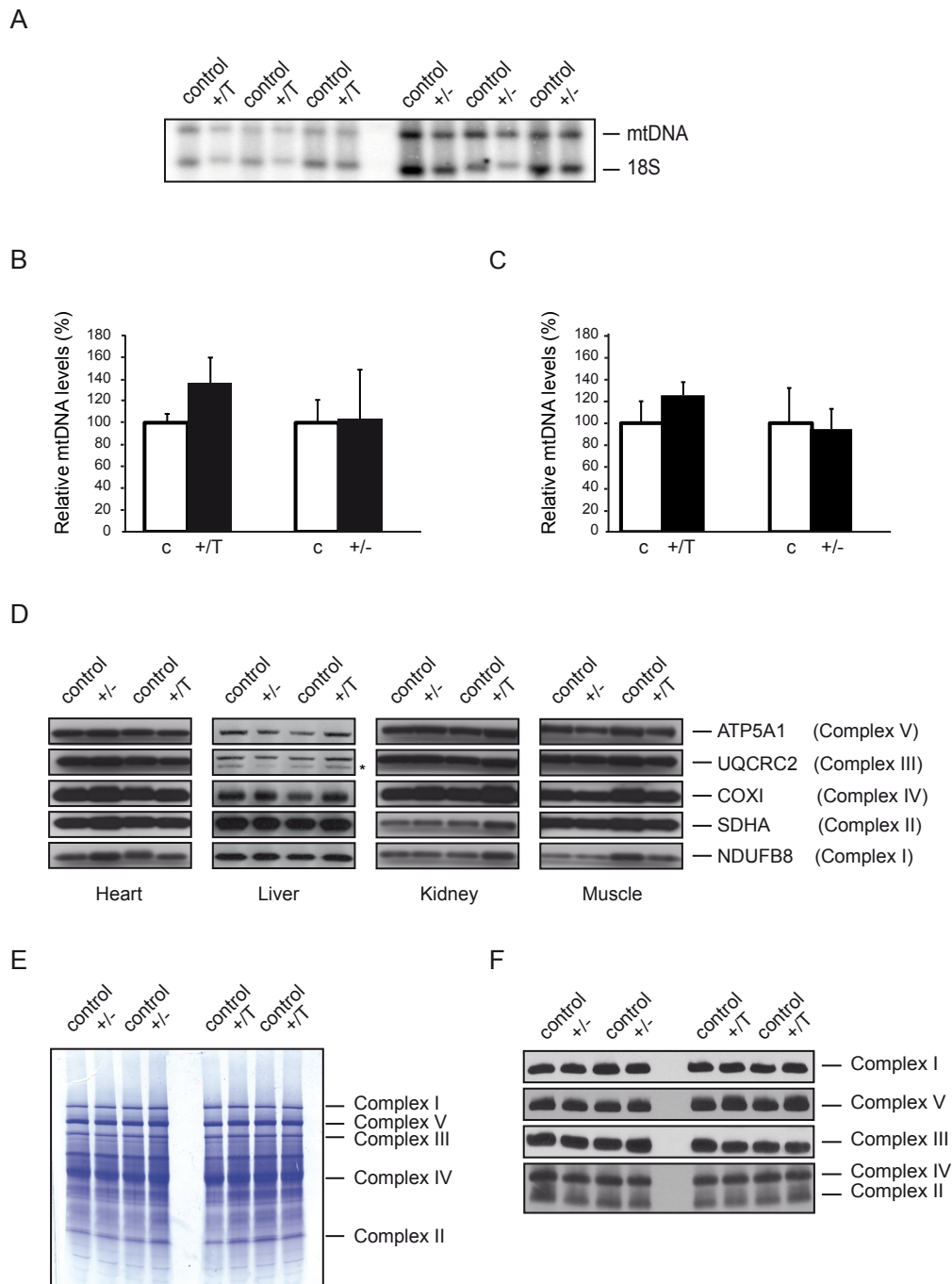
cardiomyopathy, a good indicator for mitochondrial dysfunction that was also found in mice lacking LRPPRC in the heart (Ruzzenente et al., 2012). However, *Lrpprc*^{+/-} mice were not affected as shown in **Figure 3.18 B**. Heart to body weight ratio was normal, the animals were fertile, apparently healthy and showed a normal life span.

We also generated a second transgenic mouse model moderately overexpressing LRPPRC (LRPPRC^{+T}), mediated by introduction of a Bacterial Artificial Chromosome (BAC) in the oocyte to study *in vivo* effects of slightly increased LRPPRC protein levels. As documented in **Figure 3.18 A**, these animals showed a two-fold up regulation of LRPPRC in heart, liver and kidney, but no effect on their heart to body weight ratio (**Figure 3.18 B**). Moderately decreased or increased levels of LRPPRC did not create any obvious phenotype. Both mouse models were viable, fertile and apparently healthy with a normal lifespan.

3.3.2 LRPPRC does not regulate the amount of respiratory chain complexes

We continued the analysis by investigating a regulatory function of LRPPRC regarding mtDNA levels and complexes of the respiratory chain in *Lrpprc*^{+/-} and *Lrpprc*^{+T} mice. Southern Blot experiments in liver extracts from wild type and mutant animals revealed normal mtDNA levels (**Figure 3.19 A,B**). These results were also confirmed by qPCR analysis (**Figure 3.19 C**) and are in good agreement with previous studies showing that LRPPRC has no essential role in maintaining DNA levels in mammalian mitochondria ((Liu et al., 2011; Ruzzenente et al., 2012) even though it was found being part of the mitochondrial nucleoid (Bogenhagen et al. 2008).

Mice lacking LRPPRC in the heart develop a severe complex IV deficiency and in addition decreased levels of complex I and V (Ruzzenente et al., 2012). We performed western blot analysis in protein extracts of heart, liver, kidney and muscle in *Lrpprc*^{+/-} and *Lrpprc*^{+T} mice to study potential effects of moderately changed LRPPRC protein levels on respiratory chain complexes in these mice. Antibodies against subunits of all complexes of the oxidative phosphorylation system showed normal levels of NDUFB8 (complex I), SDHA (complex II), UQCRC2 (complex III), COXI (complex IV) and ATP5A1 (complex V) in *Lrpprc*^{+/-} and *Lrpprc*^{+T} mice (**Figure 3.19 D**). In addition, Blue Native PAGE experiments (**Figure 3.19 E**) followed by western blot (**Figure 3.19 F**) were performed to study the assembly of super complexes of the respiratory chain. Moderately altered LRPPRC protein level did neither influence proper assembly of subunits nor super complexes of the respiratory chain in both mice models.



Harmel et al., JBC, 2013

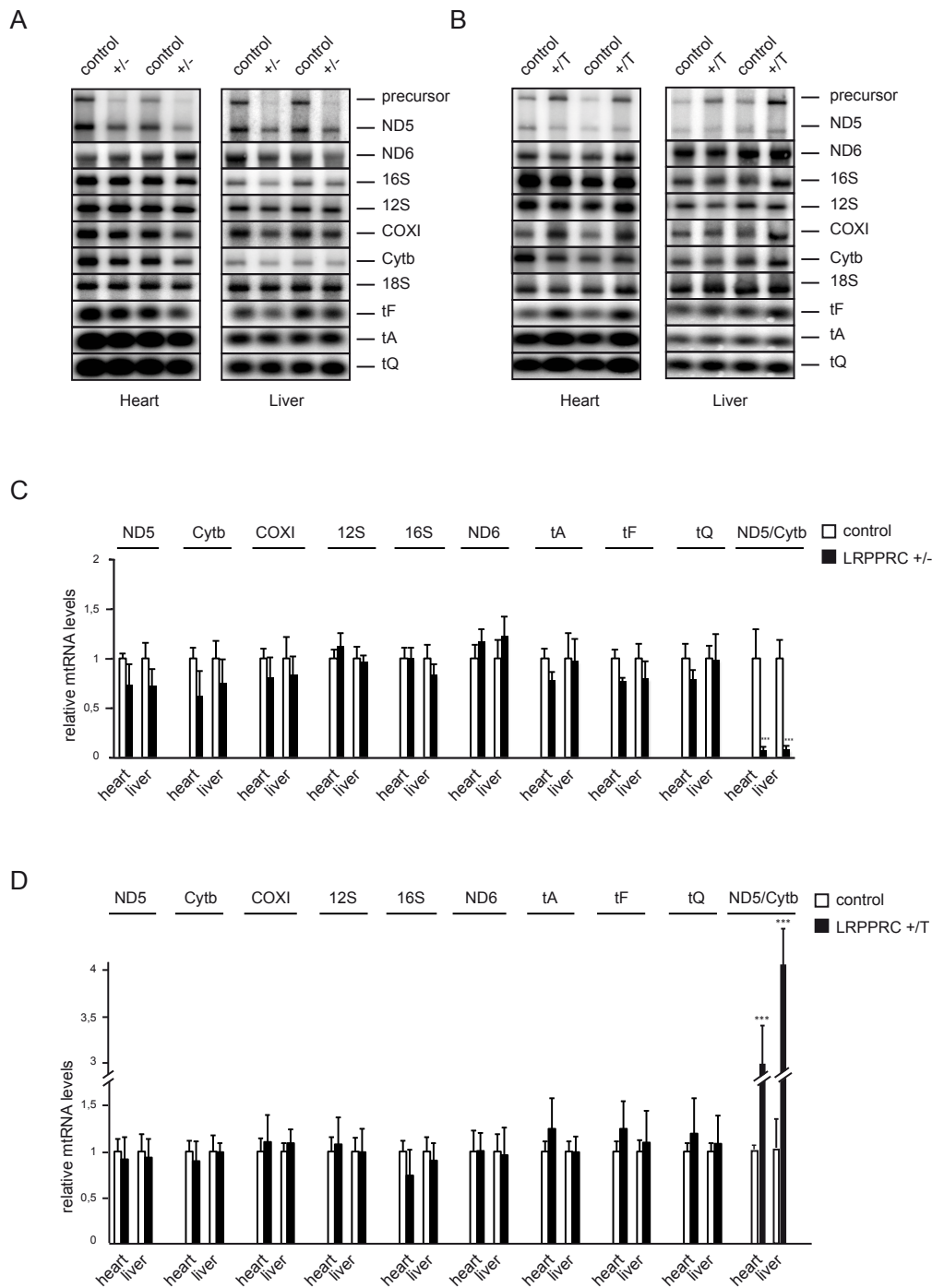
Figure 3.19: LRPPRC does not affect oxidative phosphorylation capacity. A. Southern Blot analysis of mtDNA levels in liver from control, heterozygous *Lrpprc* knockout (+/-) and *Lrpprc* overexpressing (+/T) mice at age 10 weeks. Number of studied animals: n=3 (control), n=3 (+/-), n=3 (+/T). The nucleus-encoded 18S rRNA gene was used as loading control. B. Quantification of mtDNA levels as determined by Southern blot analysis in panel A. Relative mtDNA levels in control, heterozygous *Lrpprc* knockout (+/-) and *Lrpprc* overexpressing (+/T) mice at age 10 weeks are shown. Number of studied animals: n=3 (control), n=3 (+/T), n=3 (+/-). Error bars indicate SD. C. Quantitative PCR analysis of mtDNA levels in control, heterozygous *Lrpprc* knockout (+/-) and *Lrpprc* overexpressing (+/T) mice at age 10 weeks. Number of studied animals: n=5 (control), n=5 (+/-), n=5 (+/T). Error bars indicate s.e.m. D. Western blot analysis of subunits of the respiratory chain complexes in mitochondrial extracts of heart, liver, kidney and muscle from control, heterozygous *Lrpprc* knockout (+/-) and *Lrpprc* overexpressing (+/T) mice at age 10 weeks. Nuclear encoded Complex II was used as loading control. *crossreacting band. E. Coomassie staining of blue native polyacrylamide

gel of mitochondrial extracts from liver of control, heterozygous *Lrpprc* knockout (+/-) and *Lrpprc* overexpressing (+/T) mice at age 10 weeks. F. Western blot analysis of levels of respiratory chain complexes in mitochondrial extracts of liver after separation in blue native polyacrylamide gels. Levels in control, heterozygous *Lrpprc* knockout (+/-) and *Lrpprc* overexpressing (+/T) mice are shown. The exclusively nuclear encoded complex II was used as loading control.

3.3.3 LRPPRC strongly influences levels of the ND5-Cytb precursor transcript

It has been shown previously, that reduced levels of LRPPRC lead to a severe decrease of all mitochondrial mRNAs encoded on the heavy strand (Ruzzenente et al., 2012; Sasarman et al., 2010), whereas overexpression of this protein has been reported to upregulate transcription of the same mRNAs (Liu et al., 2011; Ruzzenente et al., 2012). We therefore performed northern blot analysis in heart and liver from *Lrpprc*^{+/-} and *Lrpprc*^{+T} to field the question of a regulatory role of LRPPRC in mtDNA transcription. All transcript levels of mitochondrial mRNAs, rRNAs and tRNAs appeared unaffected comparing the transgenic with the wild type mouse models (**Figure 3.20** A-D). Previous studies in our group demonstrated that tRNA levels often go hand in hand with the transcription activity in mitochondria (Cámara et al., 2011; Metodiev et al., 2009; Park et al., 2007). Thus, normal tRNA levels in *Lrpprc*^{+/-} and *Lrpprc*^{+T} indicates LRPPRC likely being not involved in mtDNA transcription regulation.

Interestingly, the ND5/Cytb precursor transcript, an unprocessed fusion transcript of ND5 and Cytb, showed massively decreased levels in *Lrpprc*^{+/-} mice (**Figure 3.20** A,C), whereas it appeared to be strongly upregulated in *Lrpprc*^{+T} animals (**Figure 3.20** B,D). The apparent correlation between LRPPRC protein levels and the amount of the precursor allows speculations about a putative function of LRPPRC being involved in mitochondrial precursor maturation. Knockdown of the bicoid stability factor (BSF), the homologue of LRPPRC in the fruit fly *Drosophila melanogaster*, revealed similar results as loss of this protein also leads to RNA processing defects (Bratic et al., 2011). In summary, LRPPRC does not affect transcription of mitochondrial mRNAs, rRNAs and tRNAs, but could play a role in the maturation of mitochondrial ND5/Cytb precursor.

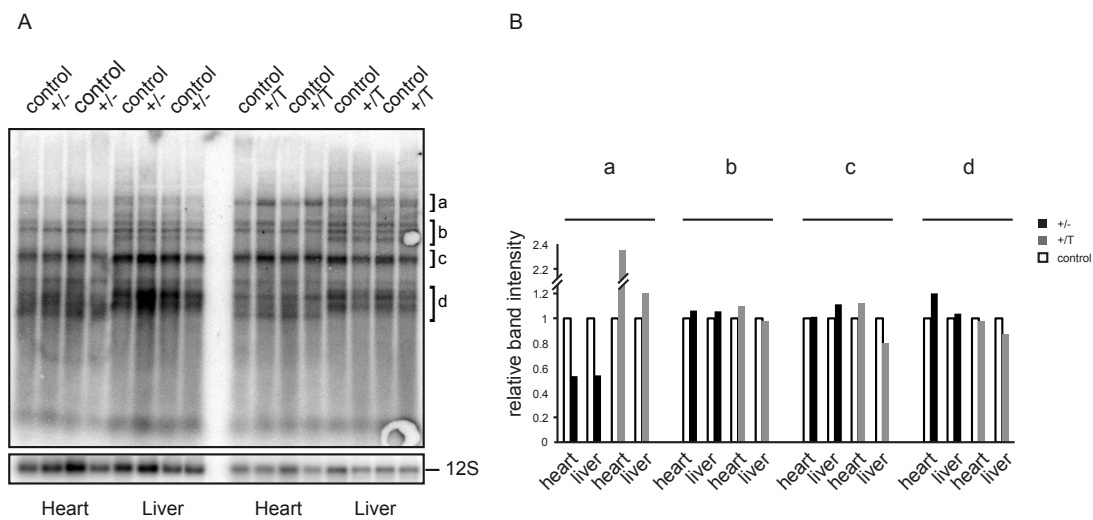


Harmel et al., JBC, 2013

Figure 3.20: Steady state levels of mitochondrial transcripts. A. Northern blot analysis of RNA isolated from heart and liver of control and heterozygous *Lrpprc* knockout (+/-) mice at 10 weeks of age. A separate autoradiograph is shown for every analyzed transcript. Nucleus-encoded 18S ribosomal RNA (18S) was used as a loading control. B. Northern blot analysis of RNA isolated from heart and liver of control and LRPPRC overexpressing (+/T) mice at 10 weeks of age. A separate autoradiograph is shown for every analyzed transcript. The nucleus-encoded 18S ribosomal RNA (18S) was used as a loading control. C. Quantification of steady-state levels of the transcripts from control (+/+; n=5) and heterozygous *Lrpprc* knockout (+/-; n=5) mice at 10 weeks of age. Error bars indicate s.e.m. ***P=0.001, Student's t-test. D. Quantification of steady-state levels of mitochondrial mRNAs, tRNAs and rRNAs from control (n=6) and *Lrpprc* overexpressing (+/T; n=6) mice at 10 weeks of age. Error bars indicate s.e.m. ***P=0.001, Student's t-test.

3.3.4 LRPPRC does not activate mitochondrial transcription

The *in vivo* function of LRPPRC is still highly debated in literature, despite strong evidence evolved from *in vivo* mouse models and patient cells supporting LRPPRC being necessary for mRNA stability, coordination of mitochondrial translation and polyadenylation of mitochondrial transcripts (Chujo et al., 2012; Ruzzenente et al., 2012; Sasarman et al., 2010). Cooper et al. recently reported LRPPRC being a part of the mitochondrial transcription machinery acting as transcriptional activator through direct interaction with the RNA polymerase (Liu et al., 2011). With two transgenic mouse models at hand, we performed *in organello* transcription experiments in heart and liver of *Lrpprc*^{+/-} and *Lrpprc*^{+T} animals in order to study a role of LRPPRC in mitochondrial transcription. Active mitochondria from heart and liver tissue were incubated in rotation for 1 hr with [α -³²P] UTP, to allow incorporation of the radiolabeled base pair in *de novo* synthesized RNAs. Levels of newly synthesized transcripts were unaffected by moderately increased or decreased LRPPRC protein levels, respectively as shown in *de novo* transcription experiments in **Figure 3.21 A, B**. However, we detected differences in the abundance of some high molecular weight transcripts, which were decreased in *Lrpprc*^{+/-} mice and increased in *Lrpprc*^{+T} mice (**Figure 3.21 A**). These findings are in agreement with the previously observed varying amounts of the ND5/Cytb precursor transcript and the putative role of LRPPRC in precursor maturation.



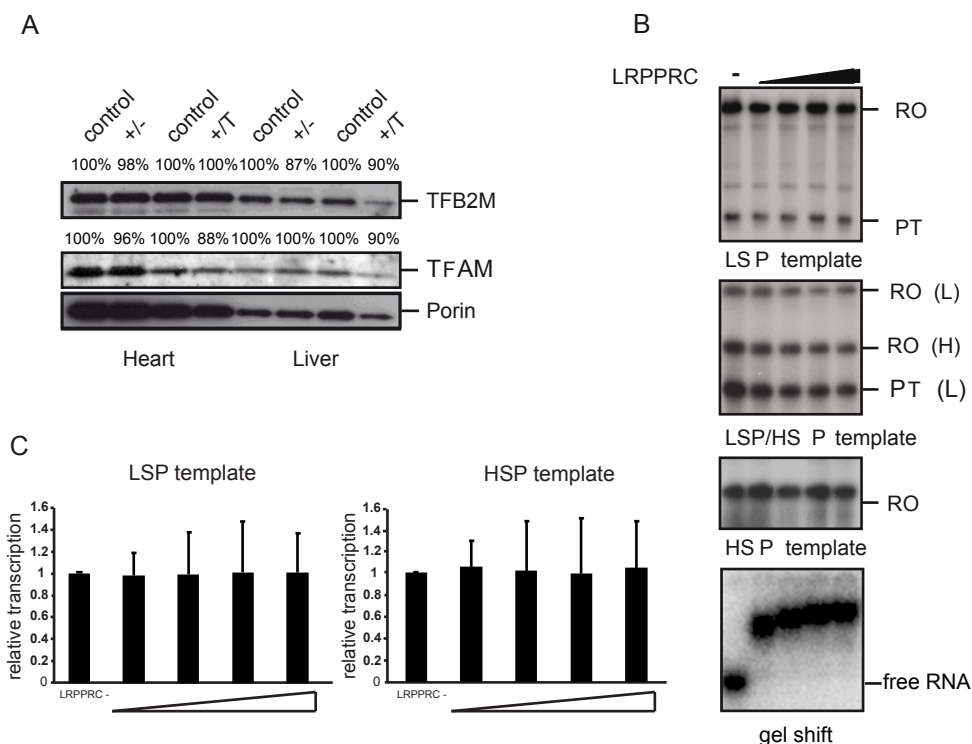
Harmel et al., JBC, 2013

Figure 3.21: *In organello* transcription analysis in *Lrpprc*^{+/-} and *Lrpprc*^{+T} mice. A. *In organello* transcription in heart and liver mitochondria from control, heterozygous *Lrpprc* knockout (+/-) and *Lrpprc* overexpressing (+/T) mice. The 12S rRNA was used as loading control. B. Quantification of areas a – d of panel A.

We also performed western blot analysis studying protein steady state levels of the components of the transcriptional core machinery. No difference in the steady state levels of TFAM and TFB2M were found in heart and liver mitochondria from *Lrpprc*^{+/-} and *Lrpprc*^{+T} mice confirming the normal transcription activity observed in the *in organello* transcription assay (**Figure 3.22A**).

Next, *in vitro* transcription experiments were performed to further analyze the effect of LRPPRC on mitochondrial transcription. Addition of recombinant LRPPRC protein to an *in vitro* transcription system was previously shown to activate transcription (Liu et al., 2011). However, we recently reported that such recombinant systems are very sensitive to even small changes of salt concentrations, which can cause misleading results concerning the activation or deactivation of the *in vitro* transcription system, respectively (Shi et al., 2012).

For that reason, we carefully controlled the conditions of the recombinant system by using physiologically relevant salt concentrations and keeping concentrations and buffer conditions of all recombinant components constant. Implementing these requirements TFAM, TFB2M and POLRMT were mixed with templates containing the heavy strand promoter 1 and 2 (HSP1 and 2) and light strand promoter (LSP), respectively in order to perform *in vitro* transcription analysis.



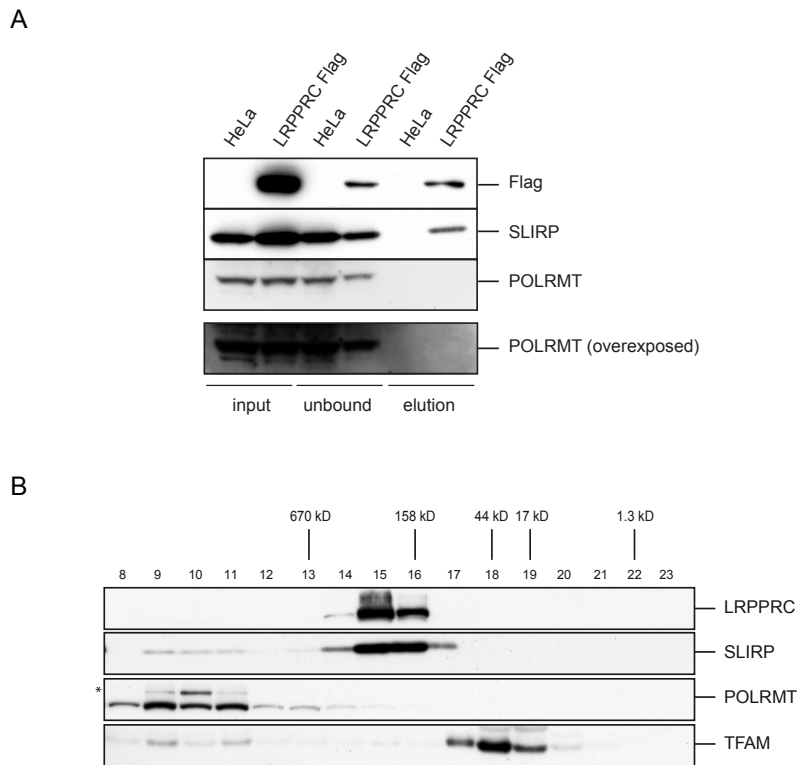
Harmel et al., JBC, 2013

Figure 3.22: LRPPRC does not activate mitochondrial transcription. A. Western blot analysis of the steady-state levels of proteins involved in regulation of mitochondrial transcription (TFAM and TFB2M) in mitochondrial extracts from heart and liver from control, heterozygous *Lrpprc* knockout

(+/-) and *Lrpprc* overexpressing (+/T) mice at 10-12 weeks of age. Porin was used as loading control. B. *In vitro* transcription was performed with purified recombinant POLRMT, TFB2M, TFAM, and the indicated mtDNA template, as described in experimental procedures. Increasing amounts of LRPPRC (0, 0.4, 0.8, 1.6, and 3.2 pmol) were added when indicated. LSP transcription generated a run-off (RO) product as well as a prematurely terminated (PT) product. A gel shift assay was used to assess whether recombinant LRPPRC had biological activity and can bind RNA. C. Quantification of HSP and LSP run-off transcripts from n=4 *in vitro* transcription experiments. For LSP the values for run-off (RO) and pre-terminated transcript at CSBII (PT) were used. The relative amount 1 indicates transcript levels in the absence of LRPPRC. Error bars indicate SD.

Finally, increasing amounts of LRPPRC were added to the reaction but no transcriptional stimulation could be detected (**Figure 3.22 B**). An electro mobility shift assay demonstrated active binding of the recombinant LRPPRC to RNA, proofing that the protein is biologically active (**Figure 3.22 B** bottom panel).

As mentioned before, LRPPRC has been reported to form a complex together with POLRMT, hence stimulating mitochondrial transcription. In order to investigate this hypothesis we performed immunoprecipitation experiments using HeLa cells with doxycycline-inducible expression of human LRPPRC-Flag. Mass spectrometric analysis of the eluate revealed interaction of LRPPRC-Flag with SLIRP, but no other binding partner was found. In addition, Western Blot analyses of the eluate using antibodies against SLIRP and POLRMT confirmed the previous results, since only SLIRP, but not POLRMT could be detected in the elution fraction (**Figure 3.23 A**).



Harmel et al., JBC, 2013

Figure 3.23: LRPPRC does not interact with mitochondrial RNA polymerase. A. Co-immunoprecipitation was performed using anti-Flag antibodies and mitochondrial extracts from HeLa cells expressing LRPPRC-Flag. The input, unbound fraction and the elution fraction obtained by Flag peptide were analyzed with western blotting to detect the LRPPRC-Flag, SLIRP and POLRMT. B. Size exclusion chromatography of mitochondrial extracts from wild-type HeLa cells. Western blot analysis was used to detect LRPPRC, SLIRP, POLRMT and TFAM in the different fractions.

However, proteins overexpressed in HeLa cells can create false positive protein protein interactions. To exclude this possibility, we used BAC-transgenic mice overexpressing LRPPRC-Flag in a physiological *in vivo* model. The BAC transgene was shown to fully rescue a germ line knockout of LRPPRC, proofing the biological functionality of the construct. The moderate expression of LRPPRC-Flag is similar to the endogenous LRPPRC expression. Immunoprecipitation experiments in protein extracts from heart, liver and kidney from LRPPRC-Flag BAC transgenic mice were performed followed by mass spectrometry analysis and again only SLIRP, but not POLRMT was identified to directly interact with LRPPRC (Table 1).

Another approach to find evidence for a potential interaction between LRPPRC and POLRMT was the performance of a size exclusion chromatography using human mitochondrial extracts from HeLa cells. Antibodies detecting LRPPRC, SLIRP, TFAM and POLRMT were used showing LRPPRC and SLIRP migrating in the same elution fraction

(Figure 3.23 B). These data confirmed the previously shown direct interaction of these two proteins (Sasarman et al., 2010). POLRMT however, was detected in a high molecular fraction together with TFAM and a small portion of SLIRP (Figure 3.23 B). These findings support the hypothesis that SLIRP binds newly synthesized mitochondrial transcripts in close proximity to the nucleoid to bind and protect mRNAs from degradation (Ruzzenente et al., 2012). Summarizing these data, LRPPRC does not form a stable complex with POLRMT.

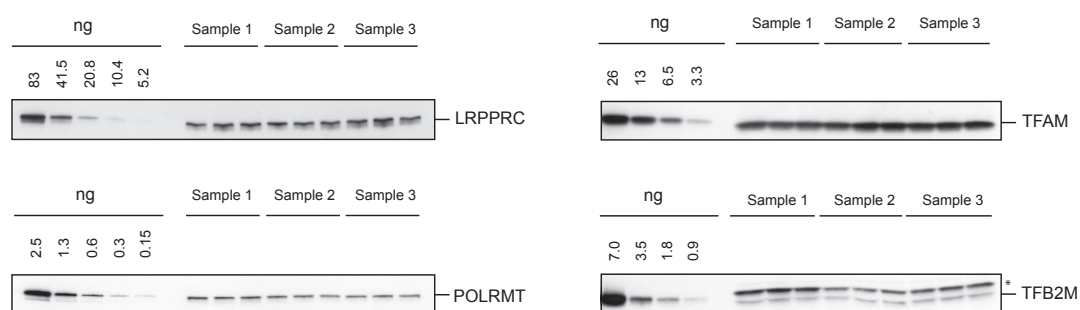
	Gene	UNIPROT	PROT NAME	PEPTIDES	SCORE	SC	emPAI
HEART MITOCHONDRIA	LRPPRC_MOUSE	Q6PB66	Leucine-rich PPR motif-containing protein	12	1273.7	10.1	0.16
	SLIRP_MOUSE	Q9D8T7	SRA stem-loop-interacting RNA-binding protein	1	107.3	10.7	0.27
	K1C10_MOUSE	P02535	Keratin, type I cytoskeletal 10	2	153.2	2.8	0.06
	K2C1_MOUSE	P04104	Keratin, type II cytoskeletal 1	1	99.3	1.9	0.05
KIDNEY MITOCHONDRIA	LRPPRC_MOUSE	Q6PB66	Leucine-rich PPR motif-containing protein	40	1779.9	30.9	1.06
	SLIRP_MOUSE	Q9D8T7	SRA stem-loop-interacting RNA-binding protein	6	279.2	49.1	1.63
	MCCA_MOUSE	Q99MR8	Methylcrotonoyl-CoA carboxylase subunit alpha	5	294.6	8.5	0.28
	MCCB_MOUSE	Q3ULD5	Methylcrotonoyl-CoA carboxylase beta chain	11	504.4	20.1	0.6
	ECHB_MOUSE	Q99JY0	Trifunctional enzyme subunit beta	1	62.0	1.9	0.06
	ECHP_MOUSE	Q9DBM2	Peroxisomal bifunctional enzyme	1	54.7	2.1	0.04
LIVER MITOCHONDRIA	LRPPRC_MOUSE	Q6PB66	Leucine-rich PPR motif-containing protein	40	1797.6	30.2	1.19
	SLIRP_MOUSE	Q9D8T7	SRA stem-loop-interacting RNA-binding protein	8	405.1	59.8	4.42
	PPA5_MOUSE	Q05117	Tartrate-resistant acid phosphatase type 5	2	94.6	9.5	0.19
	DHE3_MOUSE	P26443	Glutamate dehydrogenase 1	2	93.2	5.9	0.05
	SPA3N_MOUSE	Q91WP6	Serine protease inhibitor A3N	1	88.8	4.5	0.07
	PPIB_MOUSE	P24369	Peptidyl-prolyl cis-trans isomerase B	1	56.4	6	0.14
	ODO2_MOUSE	Q9D2G2	Dihydropolyllysine-residue succinyltransferase component of 2-oxoglutarate dehydrogenase complex	1	38.6	1.3	0.07
	DLDH_MOUSE	O08749	Dihydropolyl dehydrogenase	1	35.3	2.8	0.06
HELA CELLS	LRPPRC_HUMAN	P42704	Leucine-rich PPR motif-containing protein	37	1686.4	31.2	0.98
	SLIRP_HUMAN	Q9GZT3	SRA stem-loop-interacting RNA-binding protein	8	390.5	44.3	1.7
	DOC11_HUMAN	Q5JSL3	Dedicator of cytokinesis protein 11	2	75.7	6.8	0.5
	PGRC1_HUMAN	O00264	Membrane-associated progesterone receptor component 1	1	80.1	5.8	0.04
	ACTBL_HUMAN	Q562R1	Beta-actin-like protein 2	2	49.0	2.1	0.06

Table 1: LRPPRC Immunoprecipitation- Mass spectrometry results. Eluates after immunoprecipitation from heart, liver, kidney and HeLa cells were analysed by mass spectrometry in order to identify LRPPRC binding partners. SC= Sequence Score, emPAI= Exponentially Modified Protein Abundance Index.

3.3.5 LRPPRC is abundant in mammalian mitochondria

LRPPRC having a role in mitochondrial transcription would suggest a similar concentration of this protein as other mitochondrial transcription factors. In order to determine absolute levels of LRPPRC, POLRMT, TFB2M and TFAM western blot analyses were performed in mouse liver mitochondria using recombinant protein standards (Figure 3.24). Calculations

defining the intracellular concentration of LRPPRC revealed, that this protein is rather abundant, present at a concentration of 7fmol/ μ g of total mitochondrial protein. These data are in agreement with other reports that LRPPRC is abundant in human cells (Chujo et al., 2012). The levels of LRPPRC are lower than the levels of TFAM, which is acting as an mtDNA packaging factor in addition to its function as a transcription factor. Interestingly, the other two components of the basal mitochondrial transcription initiation machinery, POLRMT and TFB2M, were less abundant (0.15 fmol/ μ g and 0,47 fmol/ μ g) (**Figure 3.24**). The ~50-fold higher abundance of LRPPRC in comparison with POLRMT and ~14-fold higher abundance in comparison with TFB2M provide another argument against a role for LRPPRC in regulation of transcription



	ng/ μ g total mitochondrial protein	fmol/ μ g total mitochondrial protein
LRPPRC	1.1 \pm 0.09	7
POLRMT	0.02 \pm 0.04	0.15
TFAM	0.4 \pm 0.06	14.3
TFB2M	0.02 \pm 0.02	0.5

Harmel et al., JBC, 2013

Figure 3.24: LRPPRC is an abundant protein. The endogenous levels of LRPPRC, POLRMT, TFAM and TFB2M in mouse liver mitochondrial lysates were determined by western blot analyses using purified standards of the corresponding mouse proteins. * = unspecific crossreacting band.

Section 3.3 was modified from Harmel et al., The Leucine –rich pentatricopeptide repeat-containing protein (LRPPRC) does not activate transcription in mammalian mitochondria, *Journal of Biological Chemistry* , 2013, Vol. **288**, pp. 15510-15519

4 Discussion

The data presented in this work revealed surprising and unexpected insights in the regulation of mitochondrial gene expression and emphasized the importance of the usage of suitable *in vivo* models as a tool for the investigation of unknown protein functions. For several decades, results from *in vitro* studies inferred that MTERF1 terminates H-strand transcription at the 3' end of the 16s rRNA, and was believed to regulate mitochondrial ribosomal biogenesis (Daga and Attardi, 1993; Kruse et al., 1989). The 50-fold higher steady-state levels of ribosomal RNA relative to the mRNAs in mammalian mitochondria (Gelfand and Attardi, 1981) was, among other things, attributed to an independent regulation including a second H-strand promoter only responsible for transcription of ribosomal RNAs (Montoya et al., 1983). In this work, we describe the role of MTERF1 *in vivo*. Molecular characterization of MTERF1 in a knockout mouse model now contradicts the ideas based on previously obtained data from *in vitro* systems, since expression levels of ribosomal RNAs are not affected in the mouse model lacking MTERF1. We could show that this protein predominantly co-localizes with mitochondrial nucleoids, strengthening the concept, that MTERF1 is a DNA binding protein (Terzioglu et al., 2013). In addition, Chromatin Immunoprecipitation-Next Generation Sequencing (ChIP-NGS) and DNA-footprint analyses after targeting a methyltransferase into mitochondria clearly showed that MTERF1 binds a specific region in tRNA^{Leu(UUR)} gene, which is not occupied by any other protein in the absence of MTERF1. The lack of MTERF1 does not influence H-strand transcription. Instead, northern blot analysis and S1 protection assay analysis in *Mterf1* knockout mice revealed decreased 7S RNA transcripts in the LSP promoter proximal region (**Figure 3.5**). Previous studies in our lab demonstrated a strong correlation between the amount of 7S RNA and *de novo* transcription activity (Cámara et al., 2011; Park et al., 2007; Ruzzenente et al., 2012), therefore anticipating reduced transcription initiation events at the LSP promoter. However, expression of L-strand encoded proteins and tRNAs were unaffected in the *Mterf1* knockout mouse. MtDNA levels, which are known to be dependent on LSP initiated RNA primer formation, appeared to be normal. These findings, together with decreased L-strand transcript levels downstream of the MTERF1 binding site, could suggest a mechanism to terminate L-strand transcription in order to avoid promoter interference at the LSP. We propose a mechanism, whereby the transcription machinery encounters the light strand promoter leading to decreased activity of the LSP. In the phase of transcription initiation, stalling of the leading transcription machinery at the promoter region can cause unstable template interactions generated by the trailing enzyme (Zhou and Martin, 2006). Additionally, studies on T7 phage RNA polymerases have shown when multiple

polymerases are operating on the same strand, the trailing RNA polymerase can displace the leading one, causing abortive transcription (Zhou and Martin, 2006). Therefore, MTERF1 could provide an important block on the L-strand, preventing promoter collision on the LSP. Notably, heavy strand transcription also seems to be terminated before the regulatory region in the D-loop. Previous studies have revealed premature H-strand transcription termination past the termination associated sequence (TAS) region (Freyer et al., 2010) strengthening the hypothesis of a protein having a similar function on the L-strand. On the other hand it has previously been shown, that phage RNA polymerases moving in opposing directions can bypass each other without losing their transcription efficiency, which is suggested to be mediated by a temporary disconnection from the non-template strand during the collision (Ma and McAllister, 2009). These results could explain the unaffected H-strand transcription of *Mterf1* knockout mice, since converging RNA polymerases on the H-strand or L-strand can easily bypass each other without affecting the gene expression of the other strand.

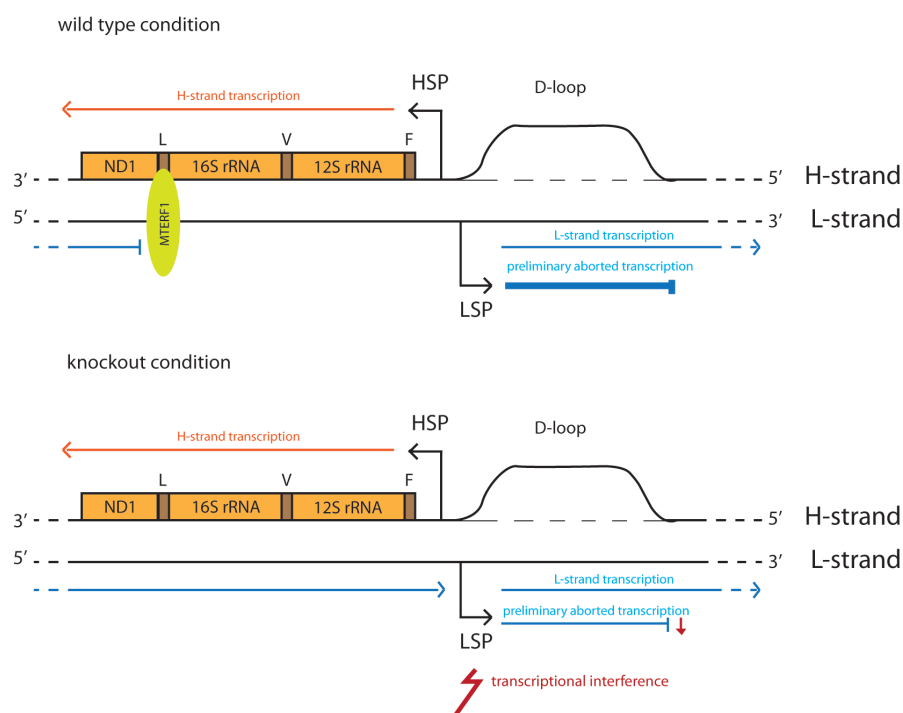


Figure 4.1: Proposed model for the mode of action of MTERF1 (upper panel) and the transcriptional consequences of loss of MTERF1 (lower panel). During wild type conditions MTERF1 blocks L-strand transcription at its binding site. Lack of MTERF1 allows POLRMT to proceed transcription to the LSP causing decreased transcription initiation events.

The first hints regarding the polarity of MTERF1 in *in vitro* analysis were published 20 years ago, when Clayton and co-workers detected a preferential termination activity of MTERF1 for transcripts originating at the LSP (Shang and Clayton, 1994). However, the idea that MTERF1 could have a regulatory function regarding the transcription of mitochondrial ribosomal RNAs by promoting a loop formation in the rDNA region of mtDNA has eclipsed

this knowledge for many years (Kruse and Attardi, 1989; Martin et al., 2005). X-ray crystallography analysis of MTERF1 by crystallization of this protein with the target sequence, revealed much more interactions and therefore stronger affinity of MTERF1 to the L-strand than the H-strand (Yakubovskaya et al., 2010). MTERF1 is reported to be a half-doughnut shaped protein, wrapping around the DNA, which partially unwinds the double helix and causes a phenomenon called “base flipping” (Yakubovskaya et al., 2010). Three nucleotides corresponding to A3243 of the light strand and T3243 and C3242 of the heavy strand are everted from the double helix and interact with the protein. Among the other members of the MTERF family this feature is unique to MTERF1, enabling this protein for an exceptionally strong interaction with its mtDNA binding site in order to ensure transcriptional blockage at the L-strand. In accordance with our data, no other specific binding site especially in the mtDNA promoter region could be identified as suggested in previous studies (Wenz et al., 2009). The structural properties of MTERF1 allow this protein to also unspecifically bind mtDNA, however, these interactions with random DNA sequences appear to be much less frequent compared to the ones with the binding site (Yakubovskaya et al., 2010). The detailed crystal structure findings together with the extensive DNA-protein interactions described above make it very unlikely that MTERF1 can simultaneously bind two dsDNA regions as previously suggested by Attardi and co-workers. Regarding our knowledge of the MTERF family members to date, MTERF1 is the only family member, which is living up to its name as transcription termination factor, since MTERF3, another MTERF-family member long time known as negative regulator of mitochondrial transcription (Park et al., 2007), was recently shown to have an additional role in ribosomal biogenesis (Wredenberg et al., 2013). Previous studies, concerning the human mitochondrial transcriptome have impressively demonstrated a massive decrease of transcription levels on the L-strand right after the MTERF1 binding site. Although there are several other non-coding areas on the L-strand, there is no region being less transcribed than the antisense of the mitochondrial ribosomal RNAs (Mercer et al., 2011). Together with foot printing analyses revealing MTERF1 binding in the tRNA^{Leu(UUR)} gene, these data support our findings of MTERF1 terminating L-strand transcription (Mercer et al., 2011).

Lack of MTERF1 does not seem to have a strong effect on knockout mouse models at the metabolic level. The mice are phenotypically healthy, with a normal lifespan and even a ketogenic diet stress does not provoke any pathological effects at mitochondrial level. In MELAS syndrome, a severe neuromuscular mitochondrial disorder, it is known that mutations in the tRNA^{Leu(UUR)} gene prevent the binding of MTERF1 to its binding site, in addition to the translational deficiencies caused by the mutation in the tRNA^{Leu(UUR)} gene product. Furthermore, it has been discovered that amino acid substitutions at two guanines, which interfere with MTERF1 protein-DNA interactions lead to mitochondrial disorders due

to the elimination of sequence recognition of MTERF1, which consequently causes loss of its transcriptional termination activity (Yakubovskaya et al., 2010). It is puzzling having healthy mice completely lacking MTERF1 on the one hand, and patients developing severe mitochondrial disorders by carrying the protein but without the capability to fulfill its function, on the other hand. Regarding the situation in MELAS patients, impaired expression of tRNA^{Leu(UUR)} or a defective charging specificity of the tRNA^{Leu} synthetase could be the reason for the clinical phenotype (Chomyn et al., 1992) since the mutation preventing the specific binding of MTERF1 is located in the coding region of the tRNA^{Leu} gene. Mutations located in the MTERF1 protein itself, lowering its binding or termination capabilities however, are not known. In addition, *in vitro* studies on fibroblasts of patients suffering from MELAS develop global mitochondrial translational deficiencies, which cannot be explained by defective transcription termination or misprocessing of the total H-strand polycistronic transcripts at the level of the tRNA^{Leu(UUR)} sequence.

Besides its closest relative MTERF1, MTERF2 is the only remaining MTERF family member exclusively being implicated in mitochondrial transcription. Recently published *in vivo* studies in *Mterf2* knockout mice revealed healthy animals not suffering from any phenotype (Wenz et al., 2009). Therefore, the mice were challenged with a high-fat, low carbohydrate diet, which activates mitochondrial biogenesis by diminishing glycolytic activity and shifting mitochondrial metabolism to oxidative phosphorylation. In a situation, when oxidative phosphorylation is the only available energy source in the cell, a lacking protein involved in mitochondrial metabolism could be more prone to provoke defects, which can be compensated under normal conditions. For many years, the ketogenic diet has successfully been implemented in the treatment of epileptic patients and patients suffering from neurodegenerative diseases such as Alzheimer's or Parkinson's disease (Stafstrom and Rho, 2012). Even though the exact mode of action is still unclear, there are several factors which may be responsible for the beneficial impact, including carbohydrate reduction, activation of ATP-sensitive potassium channels by mitochondrial metabolism, inhibition of the mammalian target of rapamycin (TOR) pathway and inhibition of glutamatergic excitatory synaptic transmission (Danial et al., 2013). The most common side effects of patients treated with a ketogenic diet, are tiredness and muscle weakness. The latter was also observed in *Mterf2* knockout mice fed with such a diet for several months (Wenz et al., 2009). These mice have been reported to develop memory deficits and muscle weakness. Notably none of these symptoms were detected in the control group, which could be expected from the experience in human patients. Previously performed molecular analysis of *Mterf2* knockout mice revealed decreased steady state mRNA levels resulting in reduced steady state protein levels of the respiratory chain complex and impaired oxidative phosphorylation activity (Wenz et al., 2009).

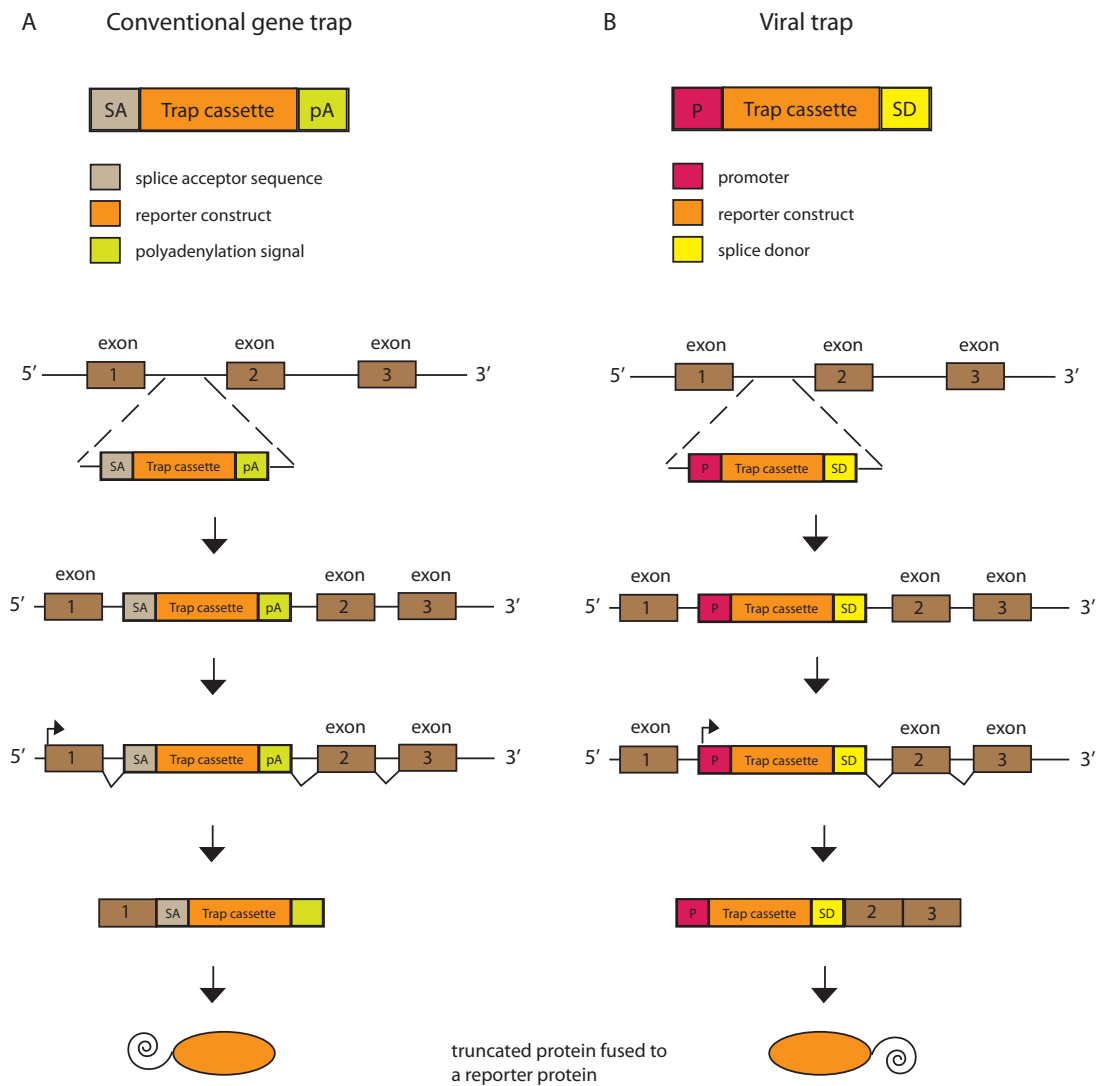


Figure 4.2: Common gene trap vs. viral trap. A. After electroporation in the cell the gene trap vector inserts randomly into a genomic locus. Transcription of the target gene from its endogenous promoter results in a truncated mRNA fused to the reporter protein, due to the interruption of endogenous splicing by a polyA signal in the vector. B. Viral traps contain their own promoter, transcribing the reporter gene as well as a truncated 3' end of the target gene. The strong viral promoter can also influence promoter activity of neighbouring genes. Figure and legend modified from www.genetrapp.org.

However, characterization of the *Mterf2* knockout mouse model created in our lab could not support these findings. Normal expression levels of mitochondrial encoded genes and tRNAs as well as unaffected steady state mRNA levels of POLRMT, TFAM and TFB2M, the mammalian core transcription machinery in mitochondria, rather argue against a role of MTERF2 in mitochondrial transcription. Unchanged mtDNA levels further confirm our findings and also indicate normal mitochondrial biogenesis. Although we cannot support a role of MTERF2 in mitochondrial transcription, we still do not know at which regulatory level this protein fulfills its function in mitochondrial metabolism. Western Blots in mitochondrial extracts from *Lrrpprc*, *Mterf3*, *Mterf4* and *Tfam* knockout mice, representing

models for different levels of regulation in mitochondrial gene expression, revealed unchanged MTERF2 protein levels and also protein steady state levels of subunits of the respiratory chain complexes as well as OXPHOS complex assembly appear normal in the absence of MTERF2. Therefore, diminished RNA stability, defective ribosome assembly and abolished transcription in mitochondria do not seem to influence MTERF2 steady state levels. An obvious difference between the *Mterf2* knockout mouse model created in our lab and the one developed in the group of Carlos Moraes is the knockout strategy used to disrupt the *Mterf2* gene. In our lab we used homologous recombination to introduce a STOP codon in exon 3 of the *Mterf2* gene, whereas Wenz et al. decided to interrupt *Mterf2* gene expression through introduction of a viral trap. Viral traps belong to the group of gene traps, a common tool to randomly generate embryonic stem cells with insertional mutations in either the intronic or the coding region of a target gene. The most common kind of a gene trap makes use of the endogenous promoter of the target gene. The target gene is expressed until it reaches a poly A signal at the 3' end of the gene trap, which inhibits splicing downstream of the construct and terminates translation causing a truncated protein (Rojas-Pierce and Springer, 2003; Yamaguchi et al., 2012). To target genes, which are not normally expressed or expressed at very low levels, so-called viral traps are used containing an own promoter and a transcription start site. The disadvantage of using strong viral promoters is their ability to negatively influence promoters of other genes located in close proximity to the target gene (Floss and Schnütgen, 2008). Just 1,6 kb upstream of the *Mterf2* gene another gene is situated encoding for cryptochrome 1 (CRY1). This protein belongs to the photolyase family, including plant blue-light receptors, which are essential components of the circadian clock. CRY1 is conserved in bacteria and animals but is quite widespread in plants, as these organisms are light-dependent regarding development and flowering. CRY1 also has a homologue CRY2, which is mostly located in the nucleus. Deletion of each gene alters behavioural rhythmicity, while deletion of both genes abolishes it completely (van der Horst et al., 1999). Besides the disturbed circadian rhythm, *Cry1* knockout mice have been reported to have a normal appearance, are fertile and do not develop any deleterious phenotypes, which are observed in the *cry1/cry2* double knockout mice (van der Horst et al., 1999). Simultaneous disruption of *cry1* in a *Mterf2* knockout mouse may therefore match with the phenotype of mice lacking MTERF2, since both mouse models are apparently healthy. Analysis of *cry1* knockout mice regarding mitochondrial metabolism did not reveal any involvement of this protein in mitochondrial transcription or OXPHOS activity. Surprisingly, we found *cry1* expression levels massively downregulated in both *Mterf2* knockout mouse models, indicating that this gene is in fact affected in the *Mterf2* knockout mice created by gene trap, but also in our *Mterf2* knockout mouse, which excludes this gene from being responsible for the different phenotypes in two knockout mouse models. The reason why the

insertion of a STOP codon should influence promoter activity of a neighbouring gene is unclear and the lack of antibodies prevented further analyses of CRY1 protein steady state levels. A direct interaction of CRY1 and MTERF2 is unlikely but not impossible,.

In vitro studies in HeLa cells revealed unspecific DNA binding capability of MTERF2 and co-localization of this protein with mitochondrial nucleoids (Pellegrini et al., 2009). This, combined with a relatively high abundance of MTERF2 corresponding to 1 protein per 265 bp DNA, suggested that it could, similar to TFAM, cover mtDNA as well as having a role in mtDNA expression. However, one should also consider potential RNA binding capabilities. The fact, that MTERF2 was found in the nucleoid does not exclude RNA binding, since for example SLIRP, an exclusively RNA binding protein was found in the nucleoid fraction in size exclusion chromatographies (**Figure 3.23 B**) where it acts as a co-factor in post-transcriptional regulation. The structure of MTERF2 has not been solved yet, but is believed to be similar to the half-doughnut shape characterizing the other MTERF-family members. This particular 3-D structure has been shown to allow the protein to wrap around its nucleic acid substrate through interactions of its positively charged surface at the concave site of the protein, which provides a path for the negatively charged nucleic acid (Spähr et al., 2010; 2012; Yakubovskaya et al., 2010). Since this feature is conserved in all other MTERF family members, it is very likely that also MTERF2 has similar attributes, which also includes a putative RNA binding capability. Regarding the *in vivo* functions of the other MTERF family members, recent studies in our lab surprisingly revealed MTERF3 and MTERF4 being RNA binding proteins with a role in mitochondrial ribosome assembly and translation (Cámara et al., 2011; Wredenberg et al., 2013). Therefore a non-transcriptional role for MTERF2 in mitochondrial RNA metabolism is not ruled out. On the other hand, ribosome assembly is not affected in mice lacking MTERF2 and due to the healthy appearance of our *Mterf2* knockout mouse model we cannot expect an indispensable role of MTERF2 in the mitochondrial RNA metabolism. Furthermore, evolutionary appearance of the MTERF family members attests MTERF3 and MTERF4 being more closely related to each other than to MTERF1 and MTERF2, which is also mirrored in their similar function. Considering this, MTERF2 might rather be a DNA binding protein with a function similar to MTERF1. The mild phenotype of *Mterf1* as well as *Mterf2* knockout mice, could also imply mutual functional compensation. However, regarding MTERF1 we could show, that no other protein is binding at the *Mterf1* binding site in the absence of this protein (**Figure 3.4 L**) and *Mterf1/Mterf2* double knockout mice in our lab are viable, fertile and show a normal life span (data not shown).

The function of MTERF1 and its homologs in other organisms is highly conserved, since mammalian MTERF1, *Drosophila melanogaster* dmTTF and sea urchin *Paracentrotus lividus* mtDBP all share the capacity to arrest progression of the mitochondrial RNA polymerase (Polosa et al., 2005; Roberti et al., 2006a; 2006b). However, their binding sites as

well as the roles of these proteins seems to be specific for each species (Roberti et al., 2006a). MTERF2 homologs, on the other hand, have not been investigated so far. Its function is, like in mammals, still awaiting identification.

Besides studying the regulation of mtDNA expression at the level of mitochondrial transcription we also covered this issue at the post-transcriptional level. The *in vivo* function of LRPPRC is still highly discussed in literature, and suggests a multiplicity of putative functions in the mitochondria as well as in the cytoplasm and the nucleus. In contrast to the existence of several striking evidences implicating that LRPPRC is an important factor in RNA stability and polyadenylation, recent reports has been claiming this protein to have a role in mitochondrial transcription (Liu et al., 2011). This brought us to further characterize a putative role for LRPPRC in mitochondrial transcription via manipulation of the *in vivo* expression of LRPPRC in two different mouse models. *Lrpprc* heterozygous mice and mice overexpressing LRPPRC mediated by BAC induction only show moderately increased or decreased LRPPRC protein levels and are therefore good models to investigate the *in vivo* function of this protein in a normal environment. The data observed in our study do not support the hypothesis that LRPPRC stimulates mitochondrial transcription. Concerted analysis regarding mtDNA transcription revealed unaffected expression levels of mitochondrial encoded genes and tRNAs as well as normal OXPHOS protein steady state levels of subunits and super complexes of the respiratory chain complex. In addition, transcription assays, *de novo* and *in vitro*, did not provide evidence of LRPPRC being a mitochondrial transcription factor. Differences between our data and previously published studies regarding the outcome and overall interpretation of identical experiments, illustrates the importance of careful handled experiments. Liu et al has recently shown recombinant LRPPRC stimulating transcription of mtDNA in an *in vitro* system (Liu et al., 2011). However, the conditions used in this experiment did not correspond to physiological conditions and may have lead to misleading results. It was recently reported, that *in vitro* transcription systems are very sensitive to even small variations in salt concentrations (Shi et al., 2012). Addition of a recombinant factor could therefore lead to the wrong assumption that this factor is stimulating or inhibiting transcription. For this reason, we thoroughly checked the exact salt concentrations and took care of a careful purification of recombinant LRPPRC before it was added to the transcription reaction. Using affinity and ion exchange chromatography, LRPPRC was finally dialyzed and diluted in a buffer containing 0.2M NaCl. The final reaction was performed in 80mM NaCl and could not detect a stimulating effect of LRPPRC on *in vitro* transcription. Furthermore, we used TFAM at a concentration of 200-600 nM for the *in vitro* assays, which corresponds to a similar TFAM/mtDNA ratio observed *in vivo* (Ekstrand et al., 2004; Pellegrini et al., 2009). TFAM concentrations used by the other group were much lower and in addition purification of recombinant LRPPRC was achieved

via His-Tag, making it susceptible for contaminations by other mitochondrial proteins (Liu et al., 2011). The low TFAM concentration allows even low concentrations of contaminating factors to significantly influence the stimulatory effect of LRPPRC on an *in vitro* transcription assay. Notably, recapitulation of this experiment with the same conditions as recently reported, revealed the same results as it has been claimed by this group (data not shown), demonstrating the need for precise performance of scientific experiments to avoid misleading contaminations. Together with our other data obtained from size exclusion chromatography and immunoprecipitation experiments we strongly support the idea of LRPPRC not interacting with POLRMT.

The only molecular phenotype detected in our mouse models with moderately increased and moderately decreased LRPPRC protein levels, is the expression level of the precursor transcript of ND5/Cytb, which always corresponds to LRPPRC protein levels in both mouse models. This is suggesting a potential additional role of LRPPRC in precursor processing. LRPPRC has been recently reported to directly bind mitochondrial precursors such as ATP6-COX3, tRNA^{Met} - ND2, tRNA^{L1} - ND1, tRNA^{Val} - 16S rRNA and tRNA^{Phe} - 12 S rRNA (Chujo et al., 2012). Since other RNA transcripts are not affected by varying amounts of LRPPRC, degradation caused by decreased transcript stability is unlikely the reason for this phenotype. Considering the fact, that reduced amount of LRPPRC causes decreased precursor levels and vice versa rather suggests an inhibitory role on precursor maturation, since its absence increases processing, which reveals reduced steady-state levels (**Figure 3.20 A**). Further analysis regarding a putative interaction of LRPPRC with other precursor transcripts is needed to evaluate a potential additional role in precursor maturation.

We found LRPPRC to be a relatively abundant protein in the mitochondria, with a concentration half as much as TFAM, but 14- and 50-fold more than TFB2M and POLRMT. This, again, argues against a role for LRPPRC in mitochondrial transcription.

Additional evidence regarding the *in vivo* function of LRPPRC is given in a LRPPRC heart and skeletal muscle specific knockout mouse model. Recent characterization of this mouse model in our lab revealed severe cytochrome c deficiency and decreased mRNA expression levels causing massively impaired complex IV activity (Ruzzenente et al., 2012). Furthermore we found a misregulated translation phenotype with some peptides being excessively translated or not translated at all and abolished polyadenylation for most of the mitochondrial mRNAs. However, *de novo* transcription appeared normal, which was also detected in both mouse models analysed in this work. The source for the phenotype in mice lacking LRPPRC in heart and skeletal muscle must therefore be a post-transcriptional event since defective transcription cannot be the reason for decreased transcript levels. Sucrose gradient sedimentation of mitochondrial extracts with subsequent qPCR analysis of single fractions revealed a mitochondrial mRNA distribution showing that LRPPRC is important for mRNA

stability, maintaining a pool of currently untranslated mRNAs in mammalian mitochondria (Ruzzenente et al., 2012).

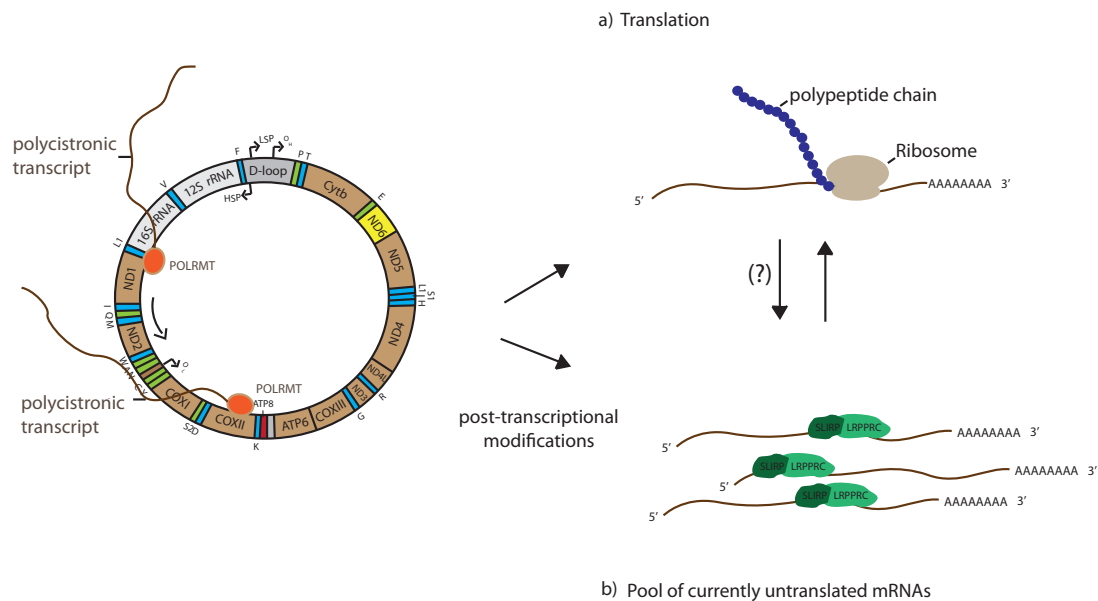


Figure 4.3: Proposed model for the post-transcriptional role of the LRPPRC/SLIRP complex. Transcription at mtDNA creates polycistronic precursor transcripts, which are processed and modified into the single RNA species. If not translated by mitochondrial ribosomes, currently untranslated mRNAs are stabilized by the LRPPRC/SLIRP complex and protected from degradation.

Considering that LRPPRC is a member of the PPR protein family, this finding is not very surprising, since PPR domain containing proteins are capable to bind RNA and known to have roles in RNA metabolism in mitochondria and chloroplasts including RNA editing, transcript processing, RNA stability and initiation of translation (Schmitz-Linneweber and Small, 2008; Zehrmann et al., 2011)

Patients suffering from an A354V amino acid substitution in the *Lrpprc* gene develop Leigh Syndrome, French Canadian Type, a disease with a similar mitochondrial biochemical profile as the conditional knockout mouse model. Analysis of patient fibroblasts revealed decreased LRPPRC protein levels, resulting in cytochrome c deficiency, downregulated transcription and defective complex assembly. *De novo* translation, however, seems to be generally decreased in patient fibroblasts, which is in contrast to the translational misregulation found in the mouse model. The LSFC patients display typical symptoms of a mitochondrial disease including poor muscle coordination (ataxia) or neurological symptoms including stroke-like episodes and seizures. These observations in patient samples, together with our observations in the mouse again argue against a role for LRPPRC in mitochondrial transcription (Ruzzenente et al., 2012).

LRPPRC is a conserved protein in metazoan organisms. The yeast protein PET309 is proposed to be a homologue of LRPPRC with 37% similarity over 300 amino acids. It is

essential for respiratory growth and important for stability and translation of mitochondrial COX1 mRNA in yeast (Tavares-Carreón et al., 2008). Mutational analysis of its PPR domains revealed an important function in translation, where none of the seven PPR motifs is dispensable. Interestingly, mRNA stability of COX1 in yeast does not seem to be mediated by PPR domains, and so far Pet309 is the only translational activator that has been found to contain PPR motifs (Tavares-Carreón et al., 2008). The bicoid stability factor (BSF) in *Drosophila melanogaster*, another homologue of LRPPRC is also shown to be a RNA binding protein involved in stability of mitochondrial mRNAs (Batic et al., 2011). BSF was initially thought to bind the 3' untranslated region (UTR) of cytoplasmic mRNAs and has been linked to a role in regulating zygotic genes by binding their 5' UTR (Mancebo et al., 2001). However, recent localization studies agree that BSF is mainly situated in mitochondria in larvae and adult flies, where it was reported to have a function highly similar to its mammalian LRPPRC, including stabilization of mitochondrial mRNAs, promotion of polyadenylation and coordination of translation (Batic et al., 2011). In summary, these studies clearly support and continue the line of evidence for a role of LRPPRC in mitochondrial RNA regulation. In several of the studies in which LRPPRC has been reported to have extramitochondrial roles, the data were based on the finding of biochemical activities in cytoplasmic or nuclear extracts and it cannot be excluded that these extracts have been contaminated with proteins from broken mitochondria. Therefore, these experiments should be repeated under more careful conditions by using nuclear or cytoplasmic extracts free from any contaminating factors.

4.1 Future perspectives

The characterization of a *Mterf1* knockout mouse model revealed surprising new insights in the *in vivo* function of MTERF1. However, there are ongoing studies investigating additional roles of MTERF1 as for example in replication. Notably, these analyses take place *in vitro* in cell lines and await further confirmation in an *in vivo* model. In our hands mtDNA levels in the *Mterf1* knockout mouse model appear normal, which rather argues against this function. Functional characterization of MTERF2, on the other hand, is far away from being complete. In our hands, mice lacking this protein are phenotypically healthy and fertile and so far we could not find any molecular phenotype even under stress conditions, which is in contrast to the *Mterf2* knockout mouse model from the Moraes Lab. It remains unclear, why we could not confirm the previously described phenotype, even not in the same the phenotype initially was detected. Data from our *Mterf2* knockout mouse model fed with a ketogenic diet have not been analyzed so far. They might give more ideas regarding the intramitochondrial role of MTERF2. Furthermore it might be interesting to elucidate why *Cry1* gene expression is

downregulated in the *Mterf2* knockout mouse model from our lab as well as from the Moraes lab. It is not clear if CRY1 can directly interact with MTERF2 or if events at the *Cry1* promoter region are responsible for this phenomenon. In addition, more detailed analysis regarding its interaction partners and nucleic acid binding capabilities could give more profound information about the *in vivo* function of MTERF2.

Taken together the results from this work with our previous data concerning the location and function of LRPPRC, we strongly agree on a posttranscriptional role of LRPPRC in mammalian mitochondria. However, there are still open-ended questions as for example its involvement in precursor maturation. Studies disclosing the influence of varying LRPPRC protein levels on other precursor transcripts could be performed. Furthermore the exact role in mitochondrial polyadenylation is still unknown. More experiments defining the influence of altering LRPPRC protein levels to the length of polyA tails and their contribution on transcript stability in an *in vivo* model can shed light on this.

Table of Figures

Figure 1.2: Schematic illustration of the five protein complexes constituting the mammalian oxidative phosphorylation system.....	3
Figure 1.3: Schematic illustration of a mammalian mtDNA molecule.....	7
Figure 1.4: Phylogenetic tree of the MTERF family proteins.....	12
Figure 1.5: Posttranscriptional modifications in mammalian mitochondria.....	19
Figure 3.1: Disruption of <i>Mterf1a</i> and <i>Mterf1b</i> in the germline.....	60
Figure 3.2: Body weight curves.....	61
Figure 3.3: Bioenergetic measurements and Blue Native PAGE analysis in <i>Mterf1</i> knockout mice.....	62
Figure 3.4 :Analysis of MTERF1 DNA-binding sites and mtDNA expression.....	64
Figure 3.5: Analysis of transcription initiation at the LSP.....	66
Figure 3.6: Phenotyping of <i>Mterf1</i> knockout mice after treatment with ketogenic diet.....	67
Figure 3.7: Targeting and screening of the <i>Mterf2</i> knockout mouse.....	70
Figure 3.8: Body weight curves and glucose tolerance tests in <i>Mterf2</i> knockout and control mice.....	71
Figure 3.9: Metabolic phenotyping of control and <i>Mterf2</i> knockout mice.....	72
Figure 3.10: MtDNA levels in controls, <i>Mterf2</i> knockout mice (T2N and T2M) and <i>Cry1</i> knockout mice.....	73
Figure 3.11: Steady state mitochondrial transcript levels in heart, kidney, liver, skeletal muscle and brain are unchanged in wild type, <i>Mterf2</i> N knockout, <i>Mterf2</i> M knockout and <i>Cry1</i> knockout mice.....	74
Figure 3.12: Steady state mRNA levels of mitochondrial encoded genes and mitochondrial transcription factors.....	75
Figure 3.13: Expression levels of MTERF family proteins.....	76
Figure 3.14: MTERF2 protein levels in different knockout mouse models.....	77
Figure 3.15: Steady state protein levels of respiratory chain subunits in wild type <i>Mterf2</i> N, <i>Mterf2</i> M and <i>Cry1</i> knockout mice.....	78
Figure 3.16: Super complex assembly is not affected by loss of MTERF2 and CRY1. ...	79
Figure 3.17: Steady state expression levels of <i>Cry1</i> in different tissues.....	80
Figure 3.18: Heart to body weight ratio is not affected by moderately altered levels of LRPPRC.....	81
Figure 3.19: LRPPRC does not affect oxidative phosphorylation capacity.....	83
Figure 3.20: Steady state levels of mitochondrial transcripts.....	85
Figure 3.21: <i>In organello</i> transcription analysis in <i>Lrpprc</i> ^{+/-} and <i>Lrpprc</i> ^{+T} mice.....	86

Figure 3.22: LRPPRC does not activate mitochondrial transcription.87

Figure 3.23: LRPPRC does not interact with mitochondrial RNA polymerase.....89

Figure 3.24: LRPPRC is an abundant protein.91

**Figure 4.1: Proposed model for the mode of action of MTERF1 (upper panel) and the
transcriptional consequences of loss of MTERF (lower panel).....93**

Figure 4.2: Common gene trap vs. viral trap.....96

**Figure 4.3: Proposed model for the post-transcriptional role of the LRPPRC/SLIRP
complex.101**

References

Adams, K.L., and Palmer, J.D. (2003). Evolution of mitochondrial gene content: gene loss and transfer to the nucleus. *Mol. Phylogenet. Evol.* *29*, 380–395.

Allen, J.F. (2003). Why chloroplasts and mitochondria contain genomes. *Comp. Funct. Genomics* *4*, 31–36.

Antico Arciuch, V.G., Elguero, M.E., Poderoso, J.J., and Carreras, M.C. (2012). Mitochondrial regulation of cell cycle and proliferation. *Antioxid. Redox Signal.* *16*, 1150–1180.

Arnold, J.J., Smidansky, E.D., Moustafa, I.M., and Cameron, C.E. (2012). Human mitochondrial RNA polymerase: structure-function, mechanism and inhibition. *Biochim. Biophys. Acta* *1819*, 948–960.

Asin-Cayuela, J., Schwend, T., Farge, G., and Gustafsson, C.M. (2005). The human mitochondrial transcription termination factor (mTERF) is fully active in vitro in the non-phosphorylated form. *J. Biol. Chem.* *280*, 25499–25505.

Barkan, A., Rojas, M., Fujii, S., Yap, A., Chong, Y.S., Bond, C.S., and Small, I. (2012). A combinatorial amino acid code for RNA recognition by pentatricopeptide repeat proteins. *PLoS Genet* *8*, e1002910.

Bender, A., Krishnan, K.J., Morris, C.M., Taylor, G.A., Reeve, A.K., Perry, R.H., Jaros, E., Hersheson, J.S., Betts, J., Klopstock, T., et al. (2006). High levels of mitochondrial DNA deletions in substantia nigra neurons in aging and Parkinson disease. *Nat. Genet.* *38*, 515–517.

Bogenhagen, D.F., and Clayton, D.A. (1978). Mechanism of mitochondrial DNA replication in mouse L-cells: kinetics of synthesis and turnover of the initiation sequence. 1–20.

Bogenhagen, D.F., and Clayton, D.A. (1977). Mouse L Cell Mitochondrial DNA Molecules Are Selected Randomly for Replication throughout the Cell Cycle. *Cell* 1–9.

Bogenhagen, D.F., Rousseau, D., and Burke, S. (2008). The layered structure of human mitochondrial DNA nucleoids. *J. Biol. Chem.* *283*, 3665–3675.

Bratic, A., Wredenberg, A., Grönke, S., Stewart, J.B., Mourier, A., Ruzzenente, B., Kukat, C., Wibom, R., Habermann, B., Partridge, L., et al. (2011). The bicoid stability factor controls polyadenylation and expression of specific mitochondrial mRNAs in *Drosophila melanogaster*. *PLoS Genet* *7*, e1002324.

Brzezniak, L.K., Bijata, M., Szczesny, R.J., and Stepień, P.P. (2011). Involvement of human ELAC2 gene product in 3' end processing of mitochondrial tRNAs. *RNA Biol* *8*, 616–626.

Bykhovskaya, Y., Casas, K., Mengesha, E., Inbal, A., and Fischel-Ghodsian, N. (2004). Missense mutation in pseudouridine synthase 1 (PUS1) causes mitochondrial myopathy and sideroblastic anemia (MLASA). *Am. J. Hum. Genet.* *74*, 1303–1308.

Camasamudram, V., Fang, J.-K., and Avadhani, N.G. (2003). Transcription termination at the mouse mitochondrial H-strand promoter distal site requires an A/T rich sequence motif and sequence specific DNA binding proteins. *Eur J Biochem* *270*, 1128–1140.

Campbell, C.T., Kolesar, J.E., and Kaufman, B.A. (2012). Mitochondrial transcription factor A regulates mitochondrial transcription initiation, DNA packaging, and genome copy number. *Biochim. Biophys. Acta* *1819*, 921–929.

Casas, K., Bykhovskaya, Y., Mengesha, E., Wang, D., Yang, H., Taylor, K., Inbal, A., and Fischel-

- Ghodsian, N. (2004). Gene responsible for mitochondrial myopathy and sideroblastic anemia (MSA) maps to chromosome 12q24.33. *Am. J. Med. Genet. A* 127A, 44–49.
- Cámara, Y., Asin-Cayuela, J., Park, C.B., Metodiev, M.D., Shi, Y., Ruzzenente, B., Kukat, C., Habermann, B., Wibom, R., Hultenby, K., et al. (2011). MTERF4 regulates translation by targeting the methyltransferase NSUN4 to the mammalian mitochondrial ribosome. *Cell Metab.* 13, 527–539.
- Cermakian, N., Ikeda, T.M., Miramontes, P., Lang, B.F., Gray, M.W., and Cedergren, R. (1997). On the evolution of the single-subunit RNA polymerases. *J. Mol. Evol.* 45, 671–681.
- Chang, J.H., and Tong, L. (2012). Mitochondrial poly(A) polymerase and polyadenylation. *Biochim. Biophys. Acta* 1819, 992–997.
- Chen, H., McCaffery, J.M., and Chan, D.C. (2007). Mitochondrial fusion protects against neurodegeneration in the cerebellum. *Cell* 130, 548–562.
- Chomyn, A., Martinuzzi, A., Yoneda, M., Daga, A., Hurko, O., Johns, D., Lai, S.T., Nonaka, I., Angelini, C., and Attardi, G. (1992). MELAS mutation in mtDNA binding site for transcription termination factor causes defects in protein synthesis and in respiration but no change in levels of upstream and downstream mature transcripts. *Proc. Natl. Acad. Sci. U.S.A.* 89, 4221–4225.
- Chujo, T., Ohira, T., Sakaguchi, Y., Goshima, N., Nomura, N., Nagao, A., and Suzuki, T. (2012). LRPPRC/SLIRP suppresses PNPase-mediated mRNA decay and promotes polyadenylation in human mitochondria. *Nucleic Acids Research* 40, 8033–8047.
- Colley, S.M., Wintle, L., Searles, R., Russell, V., Firman, R.C., Smith, S., Deboer, K., Merriner, D.J., Genevieve, B., Bentel, J.M., et al. (2013). Loss of the Nuclear Receptor Corepressor SLIRP Compromises Male Fertility. *PLoS ONE* 8, e70700.
- Cooper, M.P., Qu, L., Rohas, L.M., Lin, J., Yang, W., Erdjument-Bromage, H., Tempst, P., and Spiegelman, B.M. (2006). Defects in energy homeostasis in Leigh syndrome French Canadian variant through PGC-1 α /LRP130 complex. *Genes Dev.* 20, 2996–3009.
- Cotney, J., Wang, Z., and Shadel, G.S. (2007). Relative abundance of the human mitochondrial transcription system and distinct roles for h-mtTFB1 and h-mtTFB2 in mitochondrial biogenesis and gene expression. *Nucleic Acids Research* 35, 4042–4054.
- Crosby, A.H., Patel, H., Chioza, B.A., Proukakis, C., Gurtz, K., Patton, M.A., Sharifi, R., Harlalka, G., Simpson, M.A., Dick, K., et al. (2010). Defective mitochondrial mRNA maturation is associated with spastic ataxia. *Am. J. Hum. Genet.* 87, 655–660.
- Cusack, S. (1997). Aminoacyl-tRNA synthetases. *Curr. Opin. Struct. Biol.* 7, 881–889.
- Daga, A., and Attardi, G. (1993). Molecular Characterization of the Transcription Termination Factor from Human Mitochondria. *The Journal of Biological Chemistry* 1–8.
- Dairaghi, D., Shadel, G.S., and Clayton, D.A. (1995). Addition of a 29 Residue Carboxyl-terminal Tail Converts a Simple HMG Box-containing Protein into a Transcriptional Activator. *J. Mol. Biol.* 1–18.
- Danial, N.N., Hartman, A.L., Stafstrom, C.E., and Thio, L.L. (2013). How does the ketogenic diet work? Four potential mechanisms. *J. Child Neurol.* 28, 1027–1033.
- Davies, S.M.K., Rackham, O., Shearwood, A.-M.J., Hamilton, K.L., Narsai, R., Whelan, J., and Filipovska, A. (2009). Pentatricopeptide repeat domain protein 3 associates with the mitochondrial small ribosomal subunit and regulates translation. *FEBS Lett.* 583, 1853–1858.
- Delannoy, E., Stanley, W.A., Bond, C.S., and Small, I.D. (2007). Pentatricopeptide repeat (PPR) proteins as sequence-specificity factors in post-transcriptional processes in organelles. *Biochem. Soc. Trans.* 35, 1643–1647.

- Dubin, D.T. (1974). Methylated nucleotide content of mitochondrial ribosomal RNA from hamster cells. *J. Mol. Biol.* *84*, 257–273.
- Eaton, S., Bartlett, K., and Pourfarzam, M. (1996). Mammalian mitochondrial beta-oxidation. *Biochem. J.* *320 (Pt 2)*, 345–357.
- Ekstrand, M.I., Falkenberg, M., Rantanen, A., Park, C.B., Gaspari, M., Hulthenby, K., Rustin, P., Gustafsson, C.M., and Larsson, N.-G. (2004). Mitochondrial transcription factor A regulates mtDNA copy number in mammals. *Human Molecular Genetics* *13*, 935–944.
- Falkenberg, M., Gaspari, M., Rantanen, A., Trifunovic, A., Larsson, N.-G., and Gustafsson, C.M. (2002). Mitochondrial transcription factors B1 and B2 activate transcription of human mtDNA. *Nat. Genet.* *31*, 289–294.
- Falkenberg, M., Larsson, N.-G., and Gustafsson, C.M. (2007). DNA replication and transcription in mammalian mitochondria. *Annu. Rev. Biochem.* *76*, 679–699.
- Fernandez-Silva, P., and Attardi, G. (1997). The human mitochondrial transcription termination factor (mTERF) is a multizipper protein but binds to DNA as a monomer, with evidence pointing to intramolecular leucine zipper interactions. *The EMBO Journal* 1–14.
- FERNANDEZSILVA, P., ACINPEREZ, R., FERNANDEZVIZARRA, E., PEREZMARTOS, A., and ENRIQUEZ, J. (2007). *Methods in Cell Biology* (Elsevier).
- Floss, T., and Schnütgen, F. (2008). Conditional gene trapping using the FLEEx system. *Methods Mol. Biol.* *435*, 127–138.
- Fraga, C.G., Shigenaga, M.K., Park, J.W., Degan, P., and Ames, B.N. (1990). Oxidative damage to DNA during aging: 8-hydroxy-2'-deoxyguanosine in rat organ DNA and urine. *Proc. Natl. Acad. Sci. U.S.A.* *87*, 4533–4537.
- Freyer, C., Park, C.B., Ekstrand, M.I., Shi, Y., Khvorostova, J., Wibom, R., Falkenberg, M., Gustafsson, C.M., and Larsson, N.G. (2010). Maintenance of respiratory chain function in mouse hearts with severely impaired mtDNA transcription. *Nucleic Acids Research* *38*, 6577–6588.
- Gangelhoff, T.A., Mungalachetty, P.S., Nix, J.C., and Churchill, M.E.A. (2009). Structural analysis and DNA binding of the HMG domains of the human mitochondrial transcription factor A. *Nucleic Acids Research* *37*, 3153–3164.
- Gaspari, M., Falkenberg, M., Larsson, N.-G., and Gustafsson, C.M. (2004). The mitochondrial RNA polymerase contributes critically to promoter specificity in mammalian cells. *The EMBO Journal* *23*, 4606–4614.
- Gelfand, R., and Attardi, G. (1981). Synthesis and turnover of mitochondrial ribonucleic acid in HeLa cells: the mature ribosomal and messenger ribonucleic acid species are metabolically unstable. *Mol. Cell. Biol.* *1*, 497–511.
- Gohil, V.M., Nilsson, R., Belcher-Timme, C.A., Luo, B., Root, D.E., and Mootha, V.K. (2010). Mitochondrial and nuclear genomic responses to loss of LRPPRC expression. *J. Biol. Chem.* *285*, 13742–13747.
- Gray, M.W. (1999). Mitochondrial Evolution. *Science* *283*, 1476–1481.
- Gray, M.W., Burger, G., and Lang, B.F. (2001). The origin and early evolution of mitochondria. *Genome Biol.* *2*, REVIEWS1018.
- Haaack, T.B., Kopajtich, R., Freisinger, P., Wieland, T., Rorbach, J., Nicholls, T.J., Baruffini, E., Walther, A., Danhauser, K., Zimmermann, F.A., et al. (2013). ELAC2 Mutations Cause a Mitochondrial RNA Processing Defect Associated with Hypertrophic Cardiomyopathy. *Am. J. Hum. Genet.*

- Hatchell, E.C., Colley, S.M., Beveridge, D.J., Epis, M.R., Stuart, L.M., Giles, K.M., Redfern, A.D., Miles, L.E.C., Barker, A., MacDonald, L.M., et al. (2006). SLIRP, a small SRA binding protein, is a nuclear receptor corepressor. *Molecular Cell* 22, 657–668.
- Heijne, von, G. (1986). Why mitochondria need a genome. *FEBS Lett.* 198, 1–4.
- Hekimi, S., Lapointe, J., and Wen, Y. (2011). Taking a “good” look at free radicals in the aging process. *Trends in Cell Biology* 21, 569–576.
- Hess, J.F., Parisi, M.A., Bennett, J.L., and Clayton, D.A. (1991). Impairment of mitochondrial transcription termination by a point mutation associated with the MELAS subgroup of mitochondrial encephalomyopathies. *Nature* 351, 236–239.
- Holzmann, J., and Rossmannith, W. (2009). Mitochondrion. *Mitochondrion* 9, 284–288.
- Holzmann, J., Frank, P., Löffler, E., Bennett, K.L., Gerner, C., and Rossmannith, W. (2008). RNase P without RNA: identification and functional reconstitution of the human mitochondrial tRNA processing enzyme. *Cell* 135, 462–474.
- Hyvarinen, A.K., Pohjoismaki, J.L.O., Reyes, A., Wanrooij, S., Yasukawa, T., Karhunen, P.J., Spelbrink, J.N., Holt, I.J., and Jacobs, H.T. (2007). The mitochondrial transcription termination factor mTERF modulates replication pausing in human mitochondrial DNA. *Nucleic Acids Research* 35, 6458–6474.
- Jiménez-Menéndez, N., Fernández-Millán, P., Rubio-Cosials, A., Arnan, C., Montoya, J., Jacobs, H.T., Bernadó, P., Coll, M., Usón, I., and Solà, M. (2010). Human mitochondrial mTERF wraps around DNA through a left-handed superhelical tandem repeat. *Nature Structural & Molecular Biology* 1–3.
- Kasamatsu, H., and Vinograd, J. (1974). REPLICATION OF CIRCULAR DNA IN EUKARYOTIC CELLS. 1–25.
- Kaufmann, B., Durisic, N., Mativetsky, J., Costantino, S., and Shoubridge, E.A. (2007). The Mitochondrial Transcription Factor TFAM Coordinates the Assembly of Multiple DNA Molecules into Nucleoid-like Structures. *Mol. Biol. Cell* 1–12.
- Kennedy, A.R., Pissios, P., Otu, H., Xue, B., Asakura, K., Furukawa, N., Marino, F.E., Liu, F.F., Kahn, B.B., Libermann, T.A., et al. (2007). A high-fat, ketogenic diet induces a unique metabolic state in mice. *AJP: Endocrinology and Metabolism* 292, E1724–E1739.
- Kruse, B., Narasimhan, N., and Attardi, G. (1989). Termination of transcription in human mitochondria: identification and purification of a DNA binding protein factor that promotes termination. *Cell* 58, 391–397.
- Kruse, B., and Attardi, G. (1989). Termination of transcription in human mitochondria: Identification and Purification of a DNA binding Protein Factor that promotes termination. *Cell* 1–7.
- Kujoth, G.C., Hiona, A., Pugh, T.D., Someya, S., Panzer, K., Wohlgemuth, S.E., Hofer, T., Seo, A.Y., Sullivan, R., Jobling, W.A., et al. (2005). Mitochondrial DNA mutations, oxidative stress, and apoptosis in mammalian aging. *Science* 309, 481–484.
- Kukat, C., Wurm, C.A., Spähr, H., Falkenberg, M., Larsson, N.-G., and Jakobs, S. (2011). Super-resolution microscopy reveals that mammalian mitochondrial nucleoids have a uniform size and frequently contain a single copy of mtDNA. *Proc. Natl. Acad. Sci. U.S.A.* 108, 13534–13539.
- Lagouge, M., and Larsson, N.G. (2013). The role of mitochondrial DNA mutations and free radicals in disease and ageing. *Journal of Internal Medicine* 273, 529–543.
- Lang, B.F., Burger, G., O'Kelly, C.J., Cedergren, R., Golding, G.B., Lemieux, C., Sankoff, D., Turmel, M., and Gray, M.W. (1997). An ancestral mitochondrial DNA resembling a eubacterial genome in miniature. *Nature* 387, 493–497.

- Larsson, N.G., and Clayton, D.A. (1995). Molecular genetic aspects of human mitochondrial disorders. *Annu. Rev. Genet.* *29*, 151–178.
- Larsson, N.G., Wang, J., Wilhelmsson, H., Oldfors, A., Rustin, P., Lewandoski, M., Barsh, G.S., and Clayton, D.A. (1998). Mitochondrial transcription factor A is necessary for mtDNA maintenance and embryogenesis in mice. *Nat. Genet.* *18*, 231–236.
- Larsson, N.-G. (2010). Somatic mitochondrial DNA mutations in mammalian aging. *Annu. Rev. Biochem.* *79*, 683–706.
- Lee, H.K., Song, J.H., Shin, C.S., Park, D.J., Park, K.S., Lee, K.U., and Koh, C.S. (1998). Decreased mitochondrial DNA content in peripheral blood precedes the development of non-insulin-dependent diabetes mellitus. *Diabetes Research and Clinical Practice* 1–7.
- Lee, K.-W., Okot-Kotber, C., Lacombe, J.F., and Bogenhagen, D.F. (2013). Mitochondrial rRNA Methyltransferase Family Members are Positioned to Modify Nascent rRNA in Foci Near the mtDNA Nucleoid. *J. Biol. Chem.*
- Levinger, L., Mörl, M., and Florentz, C. (2004). Mitochondrial tRNA 3' end metabolism and human disease. *Nucleic Acids Research* *32*, 5430–5441.
- Li, X., and Guan, M.-X. (2002). A human mitochondrial GTP binding protein related to tRNA modification may modulate phenotypic expression of the deafness-associated mitochondrial 12S rRNA mutation. *Mol. Cell. Biol.* *22*, 7701–7711.
- Liesa, M., Palacin, M., and Zorzano, A. (2009). Mitochondrial Dynamics in Mammalian Health and Disease. *Physiol. Rev.* *89*, 799–845.
- Lightowlers, R.N., and Chrzanowska-Lightowlers, Z.M.A. (2008). PPR (pentatricopeptide repeat) proteins in mammals: important aids to mitochondrial gene expression. *Biochem. J.* *416*, e5–e6.
- Litonin, D., Sologub, M., Shi, Y., Savkina, M., Anikin, M., Falkenberg, M., Gustafsson, C.M., and Temiakov, D. (2010). Human mitochondrial transcription revisited: only TFAM and TFB2M are required for transcription of the mitochondrial genes in vitro. *J. Biol. Chem.* *285*, 18129–18133.
- Liu, L., Sanosaka, M., Lei, S., Bestwick, M.L., Frey, J.H., Surovtseva, Y.V., Shadel, G.S., and Cooper, M.P. (2011). LRP130 protein remodels mitochondria and stimulates fatty acid oxidation. *J. Biol. Chem.* *286*, 41253–41264.
- Liu, X., Kim, C.N., Yang, J., Jemmerson, R., and Wang, X. (1996). Induction of apoptotic program in cell-free extracts: requirement for dATP and cytochrome c. *Cell* *86*, 147–157.
- Lodeiro, M.F., Uchida, A., Bestwick, M., Moustafa, I.M., Arnold, J.J., Shadel, G.S., and Cameron, C.E. (2012). Transcription from the second heavy-strand promoter of human mtDNA is repressed by transcription factor A in vitro. *Proc. Natl. Acad. Sci. U.S.A.* *109*, 6513–6518.
- Ma, N., and McAllister, W.T. (2009). In a head-on collision, two RNA polymerases approaching one another on the same DNA may pass by one another. *J. Mol. Biol.* *391*, 808–812.
- Mancebo, R., Zhou, X., Shillinglaw, W., Henzel, W., and Macdonald, P.M. (2001). BSF binds specifically to the bicoid mRNA 3' untranslated region and contributes to stabilization of bicoid mRNA. *Mol. Cell. Biol.* *21*, 3462–3471.
- Mannella, C.A., Marko, M., and Buttle, K. (1997). Reconsidering mitochondrial structure: new views of an old organelle. *Trends Biochem. Sci.* *22*, 37–38.
- Martin, M., Cho, J., Cesare, A.J., Griffith, J.D., and Attardi, G. (2005). Termination Factor-Mediated DNA Loop between Termination and Initiation Sites Drives Mitochondrial rRNA Synthesis. *Cell* *123*, 1227–1240.

- McCulloch, V., and Shadel, G.S. (2003). Human mitochondrial transcription factor B1 interacts with the C-terminal activation region of h-mtTFA and stimulates transcription independently of its RNA methyltransferase activity. *Mol. Cell. Biol.* *23*, 5816–5824.
- Merante, F., Petrova-Benedict, R., MacKay, N., Mitchell, G., Lambert, M., Morin, C., De Braekeleer, M., Laframboise, R., Gagné, R., and Robinson, B.H. (1993). A biochemically distinct form of cytochrome oxidase (COX) deficiency in the Saguenay-Lac-Saint-Jean region of Quebec. *Am. J. Hum. Genet.* *53*, 481–487.
- Mercer, T.R., Neph, S., Dinger, M.E., Crawford, J., Smith, M.A., Shearwood, A.-M.J., Haugen, E., Bracken, C.P., Rackham, O., Stamatoyannopoulos, J.A., et al. (2011). The human mitochondrial transcriptome. *Cell* *146*, 645–658.
- Metodiev, M.D., Lesko, N., Park, C.B., Cámara, Y., Shi, Y., Wibom, R., Hultenby, K., Gustafsson, C.M., and Larsson, N.-G. (2009). Methylation of 12S rRNA is necessary for in vivo stability of the small subunit of the mammalian mitochondrial ribosome. *Cell Metab.* *9*, 386–397.
- Mili, S., and Piñol-Roma, S. (2003). LRP130, a pentatricopeptide motif protein with a noncanonical RNA-binding domain, is bound in vivo to mitochondrial and nuclear RNAs. *Mol. Cell. Biol.* *23*, 4972–4982.
- Minczuk, M., He, J., Duch, A.M., Etema, T.J., Chlebowski, A., Dzionek, K., Nijtmans, L.G.J., Huynen, M.A., and Holt, I.J. (2011). TEFM (c17orf42) is necessary for transcription of human mtDNA. *Nucleic Acids Research* *39*, 4284–4299.
- Miquel, J., Economos, A.C., Fleming, J., and Johnson, J.E. (1980). Mitochondrial role in cell aging. *Exp. Gerontol.* *15*, 575–591.
- Mitchell, P. (1961). Coupling of Phosphorylation to Electron and Hydrogen Transfer by a chemi-osmotic Type of Mechanism. 1–5.
- Mollica, M.P., Lionetti, L., Crescenzo, R., Tasso, R., Barletta, A., Liverini, G., and Iossa, S. (2005). Cold exposure differently influences mitochondrial energy efficiency in rat liver and skeletal muscle. *FEBS Lett.* *579*, 1978–1982.
- Montoya, J., Gaines, G.L., and Attardi, G. (1983). The pattern of transcription of the human mitochondrial rRNA genes reveals two overlapping transcription units. *Cell* *34*, 151–159.
- Mootha, V.K., Lepage, P., Miller, K., Bunkenborg, J., Reich, M., Hjerrild, M., Delmonte, T., Villeneuve, A., Sladek, R., Xu, F., et al. (2003). Identification of a gene causing human cytochrome c oxidase deficiency by integrative genomics. *Proc. Natl. Acad. Sci. U.S.A.* *100*, 605–610.
- Mourier, A., and Larsson, N.-G. (2011). Tracing the trail of protons through complex I of the mitochondrial respiratory chain. *PLoS Biol.* *9*, e1001129.
- Nagaike, T., Suzuki, T., Katoh, T., and Ueda, T. (2005). Human mitochondrial mRNAs are stabilized with polyadenylation regulated by mitochondria-specific poly(A) polymerase and polynucleotide phosphorylase. *J. Biol. Chem.* *280*, 19721–19727.
- Ngo, H.B., Kaiser, J.T., and Chan, D.C. (2011). The mitochondrial transcription and packaging factor Tfam imposes a U-turn on mitochondrial DNA. *Nature Structural & Molecular Biology* *18*, 1290–1296.
- Nunnari, J., and Suomalainen, A. (2012). Mitochondria: in sickness and in health. *Cell* *148*, 1145–1159.
- Nunnari, J., Marshall, W.F., Straight, A., and Walter, P. (1997). Mitochondrial transmission during mating in *Saccharomyces cerevisiae* is determined by mitochondrial fusion and fission and the intramitochondrial segregation of mitochondrial DNA

- . Mol. Biol. Cell 1–10.
- O'Brien, T.W. (1971). The general occurrence of 55 S ribosomes in mammalian liver mitochondria. *J. Biol. Chem.* 246, 3409–3417.
- Ojala, D., Montoya, J., and Attardi, G. (1981). tRNA punctuation model of RNA processing in human mitochondria. *Nature* 1–5.
- Pagliarini, D.J., Calvo, S.E., Chang, B., Sheth, S.A., Vafai, S.B., Ong, S.-E., Walford, G.A., Sugiana, C., Boneh, A., Chen, W.K., et al. (2008). A mitochondrial protein compendium elucidates complex I disease biology. *Cell* 134, 112–123.
- Parisi, M.A., and Clayton, D.A. (1991). Similarity of human mitochondrial transcription factor 1 to high mobility group proteins. *Science* 252, 965–969.
- Park, C.B., Asin-Cayuela, J., Cámara, Y., Shi, Y., Pellegrini, M., Gaspari, M., Wibom, R., Hultenby, K., Erdjument-Bromage, H., Tempst, P., et al. (2007). MTERF3 is a negative regulator of mammalian mtDNA transcription. *Cell* 130, 273–285.
- Pellegrini, M., Asin-Cayuela, J., Erdjument-Bromage, H., Tempst, P., Larsson, N.-G., and Gustafsson, C.M. (2009). MTERF2 is a nucleoid component in mammalian mitochondria. *Biochim. Biophys. Acta* 1787, 296–302.
- Perkins, G., Renken, C., Martone, M.E., Young, S.J., Ellisman, M., and Frey, T. (1997). Electron tomography of neuronal mitochondria: three-dimensional structure and organization of cristae and membrane contacts. *J. Struct. Biol.* 119, 260–272.
- Polosa, P.L., Deceglie, S., Roberti, M., Gadaleta, M.N., and Cantatore, P. (2005). Contrahelicase activity of the mitochondrial transcription termination factor mtDBP. *Nucleic Acids Research* 33, 3812–3820.
- Polosa, P.L., Roberti, M., and Cantatore, P. (2011). Mechanism and Regulation of Mitochondrial Transcription in Animal Cells. (Berlin, Heidelberg: Springer Berlin Heidelberg), pp. 271–295.
- Rackham, O., and Filipovska, A. (2012). The role of mammalian PPR domain proteins in the regulation of mitochondrial gene expression. *Biochim. Biophys. Acta* 1819, 1008–1016.
- Rackham, O., Davies, S.M.K., Shearwood, A.-M.J., Hamilton, K.L., Whelan, J., and Filipovska, A. (2009). Pentatricopeptide repeat domain protein 1 lowers the levels of mitochondrial leucine tRNAs in cells. *Nucleic Acids Research* 37, 5859–5867.
- Rackham, O., Mercer, T.R., and Filipovska, A. (2012). The human mitochondrial transcriptome and the RNA-binding proteins that regulate its expression. *Wiley Interdiscip Rev RNA*.
- Rackham, O., Shearwood, A.-M.J., Mercer, T.R., Davies, S.M.K., Mattick, J.S., and Filipovska, A. (2011). Long noncoding RNAs are generated from the mitochondrial genome and regulated by nuclear-encoded proteins. *Rna* 17, 2085–2093.
- Ringel, R., Sologub, M., Morozov, Y.I., Litonin, D., Cramer, P., and Temiakov, D. (2011). Structure of human mitochondrial RNA polymerase. *Nature* 478, 269–273.
- Roberti, M., Bruni, F., Loguercio Polosa, P., Manzari, C., Gadaleta, M.N., and Cantatore, P. (2006a). MTERF3, the most conserved member of the mTERF-family, is a modular factor involved in mitochondrial protein synthesis. *Biochim. Biophys. Acta* 1757, 1199–1206.
- Roberti, M., Bruni, F., Polosa, P.L., Gadaleta, M.N., and Cantatore, P. (2006b). The Drosophila termination factor DmTTF regulates in vivo mitochondrial transcription. *Nucleic Acids Research* 34, 2109–2116.

- Roberti, M., Polosa, P.L., Bruni, F., Manzari, C., Deceglie, S., Gadaleta, M.N., and Cantatore, P. (2009). The MTERF family proteins: Mitochondrial transcription regulators and beyond. *BBA - Bioenergetics* *1787*, 303–311.
- Rojas-Pierce, M., and Springer, P.S. (2003). Gene and enhancer traps for gene discovery. *Methods Mol. Biol.* *236*, 221–240.
- Rolo, A.P., and Palmeira, C.M. (2006). Diabetes and mitochondrial function: role of hyperglycemia and oxidative stress. *Toxicol. Appl. Pharmacol.* *212*, 167–178.
- Rorbach, J., and Minczuk, M. (2012). The post-transcriptional life of mammalian mitochondrial RNA. *Biochem. J.* *444*, 357–373.
- Rorbach, J., Nicholls, T.J.J., and Minczuk, M. (2011). PDE12 removes mitochondrial RNA poly(A) tails and controls translation in human mitochondria. *Nucleic Acids Research* *39*, 7750–7763.
- Rossmannith, J.H.P.F.E.L.K.L.B.C.G.W. (2008). RNase P without RNA: Identification and Functional Reconstitution of the Human Mitochondrial tRNA Processing Enzyme. *Cell* *135*, 462–474.
- Rossmannith, W., and Karwan, R.M. (1998). Characterization of human mitochondrial RNase P: novel aspects in tRNA processing. *Biochemical and Biophysical Research Communications* *247*, 234–241.
- Rossmannith, W. (2011). Localization of Human RNase Z Isoforms: Dual Nuclear/Mitochondrial Targeting of the ELAC2 Gene Product by Alternative Translation Initiation. *PLoS ONE* *6*, e19152.
- Rubio-Cosials, A., Sidow, J.F., Jiménez-Menéndez, N., Fernández-Millán, P., Montoya, J., Jacobs, H.T., Coll, M., Bernadó, P., and Solà, M. (2011). Human mitochondrial transcription factor A induces a U-turn structure in the light strand promoter. *Nature Structural & Molecular Biology* *18*, 1281–1289.
- Ruzzenente, B., Metodiev, M.D., Wredenberg, A., Bratic, A., Park, C.B., Cámara, Y., Milenkovic, D., Zickermann, V., Wibom, R., Hulthenby, K., et al. (2012). LRPPRC is necessary for polyadenylation and coordination of translation of mitochondrial mRNAs. *The EMBO Journal* *31*, 443–456.
- Sanchez, M.I.G.L., Mercer, T.R., Davies, S.M.K., Shearwood, A.-M.J., Nygård, K.K.A., Richman, T.R., Mattick, J.S., Rackham, O., and Filipovska, A. (2011). RNA processing in human mitochondria. *Cell Cycle* *10*, 2904–2916.
- Sasarman, F., Brunel-Guitton, C., Antonicka, H., Wai, T., Shoubridge, E.A., LSFC Consortium (2010). LRPPRC and SLIRP interact in a ribonucleoprotein complex that regulates posttranscriptional gene expression in mitochondria. *Mol. Biol. Cell* *21*, 1315–1323.
- Scarpulla, R.C. (2008). Transcriptional paradigms in mammalian mitochondrial biogenesis and function. *Physiol. Rev.* *88*, 611–638.
- Schmitz-Linneweber, C., and Small, I. (2008). Pentatricopeptide repeat proteins: a socket set for organelle gene expression. *Trends Plant Sci.* *13*, 663–670.
- Seidel-Rogol, B.L., McCulloch, V., and Shadel, G.S. (2003). Human mitochondrial transcription factor B1 methylates ribosomal RNA at a conserved stem-loop. *Nat. Genet.* *33*, 23–24.
- Sena, L.A., and Chandel, N.S. (2012). Physiological roles of mitochondrial reactive oxygen species. *Molecular Cell* *48*, 158–167.
- Shang, J., and Clayton, D.A. (1994). Human mitochondrial transcription termination exhibits RNA polymerase independence and biased bipolarity in vitro. *J. Biol. Chem.* *269*, 29112–29120.
- Shi, Y., Dierckx, A., Wanrooij, P.H., Wanrooij, S., Larsson, N.-G., Wilhelmsson, L.M., Falkenberg, M., and Gustafsson, C.M. (2012). Mammalian transcription factor A is a core component of the mitochondrial transcription machinery. *Proc. Natl. Acad. Sci. U.S.A.* *109*, 16510–16515.

- Small, I.D., and Peeters, N. (2000). The PPR motif - a TPR-related motif prevalent in plant organellar proteins. *Trends Biochem. Sci.* 25, 46–47.
- Smidansky, E.D., Arnold, J.J., Reynolds, S.L., and Cameron, C.E. (2011). Human mitochondrial RNA polymerase: evaluation of the single-nucleotide-addition cycle on synthetic RNA/DNA scaffolds. *Biochemistry* 50, 5016–5032.
- Sologub, M., Litonin, D., Anikin, M., Mustaev, A., and Temiakov, D. (2009). TFB2 is a transient component of the catalytic site of the human mitochondrial RNA polymerase. *Cell* 139, 934–944.
- Spåhr, H., Habermann, B., Gustafsson, C.M., Larsson, N.-G., and Hällberg, B.M. (2012). Structure of the human MTERF4-NSUN4 protein complex that regulates mitochondrial ribosome biogenesis. *Proc. Natl. Acad. Sci. U.S.A.* 109, 15253–15258.
- Spåhr, H., Samuelsson, T., Hällberg, B.M., and Gustafsson, C.M. (2010). Structure of Mitochondrial Transcription Termination Factor 3 reveals a novel nucleic acid-binding domain. *Biochemical and Biophysical Research Communications* 1–5.
- Springer, P.S. (2000). Gene traps: tools for plant development and genomics. *Plant Cell* 12, 1007–1020.
- Stafstrom, C.E., and Rho, J.M. (2012). The ketogenic diet as a treatment paradigm for diverse neurological disorders. *Front Pharmacol* 3, 59.
- Sterky, F.H., Ruzzenente, B., Gustafsson, C.M., Samuelsson, T., and Larsson, N.-G. (2010). LRPPRC is a mitochondrial matrix protein that is conserved in metazoans. *Biochemical and Biophysical Research Communications* 398, 759–764.
- Stewart, J.B., Freyer, C., Elson, J.L., and Larsson, N.-G. (2008). Purifying selection of mtDNA and its implications for understanding evolution and mitochondrial disease. *Nat. Rev. Genet.* 9, 657–662.
- Stock, D., Leslie, A.G., and Walker, J.E. (1999). Molecular architecture of the rotary motor in ATP synthase. *Science* 286, 1700–1705.
- Suomalainen, A. (2011). Therapy for mitochondrial disorders: little proof, high research activity, some promise. *Semin Fetal Neonatal Med* 16, 236–240.
- Taanman, J.-W. (1998). The mitochondrial genome: structure, transcription, translation and replication. 1–21.
- Tavares-Carreón, F., Camacho-Villasana, Y., Zamudio-Ochoa, A., Shingú-Vázquez, M., Torres-Larios, A., and Pérez-Martínez, X. (2008). The pentatricopeptide repeats present in Pet309 are necessary for translation but not for stability of the mitochondrial COX1 mRNA in yeast. *J. Biol. Chem.* 283, 1472–1479.
- Tavtigian, S., Simard, J., Teng, D., and Cannon-Albright, L. (2001). A candidate prostate cancer susceptibility gene at chromosome 17p. *Nature Article* 1–9.
- Temperley, R.J., Wydro, M., Lightowers, R.N., and Chrzanowska-Lightowers, Z.M. (2010). Human mitochondrial mRNAs--like members of all families, similar but different. *Biochim. Biophys. Acta* 1797, 1081–1085.
- Terzioglu, M., Ruzzenente, B., Harmel, J., Mourier, A., Jemt, E., López, M.D., Kukat, C., Stewart, J.B., Wibom, R., Meharg, C., et al. (2013). MTERF1 binds mtDNA to prevent transcriptional interference at the light-strand promoter but is dispensable for rRNA gene transcription regulation. *Cell Metab.* 17, 618–626.
- Tiranti, V., Savoia, A., Forti, F., D'Apolito, M.F., Centra, M., Rocchi, M., and Zeviani, M. (1997). Identification of the gene encoding the human mitochondrial RNA polymerase (h-mtRPO) by cyberscreening of the Expressed Sequence Tags database. *Human Molecular Genetics* 6, 615–625.

- Tomecki, R., Dmochowska, A., Gewartowski, K., Dziembowski, A., and Stepień, P.P. (2004). Identification of a novel human nuclear-encoded mitochondrial poly(A) polymerase. *Nucleic Acids Research* 32, 6001–6014.
- Topisirovic, I., Siddiqui, N., Orolicki, S., Skrabanek, L.A., Tremblay, M., Hoang, T., and Borden, K.L.B. (2009). Stability of eukaryotic translation initiation factor 4E mRNA is regulated by HuR, and this activity is dysregulated in cancer. *Mol. Cell. Biol.* 29, 1152–1162.
- Trifunovic, A. (2005). Progressive parkinsonism in mice with respiratory-chain-deficient dopamine neurons. *Proc. Natl. Acad. Sci. U.S.A.* 1–6.
- Trifunovic, A., Wredenberg, A., Falkenberg, M., Spelbrink, J.N., Rovio, A.T., Bruder, C.E., Bohlooly-Y, M., Gidlöf, S., Oldfors, A., Wibom, R., et al. (2004). Premature ageing in mice expressing defective mitochondrial DNA polymerase. *Nature* 429, 417–423.
- Tuppen, H.A.L., Blakely, E.L., Turnbull, D.M., and Taylor, R.W. (2010). Mitochondrial DNA mutations and human disease. *Biochim. Biophys. Acta* 1797, 113–128.
- Vafai, S.B., and Mootha, V.K. (2012). Mitochondrial disorders as windows into an ancient organelle. *Nature* 491, 374–383.
- van der Horst, G.T., Muijtjens, M., Kobayashi, K., Takano, R., Kanno, S., Takao, M., de Wit, J., Verkerk, A., Eker, A.P., van Leenen, D., et al. (1999). Mammalian Cry1 and Cry2 are essential for maintenance of circadian rhythms. *Nature* 398, 627–630.
- Vandecasteele, G., Szabadkai, G., and Rizzuto, R. (2001). Mitochondrial calcium homeostasis: mechanisms and molecules. *IUBMB Life* 52, 213–219.
- Vilardo, E., Nachbagauer, C., Buzet, A., Taschner, A., Holzmann, J., and Rossmannith, W. (2012). A subcomplex of human mitochondrial RNase P is a bifunctional methyltransferase--extensive moonlighting in mitochondrial tRNA biogenesis. *Nucleic Acids Research* 40, 11583–11593.
- Viña, J., Borras, C., Abdelaziz, K.M., Garcia-Valles, R., and Gomez-Cabrera, M.C. (2013). The free radical theory of aging revisited: the cell signaling disruption theory of aging. *Antioxid. Redox Signal.* 19, 779–787.
- WALLACE, D.C. (1992). Diseases of the mitochondrial DNA. *Annu. Rev. Biochem.* 61, 1175–1212.
- Wallace, D.C. (2005). A Mitochondrial Paradigm of Metabolic and Degenerative Diseases, Aging, and Cancer: A Dawn for Evolutionary Medicine. *Annu. Rev. Genet.* 1–51.
- Wallace, D.C. Mitochondrial DNA mutations in disease and aging. *Environ. Mol. Mutagen.* n/a–n/a.
- Wallace, D.C., and Fan, W. (2010). Energetics, epigenetics, mitochondrial genetics. *Mitochondrion* 10, 12–31.
- Wallace, D.C., Singh, G., Lott, M.T., Hodge, J.A., Schurr, T.G., Lezza, A., Elsas, L., II, and Nikoskelainen, E.K. (1988). Mitochondrial DNA mutation associated with Leber's Hereditary Optic Neuropathy. *Science* 1–4.
- Wenz, T., Luca, C., Torraco, A., and Moraes, C.T. (2009). mTERF2 Regulates Oxidative Phosphorylation by Modulating mtDNA Transcription. *Cell Metab.* 9, 499–511.
- Whelan, S.P., and Zuckerbraun, B.S. (2013). Mitochondrial signaling: forwards, backwards, and in between. *Oxid Med Cell Longev* 2013, 351613.
- Wredenberg, A., Lagouge, M., Bratic, A., Metodiev, M.D., Spähr, H., Mourier, A., Freyer, C., Ruzzenente, B., Tain, L., Grönke, S., et al. (2013). MTERF3 regulates mitochondrial ribosome biogenesis in invertebrates and mammals. *PLoS Genet* 9, e1003178.

- Xu, F., Ackerley, C., Maj, M.C., Addis, J.B.L., Levandovskiy, V., Lee, J., Mackay, N., Cameron, J.M., and Robinson, B.H. (2008). Disruption of a mitochondrial RNA-binding protein gene results in decreased cytochrome b expression and a marked reduction in ubiquinol-cytochrome c reductase activity in mouse heart mitochondria. *Biochem. J.* *416*, 15–26.
- Xu, F., Morin, C., Mitchell, G., Ackerley, C., and Robinson, B.H. (2004). The role of the LRPPRC (leucine-rich pentatricopeptide repeat cassette) gene in cytochrome oxidase assembly: mutation causes lowered levels of COX (cytochrome c oxidase) I and COX III mRNA. *Biochem. J.* *382*, 331–336.
- Yakubovskaya, E., Mejia, E., Byrnes, J., Hambardjieva, E., and Garcia-Diaz, M. (2010). Helix unwinding and base flipping enable human MTERF1 to terminate mitochondrial transcription. *Cell* *141*, 982–993.
- Yamaguchi, T., Morikawa, A., and Miyoshi, H. (2012). Biochemical and Biophysical Research Communications. *Biochemical and Biophysical Research Communications* *425*, 297–303.
- Zehrmann, A., Verbitskiy, D., Härtel, B., Brennicke, A., and Takenaka, M. (2011). PPR proteins network as site-specific RNA editing factors in plant organelles. *RNA Biol* *8*, 67–70.
- Zhou, Y., and Martin, C.T. (2006). Observed instability of T7 RNA polymerase elongation complexes can be dominated by collision-induced "bumping". *J. Biol. Chem.* *281*, 24441–24448.
- Zollo, O., Tiranti, V., and Sondheim, N. (2012). Transcriptional requirements of the distal heavy-strand promoter of mtDNA. *Proc. Natl. Acad. Sci. U.S.A.* *109*, 6508–6512.

Acknowledgements

First of all I want to thank my boss Prof. Dr. Nils-Göran Larsson for giving me the opportunity to do my PhD in his lab. Your input on my scientific work helped me to successfully deal with my different projects, adopt a multitude of methods and to learn how to organize myself. I really enjoyed my time in your lab and I met many colleagues there, who I can call friends now.

I thank my committee members Prof. Dr. Thomas Langer and Prof. Dr. Peter Kloppenburg for your time to evaluate my thesis.

A big Thank You goes to my supervisor and friend Mügen Terzioglu. Your friendship and support over the last four years was the base for our successful teamwork and helped me to survive in difficult moments. We always had a lot of fun together in the lab, at lunch or wherever. I am already looking forward to visit you in Cyprus, Istanbul or Helsinki ☺

I also want to say “Thank you so much” to Benedetta Ruzzenente, my friend, colleague and somehow “second supervisor”. You always had an answer for my endless questions and you taught me so much about science even if you actually did not have time for it. There is no other person I know who is so much passionate about science and transfers this to his environment. I am very happy to be your friend.

To the “chicken lab” Ana, Dusanka, Stanka, Francesca, Marie and Avan: Thank you girls for the nice atmosphere, for your help and advices. I enjoyed working and laughing with you together.

I also want to thank Arnaud, Metodi, Nina, Chris, Hyun Ju Henrik, Elisa, Inge, Timo, Johanna and Jacob for your help whenever I needed it and for being really nice colleagues to have around.

Jim, thank you for dealing with my thesis and spending so much time with it.

The technicians Avan, Lysann, Regina and Steffi: You did (and do) a great job. Thank you for your support and lab organization as well as many nice chats we had.

Miriam and Corry: Thanks a lot for dealing with all the administrative stuff besides bench work. Your organization made my life much easier.

Besonderer Dank geht außerdem an meine Familie, die zu jeder Zeit hinter mir stand, mich aufgefangen und motiviert hat. Danke Mitch, dass Du meine Launen ertragen und mir immer den Rücken gestärkt hast. Du warst da wenn ich Dich brauchte und hast mich unermüdlich daran erinnert die schönen Seiten im Leben zu genießen.

Meinen Eltern Marita und Ulrich, sowie meinem Bruder Jens danke ich für Eure grenzenlose Liebe und Unterstützung zu jeder Zeit. Euer stetes Interesse an dem was ich Tue und der Rückhalt den Ihr mir bietet und bedeutet mir sehr viel.

Erklärung

Ich versichere, dass ich die von mir vorgelegte Dissertation selbstständig angefertigt, die benutzten Quellen und Hilfsmittel vollständig angegeben und die Stellen der Arbeit – einschließlich Tabellen, Karten und Abbildungen –, die anderen Werken im Wortlaut oder dem Sinn nach entnommen sind, in jedem Einzelfall als Entlehnung kenntlich gemacht habe; dass sie abgesehen von unten angegebenen Teilpublikationen – noch nicht veröffentlicht worden ist sowie, dass ich eine solche Veröffentlichung vor Abschluss des Promotionsverfahrens nicht vornehmen werde.

Die Bestimmungen dieser Promotionsordnung sind mir bekannt. Die von mir vorgelegte Dissertation ist von Prof. Dr. Nils-Göran Larsson betreut worden.

Julia Harmel

Nachfolgende Teilpublikationen liegen vor:

1. **Harmel J**, Ruzzenente B, Terzioglu M, Spåhr H, Falkenberg M, Larsson NG. The leucine rich pentatricopeptide repeat-containing protein (LRPPRC) does not activate transcription in mammalian mitochondria J Biol Chem. 2013 May 31;288(22):15510-9.
2. Terzioglu M, Ruzzenente B, **Harmel J**, Mourier A, Jemt E, López MD, Kukat C, Stewart JB, Wibom R, Meharg C, Habermann B, Falkenberg M, Gustafsson CM, Park CB, Larsson NG. MTERF1 binds mtDNA to prevent transcriptional interference at the light-strand promoter but is dispensable for rRNA gene transcription regulation. Cell Metab. 2013 Apr 2;17(4):618-26.

CURRICULUM VITAE

Julia Harmel

Adresse Frankenweg 18
 Wohnort Bonn
 Email Jharmel1@web.de

Geburtsdatum 01.08.1983

Geburtsort Karlsruhe

Familienstand ledig

Nationalität deutsch

AUSBILDUNG

- Januar 2014 **Promotion** im Fach Molekulargenetik
 Titel der Promotionsarbeit:
 Posttranscriptional regulation of mitochondrial DNA
 expression in mammalian mitochondria
- Okt. 2009 – März 2014 Doktorandin am **Max Planck Institut für Altersforschung**,
 Köln im Bereich **mitochondriale Genetik**
 in der Arbeitsgruppe von Prof. Nils-Göran Larsson
- Okt. 2005 – Dez. 2008 **Rheinische Friedrich-Wilhelms Universität Bonn**
 Diplomarbeit am **Institut für Zellbiologie** in der
 Arbeitsgruppe von Prof. Jörg Höfeld
- Okt. 2003 – Aug. 2005 **Heinrich-Heine Universität Düsseldorf**
 Grundstudium der Biologie mit Abschluss Vordiplom
- Aug. 1994 – Apr. 2003 **Kreisgymnasium Heinsberg** mit Abschluss Abitur
- Aug. 1990 – Juli 1994 **Gartenschule Karlsruhe** (Grundschule)